Accepted Manuscript

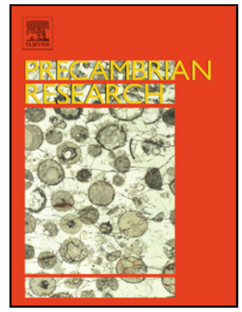

Title: Geochronological, geochemical and Nd-Hf-Os isotopic fingerprinting of an early Neoproterozoic arc-back-arc system in South China and its accretionary assembly along the margin of Rodinia

Author: Yuejun Wang Aimei Zhang Peter A. Cawood Weiming Fan Jifeng Xu Guowei Zhang Yuzhi Zhang

PII: S0301-9268(13)00106-X
DOI: http://dx.doi.org/doi:10.1016/j.precamres.2013.03.020
Reference: PRECAM 3747

To appear in: *Precambrian Research*

Received date: 20-10-2012
Revised date: 26-3-2013
Accepted date: 28-3-2013

Please cite this article as: Wang, Y., Zhang, A., Cawood, P.A., Fan, W., Xu, J., Zhang, G., Zhang, Y., Geochronological, geochemical and Nd-Hf-Os isotopic fingerprinting of an early Neoproterozoic arc-back-arc system in South China and its accretionary assembly along the margin of Rodinia, *Precambrian Research* (2013), http://dx.doi.org/10.1016/j.precamres.2013.03.020

This is a PDF file of an unedited manuscript that has been accepted for publication. As a service to our customers we are providing this early version of the manuscript. The manuscript will undergo copyediting, typesetting, and review of the resulting proof before it is published in its final form. Please note that during the production process errors may be discovered which could affect the content, and all legal disclaimers that apply to the journal pertain.

ACCEPTED MANUSCRIPT

► The metabasic rocks in Cathaysia yield U-Pb ages of 969-984 Ma and $T_{DM(Hf)}$ of 0.92-1.44 Ga.

► They originated from a subduction-modified MORB-like source linked to an arc-back-arc setting.

► The South China Block was created by episodic amalgamation of a series of arc fragments between ~970-820 Ma.

► The South China Block is an exterior accretionary orogen along the periphery of Rodinia rather than in the interior.

Accepted Manuscript

ACCEPTED MANUSCRIPT

Geochronological, geochemical and Nd-Hf-Os isotopic fingerprinting of an early Neoproterozoic arc-back-arc system in South China and its accretionary assembly along the margin of Rodinia

Yuejun Wang [1, 2, *] Aimei Zhang [1] Peter A. Cawood [3, 4]
Weiming Fan [1] Jifeng Xu [1] Guowei Zhang [2] Yuzhi Zhang [1]

1 State Key Laboratory of Isotope Geochemistry, Guangzhou Institute of Geochemistry, Chinese Academy of Science, Guangzhou 510640, China
2 State Key Laboratory of Continental Dynamics, Northwest University, Xi'an, 710069, China
3 Department of Earth Sciences, University of St. Andrews, St. Andrews, KY16 9AL, UK.
4 School of Earth and Environment, University of Western Australia, Crawley, 35 Stirling Highway, WA, 6009, Australia

* Corresponding author
Current address: Guangzhou Institute of Geochemistry,
Chinese Academy of Sciences,
P.O. Box 1131, Guangzhou 510640,
People's Republic of China
Fax: 86-20-85290227, Tel: 86-20-85290227
Email: yjwang@gig.ac.cn

Accepted Manuscript

ACCEPTED MANUSCRIPT

Abstract

U-Pb geochronology along with elemental and Nd-Hf-Os isotopic data from the earliest Neoproterozoic metabasic rocks within the Cathaysia Block of the South China Block (SCB) constrain the tectonic setting and paleogeography of the block within the Rodinia supercontinent. The metabasic rocks give zircon U-Pb ages of 969-984 Ma, $\varepsilon_{Hf}(t)$ values of +1.8-+15.3 and Hf model ages of 0.92-1.44 Ga. They are subalkaline basalts that can be geochemically classified into four groups. Group 1 has low Nb contents (1.24-4.33 ppm), highly positive $\varepsilon_{Nd}(t)$ values (+4.3-+5.2), and REE and multi-elemental patterns similar to fore-arc MORB-type basalt. Group 2 has Nb contents ranging from 3.13 ppm to 6.48 ppm, $\varepsilon_{Nd}(t)$ of +3.1 to +6.2, low Re and Os contents and high initial Os isotopic ratios, and displays an E-MORB geochemical signature. Group 3 has Nb = 7.18-29.87 ppm, Nb/La = 0.60-1.40, Nb/U = 5.0-37, Ce/Pb = 1.1-6.6, $\varepsilon_{Nd}(t)$ = +2.9 to +7.0, $^{187}Re/^{188}Os$ = 5.87-8..87 and γOs (t) = 178-772, geochemically resembling to the Pickle Nb-enriched basalt. Group 4 has strong LREE/HREE and HREE fractionation and high $\varepsilon_{Nd}(t)$ values (+2.3 to +5.6), and is characterized by similar element patterns to arc volcanic rocks. Serpentinites coeval to Group 4 show $^{187}Os/^{188}Os$ of 0.1143-0.1442 and γOs (t) of -7.8- +0.1. Groups 1 and 2 are interpreted to originate from the N-MORB and E-MORB-like sources with the addition of an arc-like component, genetically linked to fore- and back-arc settings, respectively. Groups 3 and 4 show inputs of newly subduction-derived melt and fluid in the wedge source. These geochronological and geochemical signatures fingerprint the development of an earliest Neoproterozoic (~970 Ma) arc – back-arc system along the Wuyi-Yunkai domain of the Cathaysia Block. Regional relationships indicate that the Wuyi-Yunkai arc – back-arc system was one of a series of separate convergent margin settings, which included the Shuangxiwu (~970-880 Ma) and Jiangnan (~870-820 Ma)

Accepted Manuscript

ACCEPTED MANUSCRIPT

systems that developed in the SCB. The formation and closure of these arc – back-arc systems resulted in the northwestwardly episodic amalgamation of various pieces of the Yangtze and Cathaysia to finally form the SCB. These signatures require the SCB to occupy an exterior accretionary orogen along the periphery of Rodinia during 990-820 Ma, rather than to have formed through Mesoproterozoic Sibao orogenesis within the interior of Rodinia.

Keywords: metabasic rocks, MORB- and/or arc-like geochemical signatures, earliest Neoproterozoic, arc and back-arc system, eastern South China Block, periphery of Rodinia

1 Introduction

The South China Block (SCB) is composed of the Yangtze Block to the northwest and the Cathaysia Block to the southeast. The two blocks have been considered to have amalgamated at the end of the Mesoproterozoic to form the Sibao Orogen (inset of Fig. 1) associated with the assembly of Rodinia and to occupy an intra-cratonic keystone position between Australia and Laurentia (e.g., Li et al., 1995, 2002, 2008c; Charvet et al., 1996; Ye et al., 2007; Boger et al., 2000; Li et al., 2008b, 2009). However, an interior location within Rodinia does not fit readily with the presence of early Neoproterozoic (~970-900 Ma) rock units of arc or back-arc basin affinities in the easternmost Yangtze Block (e.g., Shui, 1988; Li et al., 2003, 2008a; Li et al., 2006, 2009; Ye et al., 2007; Gao et al., 2009; Chen et al., 2009a, b Shu et al., 2011; Cawood et al., in press). Furthermore, additional age-data suggest that final assembly along the Jiangnan domain did not occur until at least ~830 Ma (e.g., Wang et al., 2006, 2007b, 2008b, c, 2011a; Wu et al., 2006; Zhou et al., 2007, 2009; Zheng et al., 2007, 2008; Zhao et al., 2011; Zhang et al., 2011c, 2012c; Zhao and Guo, 2012). As a

Accepted Manuscript

ACCEPTED MANUSCRIPT

result, the SCB has either been placed on the margin of Rodinia or external to the supercontinent (e.g., Zhao and Cawood, 1999; Torsvik et al., 2001; Yang et al., 2004). New field, geochronological, geochemical and Nd-Hf-Os isotopic data presented herein for the mafic igneous rocks from the Cathaysia Block of the SCB demonstrate that they formed in the earliest Neoproterozoic (985-970 Ma) and have geochemical affinities to MORB, Nb-enriched basalt and island-arc basalt. These and other data enable the recognition of a series of early Neoproterozoic (980-820 Ma) arc and back-arc systems across the SCB, and constrain its location to the margin of Rodinia, likely adjacent to West Australia, East Antarctica and India.

2 Geological background and petrology

The Yangtze and Cathaysia blocks of the SCB consist of distinctive Achaean and Paleoproterozoic crystalline basement that are overlain with angular unconformity by a middle-upper Neoproterozoic and lower Paleozoic (~810-430 Ma) package deposited in a failed rift environment (e.g., Wang and Li, 2003; Shu et al., 2008, 2011; Yu et al., 2010; Wan et al., 2010; Wang et al., 2012a; Zhang et al., 2012c, Zhao and Cawood, 2012 and reference therein). The eastern SCB can be subdivided into eastern Cathaysia, western Cathaysia and eastern Yangtze regions (Fig. 1; Xu et al., 2007; Yu et al., 2009; Wang et al., 2012b) of which the Eastern Cathaysia is largely covered by the Mesozoic volcanic rocks and separated from the western Cathaysia by the Zhenghe- Dapu fault and its inferred southern extension, the Gaoyao-Huilai Fault, along the Nanling and Yunkai domains (Fig. 1, e.g., Chen WS et al., 2002; Wang et al., 2012a). Western Cathaysia contains a series of structurally disrupted Proterozoic metamorphic domains including the Wuyi, Nanling and Yunkai domains (e.g., Fujian BGMR, 1985; Wang YJ et al., 2012c). The Neoproterozoic boundary between the Cathaysia and Yangtze blocks has traditionally been taken as the Jiangshan-Shaoxing Fault at the eastern Jiangnan

Accepted Manuscript

ACCEPTED MANUSCRIPT

Domain (e.g., Shui et al., 1988, Ye et al., 2007; Zhang and Wang, 2007; Shu et al., 2008; Li et al., 2008b, 2009). However, its southward extension is uncertain with some authors postulating the Anhua- Luocheng Fault of the Central and Southern Jiangnan domains (e.g., Chen and Jahn, 1998; Jia et al., 2004; Ding et al., 2008) whereas others have suggested the Chenzhou- Linwu Fault, which is used herein as the boundary (Fig. 1; Wang et al., 2010).

The Cathaysia basement was considered to consist largely of Paleoproterozoic high-grade metamorphic schist, gneiss, quartzite, marble, amphibolite and migmatite based on data from the Wuyi, Nanling and Yunkai domains, which are regionally named as the Badou (SW Zhejiang), Mayuan (North Fujian), Chencai (NW Zhejiang) and Yunkai (West Guangdong and East Guangxi) groups in Chinese literature (Fig. 2a, b; e.g., Zhao and Cawood, 1999, 2012; Yu et al., 2009, 2010; Li 1997; Li et al., 2010a; Liu et al., 2010; Li et al., 2010c; Wang et al., 2012b, c). Recent geochronological data have shown that the Neoproterozoic and even Paleozoic units are additionally presented within the previously-mapped basement succession (e.g., Li et al., 1998; Wang et al., 2007c, 2010b, 2011b, 2012c; Wan et al., 2007, 2010; Yu et al., 2009, 2010; Yu et al., 2010; Li et al., 2010a; Li et al., 2010c; Li et al., 2011). Within the Cathaysia basement, there are small amounts of mafic and ultramafic rocks (e.g., amphibolite, metagabbro, metadiabase, metabasite, peridotite and pyroxenite), which occur mainly as lens, pods and fragments (e.g., Fujian BGMR, 1985; Guangdong BGMR, 1988; Zhejiang BGMR, 1989; Zhang et al., 2012a). These rocks have previously been considered to either part of the Paleoproterozoic (~1.8 Ga) Cathaysia basement (e.g., Shui, 1988; Zhou and Zhu, 1993; Li et al., 1998, 1999) or the Neoproterozoic (even early Mesozoic) ophiolitic mélange (e.g., Li, 1993; Guangdong BGMR, 1988; Peng et al., 1999, 2006; Qin et al., 2007).

Accepted Manuscript

ACCEPTED MANUSCRIPT

In this paper, we focus on the plagioclase amphibolites, amphibolite, metagabbro and metadiabase that are collected from the Wuyi and Yunkai domains and ultramafic rocks from Shitun to the western side of the Zhenghe-Dapu fault (Figs. 2a-b). The amphibolite and plagioclase amphibolites show blastoaplitic and blastoporphyritic textures but with the primary igneous texture often destroyed by later deformation and metamorphism (Figs. 3a-b). The amphibolite consists of 60-80% chloritized hornblende, 20-30 % plagioclase, quartz and pyroxene (Fig. 3a). The mineral assemblage of plagioclase amphibolite mainly includes pleochroic amphibole (~40-60 %) + plagioclase (20-45 %) + quartz (~3 %) ± pyroxene (~5 %) and small amounts of sericite, clinozoisite, chlorite and magnetite (Figs. 3b-c). Amphibole is present as secondary overgrowths and large elongate crystals in a fine-grained groundmass of plagioclase and opaque oxide minerals. The metagabbro samples from Huangtian (Wuyi) and Liuwan (Yunkai) preserve a primary igneous texture with major mineral association of pyroxene (~20 %) + amphibole (~30-35 %) + plagioclase (~20-30 %) (Fig. 3d). Metadiabase samples were collected from the Shitun mafic-ultramafic complex and show typical diabasic texture (Fig. 3e) and the coeval ultramafic rocks are now serpentinites (Fig. 3f).

3 Zircon U-Pb geochronology

Six mafic samples (09WG-66A, 09WG-53A, 09WG-58D and 09WG-74C from the Wuyi and 09YK-3e and YK-9A from the Yunkai, see Figs. 2a-b for the sampling locations) were selected for zircon U-Pb dating, trace elements and in-situ Lu-Hf isotopic measurement. Zircons grains are mostly transparent, light-brown or colorless subhedral grains or crystal fragments, and are ~50-120 μm in length with length to width ratios of 1:1 to 3:1.

U-Pb isotopic measurements were undertaken on a Cameca IMS 1280 SIMS at

Accepted Manuscript

ACCEPTED MANUSCRIPT

the Institute of Geology and Geophysics (IGG), Chinese Academy Sciences (CAS), the SHRIMP II at the Curtin SHRIMP Center, and an LA-ICPMS at the at the Guangzhou Institute of Geochemistry (GIG), CAS and IGG, CAS. Zircon trace elements and in-situ Lu-Hf isotopic analysis was carried out using MC-ICPMS with a Geolas-193 laser-ablation microprobe at the GIG (CAS), IGG (CAS) and the University of the Hong Kong. The analytical methods are described in detail in Supplementary Data File 1 and the analytical results for SHRIMP, SIMS and LA-ICPMS zircons U-Pb dating, trace elements and Lu-Hf isotopic compositions are listed in Supplementary Data Tables 1-5.

09WG-66A is an amphibolite from Chatian (Longquan) in SW Zhejiang Province. Eleven grains for SHRIMP zircon U-Pb dating show weakly oscillatory zoning (Fig. 4a) and have relatively wide Th/U ratios of 0.20-0.79 (Fig. 4a). They form a coherent cluster and give a weighted $^{206}Pb/^{238}U$ mean age of 969 ± 13 Ma with MSWD = 4 (Fig. 5a), and interpreted to represent the crystallization age of the sample. Six grains have Th/U ratio of < 0.20 and yield the weighted mean age of 422 ± 8 Ma (MSWD = 6), which is considered the time of the metamorphism for the sample. The remaining 13 grains yield older $^{207}Pb/^{206}Pb$ apparent ages of 1377-2807 Ma, herein interpreted as the ages of xenocrysts. Other grains were measured by the LA-ICPMS method at the University of Hong Kong and GIG, CAS and the results are shown in Fig. 5b. Fourteen of 40 grains, which are generally round in morphology and mostly oscillatory zoned, yield the $^{207}Pb/^{206}Pb$ ages of 1252-2718 Ma with variable εHf(t) values (Fig. 5h). The remaining 26 grains form a well-defined discordia with an upper intercept age of 993 ± 59 Ma and lower intercept at 410 ± 87 Ma, with eighteen spots yielding a weighted mean age of 984 ± 6 Ma (MSWD = 1) with εHf(t) values of +6.3 to +15.3 and Hf model age of 0.92-1.42 Ga (Figs. 5b and 5h). In CL images, the 18

ACCEPTED MANUSCRIPT

grains with the U-Pb ages of ~984 Ma mostly show wide and parallel oscillatory structure in CL image, a feature typical of basic zircons (Fig. 4a), and display subparallel REE patterns with significant depletion in LREE, enrichment in HREE, positive Ce and negative Eu anomalies (Fig. 6a), distinct from those of the xenocrysts. Thus, the age of 984 Ma determined by LA-ICPMS is identical, within error, to the SHRIMP age, and is herein interpreted as the formation age of the sample.

09WG-53A is metadiabase taken from Shitun (Zhenghe in Fujian) in the Wuyi Domain. It, together with the lensoid metagabbro and ultramafic rocks, has been previously proposed as members of early Paleozoic or early Mesozoic "Zhenghe ophiolitic mélange" (Guo et al., 1989; Xiao and He, 2005). The grains are mostly subhedral or crystal fragments and CL images reveal a weakly oscillatory internal zonation with low to variable luminescence (Fig. 4b). SIMS dating result show that seven spots have Th/U ratios of 0.12-0.92 and yield the weighted mean age of 978 ± 11 Ma with MSWD = 2.8 (Fig. 5c). The remaining eight spots give $^{207}Pb/^{206}Pb$ apparent ages ranging from 1114 Ma to 2593 Ma, and are interpreted as xenocrystic grains. An additional seventeen grains from the sample were measured by the LA-ICPMS method and show subparallel and left-sloped REE patterns with positive Ce and negative Eu anomalies (Fig. 6b). Five of these grains yield a weighted mean age of 970 ± 10 Ma with MSWD = 1, εHf(t) values of +4.5 to +10.2 and Hf model ages of 1.11-1.33 Ga (Figs. 5d and 5h). The remaining grains give the $^{207}Pb/^{206}Pb$ apparent ages of 1117-3517 Ma (Fig. 5d) with the variable εHf(t) values and Hf model ages of 1.69-3.22 Ga.

09YK-3e plagioclase amphibolite in the Yunkai Group from Tantu (Xinyi in west Guangdong) was selected for LA-ICPMS zircon U-Pb dating at GIG, CAS. Eighteen analyses on 18 zircon grains gave a relatively wide range of Th/U ratios of 0.16-1.67 and the apparent $^{207}Pb/^{206}Pb$ apparent ages of 946-2694 Ma. Seven euhedral grains with

ACCEPTED MANUSCRIPT

wide parallel and oscillatory zonation exhibit subparallel REE pattern (Figs. 4c and 6c) and positive εHf(t) values (+5.5 to +14.7) and Neoproterozoic Hf modal age (0.94-1.38 Ga, Fig. 5h). They form a coherent age-cluster and give the weighted mean age of 980 ± 8 Ma with MSWD = 0.4 (Fig. 5e), similar to that reported by Zhang et al. (2012). The remaining grains have round to subhedral crystal morphology and complex CL image (Fig. 4c), yielding old $^{206}Pb/^{206}Pb$ apparent ages of 1103-2694 Ma. These grains have distinct REE patterns from the euhedral grains and are interpreted as xenocrysts.

YK-9A is an plagioclase amphibolite from Jintong (Xinyi) in the Yunkai domain that occurs as lens in the Silurian granitoid gneiss. Zircons from this sample commonly display a poor zonation with a few grains also showing a thin rim structure. The U-Pb dating results for this sample are reported by Wang et al. (2012c) and give a weighted mean age of 221 ± 4 Ma (MSWD = 3.9) with Th/U ratios of 0.02-0.04, interpreted as the age of metamorphism of the sample. The T_{DM} model ages of Hf isotopic composition range from 0.94 Ga to 1.18 Ga (Supplementary Dataset 3). Analytical spot YK-09A-2 has the highest εHf(t) value of +14.0 and youngest Hf model age of 0.94 Ga when assuming t = 980 Ma. Spot YK-9A-20 gives an apparent age of 1384 ± 30 Ma with the model age of 2.07 Ga, and is herein considered to be an analysis of a xenocrystic zircon.

09WG-58D amphibolite was collected from Huangtian (Qinyuan) in southwest Zhejiang (Wuyi domain). Seventeen analyses yield a weighted mean age of 421 ± 6 Ma (MSWD = 0.5) with Th/U = 0.43-0.86 (Fig. 5f). All these zircons exhibit a poor zonation, lacking a core (Fig. 4d), and are interpreted as the age of metamorphism of the sample. Their Hf model ages range from 1.40 Ga to 1.06 Ga.

09WG-74C is a garnet-bearing plagioclase amphibolite from Shanlintou village (Songyang) that originally intruded into Paleoproterozoic granitic gneiss. Eighteen

ACCEPTED MANUSCRIPT

grains with CL images of typical metamorphic zircons (Fig. 4e) show similar and left-sloped REE patterns with insignificant Ce and Eu anomalies (Fig. 6d). They give the Th/U ratios of 0.03-0.26 and yield a $^{206}Pb/^{238}U$ weighted mean age of 242 ± 2 Ma (Fig. 5g, MSWD = 0.6, n = 18), similar to the results (243 ± 3 Ma and 246 ± 3 Ma) reported by Wang et al. (2012c). The Hf model ages for the analyzed zircons are in range of 1.02-1.35 Ga.

4 *Geochemical characteristics and petrogenesis*

Representative samples were selected for whole-rock elemental and Nd-Os isotopic analyses. Major oxides, trace element contents and Nd-Os isotopic ratios were measured at the GIG, CAS and details of the analytical methods are given in Supplementary Data File 1. Analytical results for the samples are listed in Tables 1 and 2, which also includes data for additional samples published in Li et al. (1999a, b), Qin et al. (2005, 2007) and Zhang et al. (2012a).

The analyzed samples have experienced greenschist- to amphibolite-facies metamorphism and almost all have LOI of less than 2 wt %. Discussion of petrogenesis focuses on the high field strength elements, which are considered least susceptible to metamorphism and alteration (e.g., Nb, Ta, Zr, Hf, REE, Th, Ti, Y, V and Sc) rather than those that are considered to be more mobile (e.g. Rb, Sr, K; Kerrich and Fryer, 1979; LaFleche et al., 1992; Arndt, 1994). The samples have SiO_2 = 44.0-52.2 wt % (volatile-free), MgO = 3.90-12.4 wt %, Al_2O_3 = 11.8-18.6 wt %, FeOt = 8.98-18.0 wt %, TiO_2 = 0.82-3.47 wt % and P_2O_5 = 0.05-0.39 wt % (Table 1, Figs. 7a and 8a-f). They show mg-numbers ranging from 33 to 72, Ni from 38 ppm to 376 ppm, and Cr from 15 ppm to 865 ppm (Table 1 and Figs. 8g-h). In the Zr/TiO_2 vs SiO_2 and Nb/Y diagrams (Figs. 7a-b), the samples plot in the field of the subalkaline basalt. Four distinct geochemical groups, here referred to as groups 1-4, can be classified on

Accepted Manuscript

ACCEPTED MANUSCRIPT

the basis on their Nb contents, chondrite-normalized REE and primitive mantle-normalized multi-element patterns (Figs. 7-10). These groups are geochemically similar to MORB, back-arc basin basalt, Nb-enriched basalt and arc volcanic rocks, respectively.

4.1 Group 1: N-MORB-like source modified by an arc component

Group 1 samples are from the Mala-Jintong (Xinyi), Liuwan-Licun (Rongxian) and Shiwo (Beiliu) regions in the Yunkai domain and from Zhulu (Longquan) in the Wuyi domain (see Figs. 2a-b for sampling location). They have SiO_2 contents ranging from 47.0 wt % to 50.8 wt % and MgO from 6.01 wt % to 12.2 wt % with mg-numbers of 46-72 (Table 1 and Fig. 8). Their Cr and Ni contents are in range of 107-865 ppm and 61-376 ppm, respectively. Group 1 has Nb contents of 1.24-5.33 ppm and exhibits more depleted LREE relative to HREE with (La/Yb)cn (cn noting chondrite-normalized) =0.56-1.03 and (Gd/Yb)cn=0.79-1.15, showing a chondrite-normalized pattern similar, but with higher overall REE contents, to average N-MORB and New Caledonia fore-arc basin basalt (Fig. 9a). The highly incompatible elements (e.g., Th, Nb, Ta, La and Ce) are more depleted relative to moderately incompatible elements (e.g., Zr, Sm, Yb and Y), with (Nb/La)n (n noting primitive mantle-normalized) = 0.51-0.86, (Th/La)n = 0.55-1.02 and (Hf/Sm)n = 0.82-1.19. The majority of the Group 1 samples show similar multi-elemental patterns to average N-MORB and New Caledonia fore-arc basin basalt (Fig. 10a) with the exception of weakly negative P and Ti anomalies, but several samples display the patterns similar to average Lesser Caucasus back-arc basin basalt due to relatively high (Th/Nb) ratios of 1.42-2.64 (e.g., Pearce et al., 1995; Shinjo et al., 1999; Cluzel et al., 2001; Rolland et al., 2009; Hässig et al., 2012). The measured Nd isotopic ratios of the samples range from 0.512856 to 0.512954, and the corresponding ε_{Nd} (t = 980 Ma) values from

ACCEPTED MANUSCRIPT

+4.3 to +5.2 (Table 1; Li et al., 1999a, b).

Cr and Ni contents decrease and SiO_2 increases markedly with decreasing MgO, (Figs. 8d and g-h), suggesting fractional crystallization of clinopyroxene and olivine from the similar parental magma of Group 1. Poor correlations between SiO_2 and CaO, Al_2O_3, TiO_2 and P_2O_5 (Figs. 8a-f), the minimal Eu anomaly and weak P-Ti depletions (Figs. 9a and 10a) suggest only a limited role of plagioclase, Ti-Fe oxides and apatite fractionation in magma differentiation. The relatively constant Nb/La ratios and $\varepsilon_{Nd}(t)$ values irrespective of MgO argue for insignificant crustal assimilation (Figs. 12a-b). The samples with low MgO (6.01-8.94 wt %) show higher TiO_2 content than those with high MgO (10.8-12.2 wt %), also arguing against significant shallow-level crustal assimilation. This is further supported by the depletion in LREEs and LILEs relative to HREEs and HFSEs for Group 1.

Group 1 samples show Nb/La of 0.51-0.97 (< 1), Hf/Ta of 7.5-18.2 (> 5) and Ce/Nb = 2.5-5.4 (> 2.0). The TiO_2 contents range from 0.82 wt % to 1.66 wt %, Nb from 1.24 ppm to 5.33 ppm (< 7.0 ppm) and Ta from 0.10 to 0.24 ppm (< 0.7 ppm). Such characteristics, together with LREEs/HREEs commonly less than 1.0, more depleted highly incompatible elements relative to moderately incompatible elements, and the highly positive $\varepsilon_{Nd}(t)$ values, argue for an affinity to an N-MORB source (cf., Figs. 13a-b). However, (1) Group 1 has generally higher incompatible element abundances and Th/Yb and Th/Zr ratios but lower Nb/Th ratios than those of average N-MORB (Fig. 14a-d); (2) It is characterized by negative P and Ti anomalies, distinct from those of average N-MORB; (3) Some samples show similar Th/Yb, La/Yb, Sm/Nd, Ti/V and Th/Nb ratios and incompatible elemental patterns similar to those of New Caledonia fore-arc basin and Lesser Caucasus back-arc basin basalts (Figs. 9a and 10a), and plot in the fields of island-arc tholeiite or back-arc basin basalt (Figs. 13a-d

Accepted Manuscript

ACCEPTED MANUSCRIPT

and 14b-c); (4) Group 1 samples have low Nb/La and plot in the field of the arc-volcanic rocks or the region between N-MORB and arc-volcanic rocks (Figure 14a). The combined Nd/Pb and Nb/Y ratios with isotope compositions can be used to effectively evaluate the nature of subduction components since Nd, Nb and Y are fluid-immobile and dominated by sediment- and slab-derived melt, whereas Pb contribution is mainly controlled by fluid composition (Elliott et al., 1997; Class et al., 2002; Petrone and Ferrari, 2008; Castillo et al., 2002, 2007; Wang et al., 2013). In Figures 15a-b, Group 1 samples fall in the range of the source with proportional addition of recycled sediment-derived melts plus slab-fluid, indicating the involvement of an arc-like component related to the fluid metasomatism in the magma source. In the plot of Cr and Ni (Fig. 15d), Group 1 samples have higher Ni contents than the supposed range of mantle-derived melt, and plot in the field of high-mg andesite or along the mixing line between slab-derived component and primitive mantle, further suggesting an addition of arc-like component in the source. Collectively, Group 1 was likely derived from an N-MORB-like source modified by input of an arc-like component, probably in a fore- or back-arc basin.

4.2 Group 2: E-MORB-like source modified by subducted component

Group 2 contains twelve samples from the Zhaimen-Jintong (Xinyi) and Guiyi (Cenxi) areas in the Yunkai domain and Huangtian (Qinyuan) in the Wuyi domain. Their MgO contents are in the range 5.73-8.60 wt % with mg-numbers of 48-62. Nb=3.13-6.48 ppm, TiO_2 = 0.93-1.60 wt %, Cr = 74-280 ppm and Ni = 53-127 ppm. Group 2 samples have weak enrichment in LREEs relative to HREEs. (La/Yb)cn ratios range from 1.22 to 2.61, (Gd/Yb)cn from 1.15 to 1.51 and δEu from 0.78 to 1.05, similar to those of average E-MORB (Fig. 9b). Their multi-elemental patterns resemble those of average E-MORB, and are also similar to those of the Okinawa Trough with

Accepted Manuscript

ACCEPTED MANUSCRIPT

the exception of insignificant Nb-Ta anomalies (Fig. 10b; e.g., Pearce et al., 1995; Shinjo et al., 1999; Fan et al., 2010). The measured ($^{143}Nd/^{144}Nd$) ratios range from 0.512747 to 0.512880 and initial ε_{Nd}(t=980 Ma) values from +3.1 to +4.2. The representative samples have low Re (8.9-9.4 ppt) and Os concentrations (4.6-52.9 ppt) and the age-corrected Os isotopic ratio are 0.2453-1.66 with high γOs (t Ma) values (Table 2). In the plot of Os and $^{187}Re/^{188}Os$, they fall into the field of arc lava (Fig. 11a).

In comparison with E-MORB, the Group 2 samples are more depleted in Nb and Ta with the (Nb/La)n of 0.53-0.97. They show higher Th/Yb, Zr/Nb, Th/Ta, Tb/Ta, Th/Zr and La/Nb and lower Nb/Th relative to an average N-MORB source (Figs. 14a-d), suggesting the involvement of an arc-like component into the source. This is also supported by correlations between Nb vs Nb/U (Fig. 7d). Arc-like geochemical signatures are usually explained by the involvement of either an ancient lithospheric source or a newly metasomatised source. However, the positive εNd(t) values ranging from +3.1 to +4.2 for Group 2 indicate that the mantle source should be depleted. Thus, the first-order interpretation is that the Group 2 samples shared an E-MORB-like source with an addition of a new subduction-related component (e.g., Pearce and Peate, 1995; Shinjo et al., 1999). The following observations suggest that the addition should be characterized by subduction-related metasomatism: (1) Group 2 has (Ta/La)n ratios of 0.57-0.99 and (Hf/Sm)n of 0.94-1.28 and the majority defines the trend related to fluid-related metasomatism (e.g., LaFlèche et al., 1998); (2) their Nd/Pb ratios are lower and Nb/Y ratios are higher relative to those of depleted mantle, and the Nb/Zr ratios are mildly variable relative to Th/Zr (e.g., Figs. 15a-c; Kepezhinskas et al., 1997); (3) higher Ni contents are shown at the comparable Cr content for the inferred range of primitive mantle-derived melt (Fig. 15d). These signatures, together with similar Re-Os

ACCEPTED MANUSCRIPT

isotopic compositions to arc lava, suggest recent subduction metasomatism for Group 2. Samples from Group 2 show (La/Yb)n of 1.22-2.61, Sm/Nd of 0.28-0.35, and Ti/V of 20-50, and plot in the field of the back-arc basin basalt (BABB) in Figs.3a-d and 14c-d (e.g., Pouclet et al., 1995; Shuto et al., 2006; Sandeman et al., 2006). Thus, Group 2 might originate from a metasomatised E-MORB-like source in the back-arc environment.

4.3 Group 3: Nb-enriched basalt from a newly metasomatised wedge

Group 3 samples, including 43 plagioclase amphibolites/amphibolite and metagabbros, are taken from Qinshuikou-Shiwo (Beiliu) in the Yunkai domain and Zhulu and Zhuhuang (Longquan), Zhuyuan-Shanlintuo (Songyang), Huangtian and Chatian (Qinyuan) in the Wuyi domain (see Fig. 2a-b for sampling locations). These samples have SiO_2 = 44.0-50.8 wt % and TiO_2 = 1.03-3.47 wt %. In comparison with those of Groups 1 and 2, they show higher FeOt, TiO_2 and P_2O_5 but lower Al_2O_3, Cr and Ni (Fig. 8a-h). Group 3 has higher Nb contents (7.18-29.87 ppm) than intra-oceanic arcs basalts (generally < 2.0 ppm; e.g., Martin et al., 2005). Nb/La ratios are in range of 0.60-2.59 (with the majority from 0.70 to 1.40) and Nb/U ratios of 5.0-37.4, distinct from those of arc-volcanic rocks (Figs. 7c-d and 14a). According to the original definition of Defant et al. (1991) and Sajona et al. (1994, 1996), thirty-nine of the 43 samples can be classified as Nb-enriched basalt (Nb = 7-18 ppm) and the remaining 4 samples as high Nb basalt (Nb > 20 ppm) (Figs. 7c-d). Group 3 has higher REE, Th, Nb, Y, Zr and Hf contents than those of Groups 1 and 2 and average E-MORB, and show steeply right-sloping REE-normalized patterns with (La/Yb)cn = 1.24-3.68 and (Gd/Yb)cn = 1.03-1.69 with δEu of 0.78-1.08 (Fig. 9c). In Figure 10c, the samples display subparallel patterns similar to those of the Pickle and earliest Neoproterozoic Yunkai Nb-enriched basalts with the exception of Rb and Ba (e.g., Hollings, 2002;

ACCEPTED MANUSCRIPT

Zhang et al., 2012c). Their $\varepsilon_{Nd}(t)$ values range from +2.9 to +7.0 when assuming t = 980 Ma. The Re and Os contents for five representative samples range from 13.2 ppt to 74.5 ppt and 11.1 ppt to 46.2 ppt, respectively. The γOs (t Ma) values are in the range of 178~772 with $^{187}Re/^{188}Os$ of 5.87-8.87 and plot into the field of arc lava, similar to that of Group 2 (Fig. 11a).

Group 3 has MgO contents ranging from 3.90 wt % to 10.51 wt % with an mg-number of 33-60. SiO_2 correlates negatively to MgO, CaO and CaO/Al_2O_3 (Figs. 8a-d), suggestive of fractional crystallization of clinopyroxene and olivine from the parental magma (e.g., Russell and Nicholls, 1988). Plagioclase fractionation probably played an insignificant role in magma differentiation, as indicated by the relatively constant δEu values irrespective of MgO. However, simple fractionation cannot account for the geochemical characteristics of Group 3 involving variable Nb/La ratios and $\varepsilon_{Nd}(t)$ values, as shown in Figures 12a-d. Three petrogenetic models can be proposed for the Nb-enriched basalt involving (1) an OIB-like plume, (2) shallow-level crustal assimilation en route, and (3) a mantle wedge metasomatised by a young subduction-derived component (e.g., Storey et al., 1989; Leeman et al., 1990, 2005; Richards et al., 1990; Sajona et al. 1994, 1996; Kepezhinskas et al. 1996; Wyman et al., 2000; Polat and Kerrich, 2001; Stern, 2002; Bourdon et al., 2002; Castillo et al., 2002, 2007; Petrone et al., 2003; Smithies et al., 2005; Castillo, 2008; Petrone and Ferrari, 2008).

Group 3 samples have similar HREEs contents but lower LILEs, LREEs and HFSEs abundances relative to those of average OIB. Their Zr/Nb ratios range from 4.3 to 19.9, similar to those of the typical arc magma (e.g., Pearce et al., 1995). The Nb/U ratios range from 5 to 37 and Ce/Pb ratios from 1.1 to 6.6, lower than those of OIB (47 and 25, respectively; Figs. 7c-d). The majority of the Group 3 samples shows significant P-Ti and Nb anomalies with variable (Nb/La)n ratios (0.6-1.4), distinct from

ACCEPTED MANUSCRIPT

those derived from an OIB-like source. They have lower TiO_2, Ti/V and higher Tb/Ta and Th/Yb in comparison with average OIB (Figs. 13c-d and 14c). Our geochemical data are also in contrast to that expected for carbonatite contamination of a plume-related source, which would share highly fractionated Zr/Hf ratios (up to 100) and extremely high LREE contents (>> 100 ppm) (e.g., Woodhead, et al., 1993; Hastie et al., 2011). Most importantly, there is no geological observation supporting the development of an earliest Neoproterozoic plume in the eastern SCB (e.g., Li et al., 1995, 2002; Yu et al., 2009; Shu et al., 2011).

Geochemical and isotopic correlations suggest generation for Group 3 magma involved crustal assimilation en route to emplacement or source contamination by mixing. In shallow-level crustal assimilation, the potential assimilation component should be characterized by high La/Sm but relatively low Nb/La, $\varepsilon_{Nd}(t)$ and MgO, as shown in Figures 12b-d. However, the samples with low $\varepsilon_{Nd}(t)$ values are probably characterized by high MgO (low SiO_2) content when crystal fractionation is considered (Fig. 12a). To match the observed variation of Nb/La ratios (0.57-2.13) and $\varepsilon_{Nd}(t)$ values (+2.9-+7.0) for Group 3, variable (~30-70 %) assimilation of crustal materials into MORB-derived magma is required. Such proportional assimilation can not be reconciled with the major oxide composition and LILE- and REE-patterns of the Group 3 samples (Figs. 9c and 10c). The samples with low $\varepsilon_{Nd}(t)$ values (e.g. 09WG-66A9) show lower γOs (t) values and those with lower MgO have higher TiO_2 contents. These signatures, together with the high Nb, P_2O_5 and TiO_2 contents, argue against crustal assimilation en route. In fact, petrogenesis of the Nb-enriched basalts is generally considered to be unrelated to the shallow-level crustal assimilation (Wyman et al., 2000; Stern, 2002; Castillo et al., 2002, 2007; Smithies et al., 2005; Castillo, 2008). As a result, the correlation in Figures 12b-d most likely indicates a two end-members mixing

ACCEPTED MANUSCRIPT

source for the Group 3 magma, with one of end-members being characterized by depleted La/Sm (<1.5) and Gd/Yb (<1.3) but high in Nb/La (>2.0) and $\varepsilon_{Nd}(t)$ (>7.0) and the other having relatively high La/Sm (>3.0) and Gd/Yb (>2.0) but low Nb/La (<0.5) and $\varepsilon_{Nd}(t)$ (<3.0). Available data show that the Nb-enriched basalts (e.g., circum-Pacific and Superior Province) generally display geochemical affinities to an E-MORB source and mainly developed in convergent margin settings (e.g., Saunders et al., 1987; Crawford et al., 1989; Storey et al., 1989; Stern, 2002; Castillo et al., 2002, 2007; Petrone and Ferrari, 2008). In the circum-Pacific (e.g., Mindanao and Zamboanga), the Nb-enriched basalts are spatially and temporally associated with adakites, high-mg andesites and arc volcanic rocks (e.g., Defant et al., 1991; Maury et al., 1996; Yogodzinski et al., 2001; Viruete et al. 2007). Our samples show higher Nb/Y, Nb/Zr, Ta/Yb and Th/Ta and lower Nd/Pb ratios relative to MORB, suggestive of the involvement of an arc-related components (melt plus fluid flux) into the MORB-like source (Figs. 14a and 15a-d). This is further supported by the Re-Os isotopic plot in Figure 11a.

In general, the arc-like elemental geochemical signatures can be explained as originating from either an ancient or recent metasomatic event without consideration of the shallow-level crustal contamination. An ancient metasomatic event should result in the higher Th/Ce (> 0.1) and lower εNd(t) values than the newly subduction-related metasomatism (e.g., Hawkesworth et al., 1997; Hollings and Kerrich, 2004). The Group 3 samples have Th/Ce ratios of 0.01-0.09 and highly positive εNd(t) values of +2.9 to +7.0. Their Th/Zr ratios display a narrow variation irrespective of Nb/Zr ratios (Fig. 15c). Such signatures, together with the trends in Figures 15a-c, favor involvement of a recent "crustal" component (characterized by enrichment in Nb, Ta, Ti_2O and Na_2O). Thus, the two end-members should be represented by E-MORB and newly subducted

Accepted Manuscript

ACCEPTED MANUSCRIPT

component, respectively. The Group 3 samples show high (La/Yb)cn (1.53-5.90) and low Sm/Nd ratios (0.23-0.31), comparable to those of the BABB with continental basement (e.g., Gribble et al., 1998; Shinjo et al., 1999; Sandeman et al., 2006), which is also evidenced by the discrimination results in Figure 13a-d and 14c-d. As a result, Group 3 might originate from an enriched MORB source (with high Ti, Zr, V and Y and low Zr/Nb) metasomatised by the juvenile subducted-derived component in the back-arc setting.

4.4 Group 4 showing the geochemical affinity to arc volcanics

In the Shitun area in the Wuyi domain, there is a mafic-ultramafic complex that has previously been described as an "ophiolitic mélange" (e.g., Xiao and He, 2005). The ultramafic rocks in the complex, characterized by serpentinite, have SiO_2 of 37.25-38.77 wt. %, FeOt of 5.83-7.79 wt.% and MgO of ~39 wt. % (Table 1) with low Al_2O_3, CaO and Na_2O contents (Table 1). Four serpentinite samples show a wide variation of Os ranging from 51.2 ppt to 3275 ppt with $^{187}Os/^{188}Os$ of 0.1143-0.1442 (Table 2). Their γOs values range from -7.8 to +0.1. In $^{187}Re/^{188}Os$ vs $^{187}Os/^{188}Os$ and Os vs γOs diagrams (Figs. 11b-c), these serpentinites plot in the fields of residual peridotite and of lithospheric mantle, respectively, suggesting that the serpentinites can be interpreted as part of an ophiolite suite. The Group 4 rocks include two metadiabases (coeval with the serpentinite) from the Shitun mafic-ultramafic complex and four plagioclase amphibolites from Dajin and Liuwan (Rongxian) in the Yunkai domain. They are characterized by SiO_2 of 44.51-52.16 wt %, MgO of 6.90-12.36 wt % with mg-number of 52-69, Ni of 45-124 ppm and Cr of 113-314 ppm. MgO and Al_2O_3 display negative correlation, and CaO a positive correlation, with SiO_2 (Fig. 8a-f). The low SiO_2 samples have MgO content of more than 10 wt %, indicative of the source being characterized by low CaO (< 7.0 wt. %) and Al_2O_3 (> 17.0 wt. %). These

ACCEPTED MANUSCRIPT

characteristics suggest a refractory source, with a high-proportion of orthopyroxene, which had previously experienced melt extraction (e.g., Hirose, 1997; Falloon et al. 1988; Wang et al., 2007c).

In comparison with other groups, Group 4 samples have stronger LREEs/HREEs and HREE fractionation with (La/Yb)cn = 1.6-5.6 and (Gd/Yb)cn = 1.3-2.3 (Fig. 9d). They are characterized by "spiky" trace element patterns, with strong enrichment in LILEs and pronounced depletion in HFSEs (e.g., significant Nb–Ta, P and to lesser extent Ti). These samples have TiO_2 contents of 0.42-1.51 wt %, Nb content of 2.5-3.6 ppm, Ti/V ratios of ~25, (Th/Nb) ratios of 1.74-6.97 and (Nb/La)n ratios of 0.15 -0.41, comparable with those of the arc volcanic rocks (e.g., Gribble et al., 1998; Martin et al., 2005; Sandeman et al., 2006). Their ε_{Nd} (t = 980 Ma) values range from +2.3 to +5.6, suggestive of derivation from a depleted mantle source. In Figures 13a-b and 14a-d, Group 4 plots in the fields of island-arc tholeiite and island-arc calc-alkaline basalt. Their (Ta/La)n (0.24-0.53) and (Hf/Sm)n (0.77-1.02) values are similar with those of source regions affected by fluid metasomatism (e.g., LaFlèche et al., 1998). The variations in Figures 15a-b, together with the low Nb/Th, Nb/Y and Nb/Zr, and high Ba/Nb and La/Nb for Group 4, favor subduction component being mainly controlled by fluid (e.g., Class et al., 2002; Castillo et al., 2007). The synthesis of these geochemical characteristics suggests derivation of Group 4 from a refractory wedge source plus subducted-derived fluid flux (e.g., Woodhead et al., 1993; Hollings and Kerrich, 2000, 2004).

5 Tectonic implications

5.1 Age of the mafic igneous rocks

Zircons from representative samples of Groups 3 and 4, which show geochemical affinity to Nb-enriched basalts and arc volcanic rocks, respectively, yield weighted

ACCEPTED MANUSCRIPT

mean ages of 969 ± 13 Ma (SHRIMP for 09WG-66A), 984 ± 6 Ma (LA-ICPMS for 09WG-66A), 978 ± 11 Ma (SIMS for 09WG-53A), 970 ± 10 Ma (LA-ICPMS for 09WG-53A) and 980 ± 8 Ma (LA-ICPMS for 09YK-3e). These ages are similar to those of two metabasites from the northern Yunkai domain (Zhang et al., 2012a), which yielded the U-Pb zircon ages of 997 ± 21 Ma and 978 ± 19 Ma. The earliest Neoproterozoic zircons from these samples have εHf(t) values of +4.5 to +15.3, Hf model ages of 0.92-1.42 Ga (Fig. 5h) and similar left-sloping REE patterns with positive Ce and negative Eu anomalies (Fig. 6a-c), suggestive of a mafic igneous origin. Li et al. (1993) gave a Sm-Nd isochron age of 971 ± 69 Ma for plagioclase amphibolite in the Yunkai "Group". Nan (1994) reported the zircon U-Pb ages of ~1035-900 Ma and ~940-910 Ma for amphibolite and dacite-porphyry in the Yunkai "Group", respectively. Qin et al. (2006) and Zhang et al. (1997) also considered the plagioclase amphibolite and dacite-porphyry in the Yunkai "Group" most likely formed at ~1000-910 Ma (Lao and Hu, 1997).

Our plagioclase amphibolite, amphibolite and metadiabase occur as either lenses in middle Paleozoic (~460-420 Ma) and Neoproterozoic (~860-790 Ma) granitoid gneiss, or intrusions in Paleoproterozoic gneiss (e.g., Wang et al., 2011b, Shu et al., 2011). They have experienced middle Paleozoic and early Mesozoic high-grade metamorphism, as evidenced by metamorphic zircon ages for four plagioclase amphibolites and amphibolites (421 ± 13 Ma, 422 ± 13 Ma, 243 ± 3 Ma and 221 ± 4 Ma for 09WG- 58D, 09WG-66A, 09WG-74C and YK-9A, respectively). In addition, the reported Precambrian mafic rocks only developed during the Paleoproterozoic (~1800 Ma) and Neoproterozoic (~860-790 Ma) period in the Cathaysia Block and show the OIB-like geochemical affinities, reflective of intraplate rifting setting (e.g., Li XH et al., 1998; Li et al., 2005, 2010b; Shu et al., 2008, 2011; Li LM et al., 2010). Such

ACCEPTED MANUSCRIPT

characteristics are distinct from our mafic samples. These data place a lower limit on the formation ages of our samples as younger than ~1800 Ma and older than ~860 Ma. Taking into account the analyzed metamorphic grains for Group 1 having Hf model ages of 0.94-1.18 Ga (YK-09A), similar to those of 09WG-58D (1.06-1.40 Ga) and 09WG-74C (1.02-1.35 Ga), the ages of 984 Ma to 969 Ma for the mafic rocks can be considered to represent the formation timing of our samples. Thus our data verify the presence of the earliest Neoproterozoic (~985-970 Ma) mafic magmatism along the Wuyi and Yunkai domains of the Cathaysia Block.

5.2 Earliest Neoproterozoic arc-back-arc system along the Wuyi-Yunkai and its closure

The petrogenesis of the analyzed samples, including the modification of MORB-like sources by a subduction-derived component, suggests an overall earliest Neoproterozoic supra-subduction zone (arc-back arc) setting rather than an ocean spreading setting (cf., Hawkins, 1995; Hollings and Kerrich, 2004) in the Cathaysia Block. The presence of xenocrystic zircons in the representative samples of Groups 3 and 4 suggests the involvement of continental basement prior to their eruption/intrusion. In addition, previous data suggest that the Neoproterozoic metavolcanic rocks probably occur in the Yunkai and western Nanling domain (e.g., Kengping, Xinqiao and Shiqiao; Li et al., 1993; Nan, 1994; Shao et al., 1995; Han et al., 1998; Zhang et al., 1998; Guo et al., 2005). At Jingnan (NE Guangdong) and Hezi (South Jiangxi) of the Nanling domain, rhyolite and granodiorite with arc geochemical signatures gave the SHRIMP zircon U-Pb age of 972 ± 8 Ma and the Pb-Pb age of 996 ± 29 Ma, respectively (Fig. 16; Liu et al., 2001; Shu et al., 2008, 2011). Wang et al. (2013) reported the Silurian (434-420 Ma) gabbroic intrusions along the Yunkai and Nanling domains have the similar elemental signatures with our earliest Neoproterozoic samples and interpreted

Accepted Manuscript

ACCEPTED MANUSCRIPT

this as reflective of the presence of a paleosubduction-modified wedge column. The combined geochemical and geochronological data most likely suggest the development of the earliest Neoproterozoic wedge in an along-strike intracontinental arc-back-arc system along the Wuyi, Nanling and Yunkai domains that separated Western and Eastern Cathaysia (Fig. 16).

A younger age limit on closure of the Wuyi-Yunkai arc-back-arc system is constrained by the development of the OIB-type mafic rocks and Mamianshan bimodal volcanic rocks at the Wuyi dated at ~860-790 Ma, which were formed in a continental rift or within-plate setting (e.g., Li et al., 2005, 2010b; Shu et al., 2006, 2008, 2011). This suggests that the transformation to within-plate rifting from the arc-back-arc system occurred between ~980 Ma and 860 Ma along the Wuyi-Yunkai domain. The strongly peraluminous Tiantangshan and Longtang (Yunkai) and Masha (Wuyi) granites were dated at 906 ± 24 Ma (SHRIMP), 901 ± 16 Ma (LA-ICPMS) and 913 ± 11 Ma (SIMS) (e.g., Qin et al., 2006; authors' unpublished data), probably representing the time of crustal anatexis during the closure of the Wuyi-Yunkai intracontinental arc-back-arc basin. Detrital zircons with U-Pb ages of ~1.0-0.90 Ga (peak age being ~970 Ma) likely related to the development of the arc-back arc system are abundant in the Neoproterozoic sedimentary rocks along the Wuyi (e.g., Jianning), Nanling (e.g., Zengcheng) and Yunkai (e.g., Xinyi) domains (e.g., Yu et al, 2007, 2010; Wan et al., 2007, 2010; Wang et al., 2007c, 2008b, c 2010b; Li et al., 2011). Earliest Neoproterozoic (~1000-900 Ma) inherited grains are commonly identified in the Kwangsian granitic gneiss and Neoproterozoic gneiss with some showing positive εHf(t) values (inset of Fig. 5h, Wang et al., 2011). Thus, the Wuyi, Nanling and Yunkai arc-back-arc system was likely active since ~980 Ma to the termination of subduction at ~900 Ma. The Zhenghe-Dapu Fault (Wuyi) and its strike extension

Accepted Manuscript

ACCEPTED MANUSCRIPT

along the Gaoyao-Huilai Fault (Nanling and Yunkai) might represent the convergent boundary between Eastern and Western Cathaysia (Fig. 16).

5.3 Neoproterozoic northwesterly episodic amalgamation along the eastern SCB

Regional relations indicate that the Wuyi-Yunkai arc-back-arc system was one of a series of arc systems associated with amalgamation of the SCB that developed within the Cathaysia and Yangtze blocks during early Neoproterozoic period. The aforementioned data require development of an arc-back-arc system along the Wuyi, Nanling and Yunkai domains during earliest Neoproterozoic (~980 Ma) and its closure at ~900 Ma. Along the Shuangxiwu domain adjacent to the Jiangshan-Shaoxing Fault system (Figs. 1-2 and 16), plagiogranite and gabbro in the Zhangshudun ophiolitic suite are dated at 970-910 Ma and the ophiolite is interpreted as forming within a back-arc or intraoceanic arc setting (e.g., Li et al., 1994, 1997, 2002, 2003, 2008b; Li and Li, 2003; Gao et al., 2009; Chen et al., 2009a, b). Amphibolite-bearing tonalite and granodiorite within the domain show the geochemical signatures of arc volcanic rocks and give the SHRIMP zircon U-P ages of 915 ± 15 Ma and 905 ± 14 Ma, respectively (Ye et al., 2007). Xiwan leucogranites and Zhangcun rhyolite in the Zhangshudun ophiolitic suite, interpreted by Li et al.(2005, 2010b) as product of final closure of the Shuangxiwu arc system, yield zircon U-Pb ages of 880 ± 19 Ma and 891 ± 19 Ma, respectively (e.g., Li et al., 2005, 2010b). Thus the termination of the Shuangxiwu arc system is at around 880-890 Ma, slightly younger than that (~900 Ma) of Wuyi-Yunkai arc-back-arc system.

Along the easternmost Jiangnan domain of the Yangtze Block (Figs. 1 and 16), the Fuchuan gabbro and Zhangyuan pillow basalt exhibit geochemical affinities similar to the Mariana back-arc basin basalts with the gabbro yielding a zircon U-Pb age of 826-848 Ma (Ding et al., 2008; Zhang et al., 2010, 2011b). Along the central and

ACCEPTED MANUSCRIPT

southern parts of the domain, the Lengjiaxi Group and its equivalents, which are characterized by abyssal flysch- and turbidite-facies successions, are inferred to have accumulated in a back-arc basin between ~860 Ma and ~830 Ma (e.g., Zhang et al., 2012c, d; Zhao and Cawood, 2012 and references therein). They are uncomfortably overlain by basal conglomerates deposited at ~820 Ma and the subsequent middle to late Neoproterozoic Banxi Group and its equivalents which accumulated in a failed rift environment (e.g., Wang and Li, 2003; Zhang et al., 2011c, 2012c-d). The Cangshuipu volcanic rocks beneath the regional angular unconformity, which are interpreted as the product of a post-collisional setting, are dated at 824 ± 7 Ma and 822 ± 28 Ma (e.g., Zhang et al., 2011c, 2012c). The crystallization ages of the igneous rocks along the Jiangnan domain are commonly younger than 850 Ma with a cluster of ~850-820 Ma (Fig. 16; e.g., Li, 1999; Li et al., 2003; Wu et al., 2006; Wang XL et al., 2007b, 2008a, , 2011a; Zheng et al., 2007, 2008; Zhou et al., 2009; Ma et al., 2009; Xue et al., 2010; Dong et al., 2010; Wang LJ et al., 2010a; Zhao et al., 2011; Zhang YZ et al., 2012d, 2013). These data suggest the back-arc basin along the Jiangnan domain developed from ~850 and its cessation of subduction and final closure at ~830-820 Ma by the Jinningian Orogen (Fig. 16; e.g., Zhao et al., 2011; Zhang et al., 2011c, 2012c-d, 2013; Zhao and Cawood, 2012 and references therein). In combination with other data, it is inferred that the early Neoproterozoic SCB is characterized by a succession of blocks (e.g., eastern Yangtze, eastern and western Cathaysia) separated by magmatic arcs and back-arc basins (e.g., Wuyi-Yunkai, Shuangxiwu and Jiangnan). Episodic closure of the arc-back arc basins, including Wuyi-Yunkai (~900 Ma), Shuangxiwu (~880 Ma) and then Jiangnan (~820 Ma), resulted in progressive northwesterly amalgamation to create the SCB (inset (a) in Fig. 16).

An overall northwestward propagation of orogenic assembly of units is supported

ACCEPTED MANUSCRIPT

by the age-spectra of detrital zircons for the Neoproterozoic sedimentary rocks and their derivation from the southeast (inset (b) of Fig. 16, e.g., Wang et al., 2008a, 2010; Yu et al., 2010 Zhang et al., 2012a). The Neoproterozoic successions along the Wuyi-Yunkai domain (c.f, Xinyi, Zengcheng, Jingnan and Jianning) contain abundant earliest Neoproterozoic (~1.0 Ga) detrital zircons (inset (b) of Fig. 16), proportionally higher relative to those in the Western Cathaysia and Eastern Yangtze. The majority of the grains are euhedral in shape, distinct from those in the Western Cathaysia and Eastern Yangtze, which are mostly characterized by equigranular and rounded or subhedral, indicating detritus transported from the orogen to south or southeast (e.g., Wan et al., 2007, 2010; Yu et al., 2007, 2008, 2010; Wang et al., 2008a; Wang et al., 2010b; Li et al., 2011). Further to the west, along the Jiangnan domain, ~1.0 Ga detrital zircons are poorly identified and the age-spectra are characterized by ~0.86 Ga grains (inset (b) of Fig. 16, e.g., Wang et al., 2007b, Zhou et al., 2009; Zhao et al., 2011; Wang et al., 2012a;).

5.4 An exterior accretionary orogen for the SCB along the margin of Rodinia

The SCB has been argued to lie within or external to the Rodinia supercontinent in the latest Mesoproterozoic to earliest Neoproterozoic (e.g., Li et al., 1995, 2002; Zhao and Cawood, 1999; Yang et al., 2004; Yu et al., 2008; Zhao et al., 2011). In the model proposed by Li and others (1995, 2002), the proposed Sibao orogen is considered to range in age from 1.3 Ga to 1.0 Ga and constitutes a collisional orogen equivalent to the Grenville Orogen and is associated with Rodinia assembly. The orogen runs across the Jiangnan domain of the eastern SCB (inset in Fig. 1). However, our data show a northwesterly episodic amalgamation from ~900 Ma continuingly to ~820 Ma for the eastern SCB, significantly younger than the Grenvillian (~1.0-1.3 Ga) Orogen throughout Laurentia, Australia, east Antarctica and Africa (e.g., Boger et al.,

ACCEPTED MANUSCRIPT

2000; Jayananda et al., 2000). It is impossible for such a long-lived Neoproterozoic (~980-830) arc-back-arc system to develop within the Rodinia supercontinent, and thus it must have occupied a peripheral position. The final amalgamation along the Wuyi-Yunkai domain is roughly synchronous with the deformation of the East Ghats of India (~960 Ma) and the northern Prince Charles Mountains of East Antarctica (~990-960 Ma; e.g., Boger et al., 2000; Jayananda et al., 2000). These relationships, combined with the biogeographic consistency of the eastern SCB with Australia and the late Neoproterozoic tectonic relationship with India (e.g., Wang and Li, 2003; Yang et al., 2004; Myrow et al, 2006, 2009; Wang et al., 2010b), suggest to us that the SCB was situated along the margin of Rodinia between Australia and East Antarctica (e.g., Hoffman, 1991; Zhang et al., 1997; Yang et al., 2004), as shown in Fig. 17.

Synthesis of our geochemical and geochronological data as well as ~1000-750 Ma tectonic assembly along the western and northern margins of the Yangtze block (Zhao and Cawood, 2012 and references therein) suggests the preliminary tectonic model for the early Neoproterozoic evolution of the eastern SCB (Fig. 18). At ~0.98-0.90 Ga (Fig. 18a), Eastern Cathaysia of the eastern SCB received orogenic detritus from the latest Mesoproterozoic mountain belt that lay in the Prince Charles mountains region of Antarctica (e.g., Myrow et al., 2006, 2009; Boger et al., 2000; Jayananda et al., 2000). At the same time, the Wuyi-Yunkai arc-back-arc system was developed and the Shuangxiwu system continued until ~880 Ma. At ~880-900 Ma, the Eastern Cathaysia accreted onto Western Cathaysia and the arc-back-arc systems along the Wuyi-Yunkai and Shuangxiwu domains are in turn closed. At ~880-830 Ma (Fig. 18b), the back-arc basin was developed along the Jiangnan domain and the intraplate magmatism in the merged Cathaysia Block to the east of the Jiangshan-Shaoxing fault. At ~830-800 Ma (Fig. 18c), the amalgamation of the already assembled Cathaysia took place with the

ACCEPTED MANUSCRIPT

Yangtze along the Jiangnan domain and resulted into the closure of the Jiangnan arc-back-arc basin, which finally created the united SCB along the Jinningian orogen. The process of northwesterly episodic amalgamation for the eastern SCB constitute part of an exterior accretionary orogen situating between Western Australia and East Antarctica around the periphery of Rodinia (e.g., Cawood et al., 2007, 2010, in press).

Acknowledgements

This research was jointly funded by the NSFC project (40825009 and 40830319), "Closure of Eastern Paleotethys Ocean and assembly of South China continents" (41190073) of Major NSFC Program (41190070) "Reconstruction of East Asian blocks in Pangea" and the State Key Laboratory of Continental Dynamics, Northwest University (BJ081331). PAC acknowledges support from the University of St Andrews and NERC (NE/J021822/1). We thank Dr. L-Y Ma, F-F Zhang, Y-F Cai and H-C Liu for their help during help and geochemical analyses. We would like to thank Prof. G-C Zhao and two anonymous reviewers for their critical and constructive reviews on this paper. This is a contribution to Guangzhou Institute of Geochemistry, the Chinese Academy of Sciences.

References

Alves, S., Schiano, P., Capmas, F., Allergre, C.J., 2002. Osmium isotope binary mixing arrays in arc volcanism. Earth and Planetary Science Letters 198, 355-369

Arndt, N.T., 1994. Archean komatiites. In: Condie K.C. (Ed.), Archean Crustal Evolution. Elsevier, Amsterdam, 11–44.

Boger, S.D., Carson, C.J., Wilson, C.J.L., Fanning, C.M., 2000. Neoproterozoic deformation in the Radok Lake region of the northern Prince Charles Mountains, east Antarctica: evidence for a single protracted orogenic event. Precambrian Research 104, 1-24.

Bourdon, E., Eissen, J.P., Monzier, M., Robin, C., Martin, H., Cotton, J., Hall, M.L., 2002. Adakite-like lavas from Antisana volcano (Ecuador): evidence for slab-melt metasomatism beneath the Andean Northern volcanic zone. Journal of Petrology 43, 199-217.

Castillo, P.R., 2008. Origin of the adakite-high-Nb basalt association and its implications for post-subduction magmatism in Baja California, Mexico. Geological Society of American

Accepted Manuscript

ACCEPTED MANUSCRIPT

Bulletin 120, 451-462.

Castillo, P.R., Rigby, S.J., Solidum, R.U., 2007. Origin of high field strength element enrichment in volcanic arcs: geochemical evidence from the southern Sulu Arc, southern Philippines. Lithos 97, 271-288.

Castillo, P.R., Rigby, S.J., Solidum, R.U., 2007. Origin of high field strength element enrichment in volcanic arcs: geochemical evidence from the southern Sulu Arc, southern Philippines. Lithos 97, 271-288.

Castillo, P.R., Solidum, R.U., Punogbayan, R.S., 2002. Origin of high field strength element enrichment in the Sulu Arc, southern Philippines, revisited. Geology 30, 707-710.

Castillo, P.R., Solidum, R.U., Punogbayan, R.S., 2002. Origin of high field strength element enrichment in the Sulu Arc, southern Philippines, revisited. Geology 30, 707-710.

Cawood, P.A., Nemchin, A.A., Strachan, R.A., Prave, A.R., and Krabbendam, M., 2007, Sedimentary basin and detrital zircon record along East Laurentia and Baltica during assembly and breakup of Rodinia. : Geological Society of London Journal 164, 257–275.

Cawood, P.A., Strachan, R., Cutt, K., Kinny, P.D., Hand, M., Pisarevsky, S., 2010. Neoproterozoic orogeny along the margin of Rodinia: Valhalla orogen, North Atlantic. Geology 38(2), 99–102.

Cawood, P.A., Wang, Y.J., Xu, Y.J., Zhao, G.C., in press. Locating South China in Rodinia and Gondwana: a fragment of Greater Indian Lithosphere? Geology.

Chalot-Prat, F., Boullier, A., 1997. Metasomatism in the subcontinental mantle beneath the Eastern Carpathians (Romania): new evidence from trace element geochemistry. Contributions to Mineralogy and Petrology 129, 284-307.

Charvet, J., Shu, L.S., Shi, Y.S., Guo, L.Z., Faure. M., 1996. The building of South China: collision of Yangtze and Cathaysia blocks, problems and tentative answers. Journal of Southeast Asian Earth Science 13, 223-235.

Chen Z.H., Xing G.F., Guo K.Y., Dong Y.G., Chen R., Zeng Y., Li L.M., He Z.Y., Zhao L., 2009a. Petrogenesis of the Pingshui keratophyre from Zhejiang: Zircon U-Pb age and Hf isotope constrains. Chinese Science Bulletin 54, 610-617(in Chinese).

Chen, W.S., Yang, H.C., Wang, X., Huang, H., 2002. Tectonic setting and exhumation history of the Pingtan-Dongshan metamorphic belt along the coastal area, Fujian Province, southeast China. Journal of Asian Earth Sciences 20, 829-840.

Chen, Z.H., Guo, K.Y., Dong, Y.G., Chen, R., Li, LM., Liang, Y.M., Li, C.H., Yu, X.M., Zhao, L., Xing, G.F., 2009b. Possible early Neoproterozoic magmatism associated with slab window in the Pingshui segment of the Jiangshan-Shaoxing suture zone: Evidence from zircon LA-ICP-MS U-Pb geochronology and geochemistry. Science in China (Series D) 52(7), 925- 939.

Class, C., Miller, D. M., Goldstein, S. L., Langmuir, C.H., 2000. Distinguishing melt and fluid subduction components in Umnak Volcanics, Aleutian Arc, Geochem. Geophys. Geosyst., 1, 1004, doi:10.1029/1999GC000010.

Condie, K.C., 1997. Sources of Proterozoic mafic dykes swarms: constraints form Th/Ta and La/Yb

Accepted Manuscript

ACCEPTED MANUSCRIPT

ratios. Precambrian Research 81, 3-14.

Crawford, A.J., Falloon, T.J., Green, D.H., 1989. Classification, petrogenesis and tectonic setting of boninites. In: Crawford, A.J. (eEd.), Boninites and Related Rocks. Unwin Hyman, New York, pp.1-49.

Defant, M.J., Richerson, P.M., de Boer, J.Z., Stewart, R.H., Maury, R.C., Bellon,H., Jackson, T.E., Restrepo, J.F., 1991. Andesite and dacite genesis via contrasting processes: the geology and geochemistry of E1 Valle volcano, Panama. Contributions to Mineralogy and Petrology 106, 309-324.

Ding, B.H., Shi, R.D., Zhi, X.C., Zheng, L., Chen, L., 2008. Neoproterozoic (~850 Ma) subduction in the Jiangnan orogen: evidence from the SHRIMP U-Pb dating of the SSZ-type ophiolite in southern Anhui Province. Acta Petrologica et Mineralogica 27(5), 375-388 (in Chinese with English abstract).

Dong, S.W., Xue, H.M., Xiang, X.K., Ma, L.C., 2010. The discovery of Neoproterozoic pillow lava in spilite-Keratophyre of Lushan area, northern Jiangxi Province, and its geological significance. Geology in China 37(4), 1021-1033 (in Chinese with English abstract).

Elliott, T., T. Plank, A. Zindler, W. White, and B. Bourdon (1997), Element transport from slab to volcanic front at the Mariana Arc, Journal of Geophysical Research 102 (14), 991–15,019.

Falloon, T.J., Green, D.H., Hatton, C.J., Harris, K.L., 1988. Anhydrous partial melting of a fertile and depleted peridotite from 2 to 30 kbar and applications to basalt petrogenesis. Journal of Petrology 29, 1257–1282.

Fan, W.M., Wang, Y.J., Zhang, A.M., Zhang, F.F., Zhang, Y.Z., 2010. Permian arc–back-arc basin development along the Ailaoshan tectonic zone: Geochemical, isotopic and geochronological evidence from the Mojiang volcanic rocks, Southwest China. Lithos 119, 553–568.

Fujian BGMR (Bureau of Geology and Mineral Resources of Fujian Province), 1985. Regional Geology of the Fujian Province. Geological Publishing House, Beijing (in Chinese with English abstract).

Gao, J., Klemd, R., Long, L.L., Xiong, X.M., Qian, Q., 2009. Adakitic signature formed by fractional ophiolitic mélange belt, South China. Lithos 110, 277-293.

Gribble, R.F., Stern, R.J., Newman, S., Bloomer, S.H., O'Hearn, T., 1998. Chemical and isotopic composition of lavas from the Northern Mariana Trough: implications for magma genesis in back-arc-arc basins. Journal of Petrology 39, 125-154.

Guangdong, BGMR (Bureau of Geology and Mineral Resources of Guangdong Province), 1988. Regional Geology of the Guangdong Province. Geological Publishing House, Beijing, 1-941 (in Chinese with English abstract).

Guangxi, BGMR (Bureau of Geology and Mineral Resources of Guangxi Province), 1985. Regional Geology of the Guangxi Zhuang Autonomous Region. Geological Publishing House, Beijing, 1-853 (in Chinese with English abstract).

Guo, L.T., Hong, Y.R., Huang, J.C., Chen, Y.H., Huang, Y.H., Xu, H.S., 2005. Discovery of the

Accepted Manuscript

ACCEPTED MANUSCRIPT

Kengping spilite-keratophyre series in Xinyi, western Guangdong, China and its geological significance. Geological Bulletin of China 24(7), 648-654 (in Chinese with English abstract).

Guo, L.Z., Shi, Y.S., Lu, H.F., Ma, R.S., Dong, H.G., Yang, S.F., 1989. The pre-Devonian tectonic patterns and evolution of South China. Journal of Southeast Asian Earth Sciences 3, 87-93.

Han, Z.R., Pang, Z.R., Xie, D.Q., 1998. The establishment of the Neoproterozoic Tantou Group in central Jiangxi. Regional Geology of China 17(2), 113-117(in Chinese with English abstract).

Hässig, M., Rolland, Y., Sosson, M., Galoyan, G., M¨uller, C., Avagyan, A., Sahakyan, L., 2012. New structural and petrological data on the Amasia ophiolites (NWSevan-Akera suture zone, Lesser Caucasus): Insights for a large-scale obduction in Armenia and NE Turkey, Tectonophysics doi: 10.1016/j.tecto.2012.12.003

Hastie, W.W., Watkeys, M.K., Aubourg C., 2011. Significance of magnetic and petrofabric in Karoo-feeder dykes, northern Lebombo. Tectonophysics 513(1-4), 96-111.

Hawkesworth, C.J., McDermott, F., Peate, D.W., van Calsterern, P., 1997. U–Th isotopes in arc magmas: implications for elemental transfer from the subducted crust. Science 276, 551–555.

Hawkins, J.W., 1995. The geology of the Lau Basin. In Taylor, B. (ed), Back-arc Basins: Tectonics and Magmatism. Plenum Press, New York, 63-138.

Hirose, K., 1997. Melting experiments on lherzolite KLB-1 under hydrous conditions and generation of high-mg andesitic melts. Geology 25, 42–44.

Hoffman, P.F., 1991. Did the breakout of Laurentia turn Gondwanaland inside out? Science 252, 1409-1412.

Hollings, P., Kerrich, R., 2000. An Archean arc basalt-Nb-enriched basalt-adakite association; the 2.7 Ga confederation assemblage of the Birch–Uchi greenstone belt, Superior Province. Contributions to Mineralogy and Petrology 139 (2), 208–226.

Hollings, P., Kerrich, R., 2004. Geochemical systematics of tholeiites from the 2.86 Ga Pickle Crow Assemblage, northwestern Ontario: arc basalts with positive and negative Nb–Hf anomalies. Precambrian Research 134, 1–20.

Hu, G.R., Liu, C.Q., 2002. Geochemistry of amphibolites from the Zhoutan group, Jiangxi Province: implications for the tectonic settings. Acta Mineralogica Sinica 22(4), 336-342.

Jayananda, M., Moyen, J.F., Martin, H., Peucat, J.J., Auvray, B., Mahabaleswar, B., 2000. Late Archaean (2550-2520Ma) juvenile magmatism in the Eastern Dharwar craton, southern India: constraints from geochronology, Nd-Sr isotopes and whole rock geochemistry. Precambrian Research 99, 225-254.

Jia, B.H., Peng, H.Q., Tang, X.S., He, J.N., Guo, L.Q., 2004. Discovery of the Wenjiashi ophiolitic mélange belt in northeastern Hunan and its implications. Geoscience 2, 229-235.

Kepezhinaskas, P.K., Defant, M.J., Drummond, M.S., 1996. Progressive enrichment of island-arc mantle by melt-peridotite interaction from Kamchatka adakites. Geochimica et Cosmochimica Acta 60, 1217-1229.

Kepezhinskas, P., McDermott, F., Defant, M.J., Hochstaedter, A., Drummond, M.S., 1997. Trace

Accepted Manuscript

ACCEPTED MANUSCRIPT

element and Sr-Nd-Pb isotopic constraints on a three-component model of Kamchatka Arc petrogenesis. Geochimica et Cosmochimica Acta 61(3), 577-600.

Kerrich, R., Fryer, B.J., 1979. Archaean precious-metal hydrothermal systems, Dome Mine, Abitibi greenstone belt; II, REE and oxygen isotope relations. Canadian Journal of Earth Sciences 16 (3 Part 1), 440–458

LaFlèche, M.R., Camire, G., Jenner, G.A., 1998. Geochemistry of post-Acadian, Carboniferous continental intraplate basalts from the Maritimes Basin, Magdalen Islands, Québec, Canada. Chemical Geology 148, 115-136.

LaFleche, M.R., Dupuy, C., Dostal, J., 1992. Tholeiitic volcanic rocks of the Late Archean Blake River Group, southern Abitibi greenstone belt: origin and geodynamic implications. Canadian Journal of Earth Sciences 29, 1448–1458.

Lao, Q.Y., Hu, S.L., 1997. The $^{40}Ar/^{39}Ar$ age date of silicalite of Yunkai Group and their Geological significance. Acta Geoscientia Sinica.18, 98-101.

Leeman, W.P., Lewis, J.F., Evarts, R.C., Conrey, R.M., Streck, M.J., 2005. Petrologic constraints on the thermal structure of the Cascades arc. Journal of Volcanology and Geothermal Research 140, 67-105.

Leeman, W.P., Smith, D.R., Hildreth, W., Palacz, Z., Rogers, N., 1990. Compositional diversity of late Cenozoic basalts in a transect across the southern Washington Cascades: implications for subduction zone magmatism. Journal of Geophysical Research 95, 19561-19582.

Li, J.L., 1993. Texture of lithosphere and geological evolution of southeastern China. Beijing: Metallurgic Industry Press, 1- 217 (in Chinese with English abstract).

Li, L.M., Sun, M., Wang, Y.J., Xing, G.F., Zhao G.C., He, Y.H., He, K.J., Zhang, A.M.,2011. U-Pb and Hf isotopic study of detrital zircons from the meta-sedimentary rocks in central Jiangxi Province, South China: Implications for the Neoproterozoic tectonic evolution of South China Block. Journal of Asian Earth Sciences 41, 44-55.

Li, L.M., Sun, M., Wang, Y.J., Xing, G.F., Zhao, G.C., Lin, S.F., Xia, X.P., Chan, L.S., Zhang, F.F., Wong, J., 2010a. U–Pb and Hf isotopic study of zircons from migmatised amphibolites in the Cathaysia Block: implications for the early Paleozoic peak tectonothermal event in Southeastern China. Gondwana Research doi:10.1016/j.gr.2010. 03.009.

Li, W.X., Li, X.H., 2003. Adakitic granites within the NE Jiangxi ophiolite, South China: geochemical and Nd isotopic evidence. Precambrian Research 122, 29-44.

Li, W.X., Li, X.H., Li, Z.X., 2005. Neoproterozoic bimodal magmatism in the Cathaysia Block of South China and its tectonic significance. Precambrian Research 136, 51–66.

Li, W.X., Li, X.H., Li, Z.X., 2010b. Ca. 850 Ma bimodal volcanic rocks in northeastern Jiangxi South China: initial extension during the breakup of Rodinia. American Journal of Science 310, 951–980.

Li, W.X., Li, X.H., Li, Z.X., Lou, F.S., 2008a. Obduction-type granites within the NE Jiangxi Ophiolite: implications for the final amalgamation between the Yangtze and Cathaysia Blocks.

Accepted Manuscript

ACCEPTED MANUSCRIPT

Gondwana Research 13, 288–301.

Li, X.H., 1997. Timing of the Cathaysia Block formation: constraints from SHRIMP U-Pb zircon geochronology. Episodes 20, 188-192.

Li, X.H., 1999. U–Pb zircon ages of granites from the southern margin of the Yangtze Block: timing of the Neoproterozoic Jinning Orogeny in SE China and implications for Rodinia Assembly. Precambrian Research 43–57.

Li, X.H., Lee, C.Y., Liu, Y., Chen, D.F., Wang, Y.X., Zhao, Z.H., 1999a. Geochemistry characteristics of the Paleoproterozoic meta-volcanics in the Cathaysia block and its tectonic significance. Acta Petrologica Sinica 15(3) , 364-371

Li, X.H., Li, W.X., Li, Z.X., Liu, Y., 2008b. 850–790 Ma bimodal volcanic and intrusive rocks in northern Zhejiang, South China: A major episode of continental rift magmatism during the breakup of Rodinia. Lithos 102(1-2), 341-357.

Li, X.H., Li, W.X., Li, Z.X., Lo, C.H., Wang, J., Ye, M.F., Yang, Y.H., 2009. Amalgamation between the Yangtze and Cathaysia Blocks in South China: Constraints from SHRIMP U–Pb zircon ages, geochemistry and Nd–Hf isotopes of the Shuangxiwu volcanic rocks. Precambrian Research 174(1-2), 117-128.

Li, X.H., Li, Z.X., Ge, W.C., Zhou, H.W., Li, W.X., Liu, Y., Wingate, M.T.D., 2003. Neoproterozoic granitoids in South China: crustal melting above a mantle plume at ca. 825Ma? Precambrian Research 122, 45–83.

Li, X.H., Li, Z.X., Sinclair, J.A., Li, W.X., Carter, G., 2006. Revisiting the “Yanbian Terrane”: implications for Neoproterozoic tectonic evolution of the western Yangtze Block, South China. Precambrian Research 151, 14–30.

Li, X.H., Wang, Y.X., Zhao, Z.H., Chen, D.F., 1998. SHRIMP-U-Pb zircon geochronology for amphibolite from the Precambrian basement in SW Zhejiang and NW Fujian Provinces. Geochimica 27(4), 327-334.

Li, X.H., Wei, G.J., Liu, Y., Chen, D.F., Wang, Y.X., Zhao, Z.H., 1999b. Neodymium isotopic evidence for extremely depleted mantle in Paleoproterozoic in Cathaysia Block. Earth Science 24(2), 197-201

Li, X.H., Zhou, G.Q., Zhao, J.X., Fanning, C.M., Compston, W., 1994. SHRIMP ion microprobe zircon U-Pb age and Sm-Nd isotopic characteristics of the NE Jiangxi ophiolite and its tectonic implications. Geochimica 13, 317-325.

Li, Z.X., Bogdanova, S.V., Collins, A.S., Davidson, A., DeWaele, B., Ernst, R.E., Fitzsimons, I. C.W., Fuck, R.A., Gladkochub, D.P., Jacobs, J., Karlstrom, K.E., Lu, S., Natapov, L.M., Pease, V., Pisarevsky, S.A., Thrane, K., Vernikovsky, V., 2008c. Assembly, configuration, and breakup history of Rodinia: A synthesis. Precambrian Research 160, 179–210.

Li, Z.X., Li, X.H., Kinny, P.D., Wang, J., 1999c. The breakup of Rodinia: did it start with a mantle plume beneath South China? Earth and Planetary Science Letters 173, 171–181.

Li, Z.X., Li, X.H., Wartho, J.A., Clark, C., Li, W.X., Zhang, C.L., Bao, C.M., 2010c. Magmatic and metamorphic events during the Early Paleozoic Wuyi-Yunkai Orogeny, southeastern South China: New age constraints and P-T conditions. GSA Bulletin 122 (5-6), 772-793.

Accepted Manuscript

ACCEPTED MANUSCRIPT

Li, Z.X., Li, X.H., Zhou, H., Kinny, P.D., 2002. Grenvillian continental collision in South China: new SHRIMP U–Pb zircon results and implications for the configuration of Rodinia. Geology 30, 163–166.

Li, Z.X., Zhang, L.H., Powell, C.M.A., 1995. South China in Rodinia: part of the missing link between Australia-East Antarctica and Laurentia? Geology 23 (5), 407–410.

Liang, X.R., Wei, G.J., Li, X.H., Liu, Y., 2003. Precise measurement of ^{143}Nd/^{144}Nd and Sm/Nd ratios using multiple-collectors inductively coupled plasma-mass spectrometer (MC-ICPMS). Geochimica 32, 91-96 (in Chinese with English abstract).

Liu, B.X., Liu, C.G., Qiu, Y.Q., 2001. The Pb-Pb isotopic ages and geologic significance of gneissic granite in Hezi, Jiangxi. Volcanological Mineral Research. 22(4), 264-268 (in Chinese with English abstract)

Liu, R., Zhou, H., Zhang, L., Zhong, Z., Zeng, W., Xiang, H., Jin,S., Lu, X., Li, C.Z., 2010. Zircon U-Pb ages and Hf isotope compositions of the Mayuan migmatite complex, NW Fujian Province, Southeast China: Constraints on the timing and nature of a regional tectonothermal event associated with the Caledonian orogeny. Lithos, 119(3-4), 163-180.

Ludwig, K.R., 2001. Using Isoplot/EX, version 2.49. In: A Geochronological toolkit for Microsoft Excel, Berkeley. Berkeley Geochronological Center Special Publication, 1-55.

Ma, T.Q., Chen, L.X., Bai, D.Y., Zhou, K.J., Li, G., Wang, X.H., 2009. Zircon SHRIMP dating and geochemical characteristics of Neoproterozoic granites of northeastern Hunan. Geology in China. 36(1), 65-73 (in Chinese with English abstract).

Martin, H., Smithies, R.H., Rapp, R., Moyen, J.F., Champion, D., 2005. An overview of adakite, tonalite-trondhjemite-granodiorite (TTG), and sanukitoid: relationships and some implications for crustal evolution. Lithos 79, 1-24.

Maury, R.C., Sajona, F.G., Pubellier, M., Bellon, H., Defant, M.J., 1996. Fusion de la croûte océanique dans les zones de subduction/ collision récentes; 1'exemple de Mindanao (Philippines). Bulletin de la Société Geologique de France 167, 579-595.

Myrow, P.M., Hughes, N.C., Searle, M.P., Fanning, C.M., Peng, S.C., Parcha, S.K., 2009. Stratigraphic correlation of Cambrian–Ordovician deposits along the Himalaya: implications for the age and nature of rocks in the Mt. Everest region, Geological Society of America Bulletin Geol. Soc. Am. Bull., 120, 323-332.

Myrow, P.M., Snell, K.E., Hughes, N.C., Paulsen, T.S., Heim, N.A., Parcha, S.K., 2006. Cambrian depositional history of the Zanskar Valley region of the Indian Himalaya: Tectonic implications., Journal of Sedimentary Research 76, 364–381, doi: 10.2110/jsr.2006.020.

Pearce, J.A., Baker, P.E., Harvey, P.K., Luff, I.W., 1995. Geochemical evidence for subduction fluxes, mantle melting and fractional crystallization beneath the South Sandwich Island arc. Journal of Petrology 36, 1073–1109.

Pearce, J.A., Peate, D.W., 1995. Tectonic implications of the composition of volcanic arc magmas. Annual Review of Earth and Planetary Sciences 23, 251–285.

Accepted Manuscript

ACCEPTED MANUSCRIPT

Peng, S.B., Jin, Z.M., Fu, J.M., He, L.Q., Cai, M.H., Liu, Y.H., 2006. The geochemical evidences and tectonic significance of Neoproterozoic ophiolite in Yunkai area, western Guangdong Province, China. Acta Geologica Sinica 80 (6), 814-825 (in Chinese with English abstract).

Peng, S.B., Zhan, M.G., Peng, S.M., Zhang, Y.M., Fu, J.M., 1999. The discovery of ophiolitic mélanges and its significance in Yunkai area, Western Guangdong. Geology and Mineral Resources of South China 1, 24-25 (in Chinese with English abstract).

Petrone, C.M., Ferrari, L., 2008. Quaternary adakite-Nb-enriched basalt association in the western Trans-Mexican Volcanic Belt: is there any slab melt evidence? Contributions to Mineralogy and Petrology 156, 73-86.

Petrone, C.M., Ferrari, L., 2008. Quaternary adakite-Nb-enriched basalt association in the western Trans-Mexican Volcanic Belt: is there any slab melt evidence? Contributions to Mineralogy and Petrology 156, 73-86.

Petrone, C.M., Francalanci, L., Carlson, R.W., Ferrari, L., Conticelli, S., 2003. Unusual coexistence of subduction-related and intraplate-type magmatism: Sr,Nd and Pb isotope and trace element date from the magmatism of the San Pedro-Ceboruco graben (Nayarit, Mexico). Chemical Geology 192, 1-24.

Polat, A., Kerrich, R., 2001. Magnesian andesites, Nb-enriched basalt-andesites, and adakite from late-Archean 2.7Ga Wawa greenstone belts, Superior Province. Canada: Implications for Late Archean subduction zone petrogenetic processes. Contributions to Mineralogy and Petrology 141, 36-52.

Pouclet, A., Lee, J., Vidal, P., Cousens, B., Bellon, H., 1995. Cretaceous to Cenozoic volcanism in South Korea and in the Sea of Japan: magmatic constraints on the opening of the back-arc basin. In: Smellie, J.L., (Ed.), Volcanism Associated with Extension at Consuming Plate Margins. Geological Society of London (Special Publication) 81, 169-191.

Qin, X.F., Pan, Y.M., Li, L., Li, R.S., Zhou, F.S., Hu, G.A., Zhong, F.Y., 2006. Zircon SHRIMP U-Pb geochronology of the Yunkai metamorphic complex in southeastern Guangxi, China. Geological Bulletin of China 25 (5), 553-559.

Qin, X.F., Pan, Y.M., Xia, B., Li, R.S., Zhou, F.S., Hu, G.A., Lu, G.B., 2007. Geochemical characteristics and tectonic significances of metabasic volcanic rocks in the northern margin of Yunkai Block, SE Guangxi. Geochimica 36(3), 311-322.

Qin, X.F., Zhou, F.S., Hu, G.A., Li, G.N., Xie, L.F., Zhou, K.H., Huang, X.Q., Pan, Y.W., 2005. First discovery of MORB volcanic rock and its tectonic significance on the north margin of the Yunkai Block, SE Guangxi. Geological Science and Technology Information 24(3), 20-24 (in Chinese with English abstract).

Richards, J.P., Chappell, B.W., McCulloch, M.T., 1990. Intraplate-type magmatism in a continent-island-arc collision zone: Porgera intrusive complex, Papua New Guinea. Geology 18, 958-961.

Rolland, Y., Galoyan, G., Bosch, D., Sosson, M., Corsini, M., Fornari, M., Verati, C., 2009. Jurassic

Accepted Manuscript

ACCEPTED MANUSCRIPT

back-arc and Cretaceous hot-spot series In the Armenian ophiolites: Implications for the obduction process. Lithos 112, 163–187.
Sajona, F.G., Bellon, H., Maury, R.C., Pubellier, M., Cotton, J., Rangin, C., 1994. Magmatic response to abrupt changes in tectonic setting: Pliocene-Quaternary calc-alkaline lavas and Nb-enriched basalts of Leyte and Mindanao (Philippines). Tectonophysics 237, 47-72.
Sajona, F.G., Maury, R.C., Bellon, H., Cotton, J., Defant, M.J., 1996. High field strength element enrichment of Pliocene-Pleistocene island arc basalts, Zamboanga Peninsula, Western Mindanao (Philippines). Journal of Petrology 37, 693-726.
Sandeman, H.A., Hanmer, S., Tella, S., Armitage, A.A., Davis, W.J., Ryand, J.J., 2006. Petrogenesis of Neoarchaean volcanic rocks of the MacQuoid supracrustal belt: A back-arc setting for the northwestern Hearne subdomain, western Churchill Province, Canada. Precambrian Research 144(1-2), 126-139.
Saunders, A.D., Rogers, G., Marriner, G.F., Terrell, D.J., Verma, S.P., 1987. Geochemistry of Cenezoic volcanic rocks, Baja California, Mexico: Implications for the petrogenesis of post-subduction magmas. Journal of Volcanology and Geothermal Research 32 (1-3), 223-245.
Shi, R.D., Zhi, X.C., Chen L., Ding, B.H., 2006. Comment on the progress on the applications of Re-Os isotopic study on the ophibolite. Acta Petrologica Sinica 22(6), 1685-1695.
Shinjo, R., Chung, S.L., Kato, Y., Kimura, M., 1999. Geochemical and Sr-Nd isotopic characteristics of volcanic rocks from the Okinwa Trough and Ryukyu Arc: implications for the evolution of a young, intracontinental back arc basin. Journal Geophysical Research 104 (B5), 10591-10608.
Shirey S. B., and Walker R. J., 1998. The Re–Os isotope system in cosmochemistry and high-temperature geochemistry. Annual Review Earth and Planetary Science 26, 423–500.
Shu, L.S., Deng, P., Yu, J.H., Wang, Y.B., Jiang, S.Y., 2008. The age and tectonic environment of the rhyolitic rocks on the western side of Wuyi Mountain, South China. Science in China (series D) 51(8), 1053-1063.
Shu, L.S., Faure, M., Yu, J.H., Jahn, B.M., 2011. Geochronological and geochemical features of the Cathaysia block (South China): New evidence for the Neoproterozoic breakup of Rodinia. Precambrian Research 187 (3-4), 263-276.
Shu, L.S., Faure. M., Jiang, S.Y., Yang, Q., Wang, Y.J., 2006. SHRIMP zircon U-Pb age, litho- and biostratigraphic analyses of the Huaiyu Domain in South China-evidence for a Neoproterozoic orogen, not Late Paleozoic-Early Mesozoic collision. Episodes 29, 244-252.
Shui T., 1988. Tectonic framework of the continental basement of southeast China. Science in China (Series B) 31, 885-896.
Shuto, K., Ishimoto, H., Hirahara, Y., Sato, M., Matsui, K., Fujibayashi, N., Takazawa, E., Yabuki, K., Sekine, M., Kato, M., Rezanov, A.I., 2006. Geochemical secular variation of magma source during Early to Middle Miocene time in the Niigata area, NE Japan: Asthenosphere mantle upwelling during back-arc basin opening. Lithos 86, 1-33.

ACCEPTED MANUSCRIPT

Smithies, R.H., Champion, D.C., Van Kranendonka, M.J., Howard, H.M., Hickman, A.H., 2005. Modern-style subduction processes in the Mesoarchaean: geochemical evidence from the 3.12 Ga Whundo intra-oceanic arc. Earth Planetary Science Letter 23, 221-237.

Stern, R.J., 2002. Subduction zones, Review of Geophyshics Geophysics 40 (4),1012.

Storey, M., Rogers,G., Saunders, A.D., and Terrell, D.J., 1989, San Quintín volcanic field, Baja California, Mexico: "within-plate" magmatism following ridge subduction. Terra Nova 1, 195-202.

Sun, S.S., McDonough, W.F., 1989. Chemical and isotopic systematics of oceanic basalts: implications for mantle composition and processes. In: Saunders, A.D., Norry, M.J. (eds.), Magmatism in the ocean basins. Geological Society of Special Publication 42, 313–345.

Taylor, S.R., McLennan, S.M., 1985. The continental crust: its composition and evolution. Oxford Press Blackwell, pp.1-312.

Torsvik, T.H., Carter, L.M., Ashwal, L.D., Bhushan, S.K., Pandit, M.K., Jamtveit, B., 2001. Rodinia refined or obscured: palaeomagnetism of the Malani igneous suite (NW India). Precambrian Research 108, 319–333.

Tsuchiya, T., Suzuki, S., Kimura, J.I., Kagami, H., 2005. Evidence for slab melt/mantle reaction: petrogenesis of early Cretaceous and Eocene high-Mg andesites from the Kitakami Mountains, Japan. Lithos 79, 179– 206.

Tsuchiya, T., Suzuki, S., Kimura, J.I., Kagami, H., 2005. Evidence for slab melt/mantle reaction: petrogenesis of early Cretaceous and Eocene high-mg andesites from the Kitakami Mountains, Japan. Lithos 79, 179-206

Viruete, J.E., Contreras, F., Stein, G., Urien, P., Joubert, M., Pérez-Estaun, A., Friedman, R., Ullrich, T., 2007. Magmatic relationships and ages between adakites, magnesian andesites and Nb-enriched basalt-andesites from Hispaniola: Record of a major change in the Caribbean island arc magma sources. Lithos 99, 151-177.

Wan, Y.S., Liu, D.Y., Wilde, S.A., Cao, J.J., Chen, B., Dong, C.Y., Song, B., Du, L.L., 2010. Evolution of the Yunkai Terrane, South China: evidence from SHRIMP zircon U-Pb dating, geochemistry and Nd isotope. Journal of Asian Earth Sciences 37, 140-153.

Wan, Y.S., Liu, D.Y., Xu, M.H., Zhang, J., Song, B., Shi, Y., Du, L., 2007. SHRIMP U-Pb zircon geochronology and geochemistry of metavolcanic and metasedimentary rocks in Northwestern Fujian, Cathaysia Block, China: tectonic implications and the need to redefine lithostratigraphic units. Gondwana Research 12, 166-183.

Wang, J., Li, Z.X., 2003. History of Neoproterozoic rift basins in South China: implications for Rodinia breakup. Precambrian Research 122, 141–158.

Wang, L.J., Griffin, W.L., Yu,J.H., O'Reilly, S.Y., 2010a. Precambrian crustal evolution of the Yangtze Block tracked by detrital zircons from Neoproterozoic sedimentary rocks. Precambrian Research 177(1-2), 131-144.

Wang, L.J., Yu,J.H., O'Reilly, S.Y., Griffin, W.L., Wei, Z.Y., Jiang, S.Y., Sun, T., 2008a. Grenvillian

Accepted Manuscript

ACCEPTED MANUSCRIPT

orogeny in the Southern Cathaysia block: constraints from U-Pb ages and Lu-Hf isotopes in zircon from metamorphic basement. Chinese Science Bulletin 53(19), 3037-3050.

Wang, W., Zhou, M. F., Yan, D. P., Li, J. W., 2012a. Depositional age, provenance, and tectonic setting of the Neoproterozoic Sibao Group, southeastern Yangtze Block, South China. Precambrian Research 192-195, 107-124.

Wang, X.C., Li, X.H., Li, W.X., Li, Z.X., 2007a. Ca. 825 Ma komatiitic basalts in South China: first evidence for >1500°C mantle melts by a Rodinia mantle plume. Geology 35, 1103–1106.

Wang, X.L., Shu, L.S., Xing, G.F., Zhou, J.C., Tang, M., Shu, X.J., Qi, L., Hu, Y.H., 2011a. Post-orogenic extension in the eastern part of the Jiangnan orogen: Evidence from ca 800–760 Ma volcanic rocks. Precambrian Research doi:10.1016/j.precamres. 2011.07. 003.

Wang, X.L., Zhao, G.C., Zhou, J.C., Liu, Y.S., Hu, J., 2008b. Geochronology and Hf isotopes of zircon from volcanic rocks of the Shuangqiaoshan Group, South China: implications for the Neoproterozoic tectonic evolution of the eastern Jiangnan orogen. Gondwana Research 14 (3), 355–367.

Wang, X.L., Zhou, J.C., Griffin, W.L., Wang, R.C., Qiu, J.S., O'Reilly, S.Y., Xu, X.S., Liu, X.M., Zhang, G.L., 2007b. Detrital zircon geochronology of Precambrian basement sequences in the Jiangnan orogen: dating the assembly of the Yangtze and Cathaysia bocks. Precambrian Research 159 (1–2), 117–131.

Wang, X.L., Zhou, J.C., Qiu, J.S., Jiang, S.Y., Shi, Y.R., 2008c. Geochronology and geochemistry of Neoproterozoic mafic rocks from western Hunan, South China: implications for petrogenesis and post-orogenic extension. Geology Magazine 145 (2), 215–233.

Wang, X.L., Zhou, J.C., Qiu, J.S., Zhang, W.L., Liu, X.M., Zhang, G.L., 2006. LA-ICP-MS U–Pb zircon geochronology of the Neoproterozoic igneous rocks from Northern Guangxi, South China: implications for petrogenesis and tectonic evolution. Precambrian Research 145 (1–2), 111–130.

Wang, Y.J, Fan W.M, Peter A Cawood, Li S.Z., 2008d. Sr–Nd–Pb isotopic constraints on multiple mantle domains for Mesozoic mafic rocks beneath the South China Block. Lithos 106, 297–308.

Wang, Y.J., Fan, W.M., Zhang, G.W., Zhang, Y.H., 2012b. Phanerozoic tectonics of the South China Block: Key observations and controversies, Gondwana Research doi:10.1016 /j.gr.2012. 02.019

Wang, Y.J., Fan, W.M., Zhao, G.C., Ji, S.C., Peng, T. P., 2007c. Zircon U-Pb geochronology of gneisses in Yunkai Mountains and its implications on the Caledonian event in South China. Gondwana Research 12(4), 404-416.

Wang, Y.J., Wu, C.M., Zhang, A.M., Fan, W.M., Zhang, Y.H., Zhang, Y.Z., Peng, T.P., Yin, C.Q., 2012c. Kwangsian and Indosinian reworking of the eastern South China Block: constraints on zircon U-Pb geochronology and metamorphism of amphibolite and granulite. Lithos 127 239–260.

Wang, Y.J., Zhang, A.M., Fan, W.M., Zhang, Y.H., Zhang, Y.Z., 2013. Origin of paleosubduction -modified mantle for Silurian gabbro in the Cathaysia Block: Geochronological and

Accepted Manuscript

ACCEPTED MANUSCRIPT

geochemical evidence Lithos 160-161, 37–54.

Wang, Y.J., Zhang, A.M., Fan, W.M., Zhao, G.C., Zhang, G.W., Zhang, Y.Z., Zhang, F.F., Li, S.Z., 2011b. Kwangsian crustal anatexis within the eastern South China Block: Geochemical, zircon U-Pb geochronological and Hf isotopic fingerprints from the gneissoid granites of Wugong and Wuyi and Yunkai Domains. Lithos 127, 239-260.

Wang, Y.J., Zhang, F.F., Fan, W.M., Zhang G.W., Chen, S.Y., Cawood, P. A., Zhang, A.M., 2010b. Tectonic setting of the South China Block in the early Paleozoic Resolving intracontinental and ocean closure models from detrital zircon U-Pb geochronology. Tectonics 29,. TC6020, doi:10.1029/2010TC002750, 2010

Wei, G.J., Liang, X.R., Li, X.H., Liu, Y., 2002. Precise measurement of Sr isotopic compositions of liquid and solid base using (LP) MC-ICP-MS. Geochimica 31 (3), 295–305.

Widom E., Hoernle K. A., Shirey S. B., Schmingcke H.-U., 1999. Os isotope systematics in the Canary Ialands and Madeira: lithospheric contamination and mantle plume signatures. J. Petrol. 40, 279–296.

Widom E., Shirey S. B., 1996. Os isotope systematics in the Azores: implications for mantle plume sources. Earth Planet. Sci. Lett. 142, 451–465.

Williams, I.S., 1998. U-Th-Pb geochronology by ion microprobe. In: McKibben, M.A., Shanks, W.C., Ridley, W.I.(Eds), Applications of Microanalytical microanalytical teTechniques to Understanding understanding Mineralizing mineralizing Processesprocesses:: Reviews in Economic Geology, pp.1-35.

Woodhead, J., Eggins, S., Gamble, J., 1993. High field strength and transition element systematics in island arc and back-arc basin basalts: evidence for multi-phase melt extraction and a depleted mantle wedge. Earth and Planetary Science Letters 114(4), 491-504.

Wu, R.X., Zheng, Y.F., Wu, Y.B., Zhao, Z.F., Zhang, S.B., Liu, X.M., Wu, F.Y., 2006. Reworking of juvenile crust: element and isotope evidence from Neoproterozoic granodiorite in South China. Precambrian Research 146, 179-212.

Wyman, D.A., Ayer, J.A., Devaney, J.R., 2000. Niobium-enriched basalts from the Wabigoon subprovince, Canada: evidence for adakitic metasomatism above an Archean subduction zone. Earth and Planetary Science Letters 179, 21-30.

Xiao, W.J., He, H.Q., 2005. Early Mesozoic thrust tectonics of the northwest Zhejiang region (Southeast China). GSA Bulletin 117(7/8), 945–961, doi:10.1130/B25417.1.

Xu, J.F., Suzuki, K., Xu, Y.G., Mei, H.J., Li, J., 2007. Os, Pb, and Nd isotope geochemistry of the Permian Emeishan continental flood basalts: Insights into the source of a large igneous province. Geochimica et Cosmochimica Acta 71, 2104–2119.

Xu, X.S., O'Reilly, S.Y., Griffin, W.L., Wang, X.L., Pearson, N.J., He, Z.Y., 2007. The crust of Cathaysia: Age, assembly and reworking of two terranes. Precambrian Research 158, 51–78

Xue, H.M., Ma, F., Song, Y.Q., Xie, Y.P., 2010. Geochronology and geochemistry of the Neoproterozoic granitoid association from eastern segment of the Jiangnan orogen, China:

Accepted Manuscript

ACCEPTED MANUSCRIPT

Constraints on the timing and process of amalgamation between the Yangtze and Cathaysia blocks. Acta Petrologica Sinica 26, 3215-3244 (in Chinese with English abstract).

Yang, Z.Y., Sun, Z.M., Yang, T.S., Pei, J.L., 2004. A long connection (750-380 Ma) between South China and Australia: paleomagnetic constraints. Earth and Planetary Science Letters 220, 423-434.

Ye, M.F., Li, X.H., Li, W.X., Liu, Y., Li, Z.X., 2007. SHRIMP zircon U–Pb geochronological and whole-rock geochemical evidence for an early Neoproterozoic Sibaoian magmatic arc along the southeastern margin of the Yangtze Block. Gondwana Research 12, 144-156.

Yogodzinski, G.M., Lees, J.M., Churikova, T.G., Dorendorf, F., Woerner, G., Volynets, O.N., 2001. Geochemical evidence for the melting of subducting oceanic lithosphere at plate edges. Nature 409, 500-504.

Yu, J.H., O'Reilly, Y.S., Wang, L.J., Griffin, W.L., Jiang, S.Y., Wang, R.C., Xu, X.S., 2007. Finding of ancient materials in Cathaysia and implication for the formation of Precambrian crust. Chinese Science BulletinChin. Sci. Bull. 52, 13-22.

Yu, J.H., O'Reilly, Y.S., Wang, L.J., Griffin, W.L., Zhang, M., Wang, R.C., Jiang, S.Y., Shu, L.S., 2008. Where was South China in the Rodinia supercontinent? Evidence from U-Pb ages and Hf isotopes of detrital zircons. Precambrian Research 164 (1-2),1-15.

Yu, J.H., O'Reilly, Y.S., Wang, L.J., Griffin, W.L., Zhou, M.F., Zhang, M., Shu, L.S., 2010. Components and episodic growth of Precambrian crust in the Cathaysia Block, South China: Evidence from U-Pb ages and Hf isotopes of zircons in Neoproterozoic sediments. Precambrian Research 181, 97-114.

Yu, J.H., Wang, L.J., O'Reilly, Y.S., Griffin, W.L., Zhang, M., Li C.Z., Shu, L.S., 2009. A Paleoproterozoic orogeny recorded in a long-lived cratonic remnant (Wuyishan terrane), eastern Cathaysia Block, China. Precambrian Research 174, 347-363.

Yu, J.H., Zhou, X.M., O'Reilly, S.Y., 2005. Formation history and protolith characteristics of granulite facies metamorphic rock in Central Cathaysia deduced from U-Pb and Lu-Hf isotopic studies of single zircon grains. Chinese Science Bulletin 50(18), 2080-2089.

Yuan, X.C., Zuo, Y., Cai, X.L., Zhu, J.S., 1989. The structure of the lithosphere and the geophysics in the South China Plate. In: Progress on Geophysics in China in the 1980s, edited by the editorial board of Bulletin of Geophysics. Beijing 243-249.

Zhang Z.J., Wang, Y.H., 2007, Crustal structure and contact relationship revealed from deep seismic sounding data in South China. Physics of the Earth and Planetary Interiors 165, 114–126.

Zhang, A.M., Wang, Y.J., Fan, W.M., Zhang, Y.Z., Yang, J., 2012a. Earliest Neoproterozoic (ca. 1.0 Ga) arc-back-arc-basin nature along the northern Yunkai Domain of the Cathaysia Block: geochronological and geochemical evidence from the metabasite. Precambrian Research 220–221, 217– 233.

Zhang, C.H., Fan, W.M., Wang, Y.J., Peng, T.P., 2009. Geochronology and geochemistry of the Neoproterozoic mafic-ultramafic dykes in the Aikou area, western Hunan Province:

Accepted Manuscript

ACCEPTED MANUSCRIPT

Petrogenesis and its tectonic implications. Geotectonica et Metallogenia 33(2), 283-293 (in Chinese with English abstract).

Zhang, F.F., Wang, Y.J., Fan, W.M., Zhang, A.M., Zhang, Y.Z., 2011a. Zircon U-Pb geochronology and Hf isotopes of the Neoproterozoic granites in the Central Jiangxi Province. Geotectonica et Metallogenia 35(1), 73-84.

Zhang, F.F., Wang, Y.J., Fan, W.M., Zhang, A.M., Zhang, Y.Z., Zhang, Y.H., 2012b. Geochronological and geochemical constraints on petrogenesis of the Middle Paleozoic (Kwangsian) massive granites in the eastern South China Block. Lithos 150, 188–208.

Zhang, Y.J., Zhou, X.H., Liao, S.B., Zhang, X.D., Wu, B., Wang, G.Z., Yu, MG. 2010. Neoproterozoic crustal composition and orogenic process of the Zhanggongshan area, Anhui-Jiangxi Provinces. Acta Geologica Sinica 84(1), 1402-1427

Zhang, Y.J., Zhou, X.H., Liao, S.B., Zhang, X.D., Yu, MG., Ren, J., Yang, J., 2011b. Geological and Geochemical Characteristics and Petrogenesis of the Mafic Rocks from Zhangyuan, Northern Jiangnan Orogen. Geological Journal of China Universities 17(3), 393-405

Zhang, Y.Z., Wang, Y. J., Fan, W. M., Zhang, A. M., Zhang, F. F., 2011c. Geochronological constraints on the Neoproterozoic collision along the Jiangnan uplift: Evidence from studies on the Neoproterozoic basal conglomerates at the Cangshuipu area, Hunan Province. Geotectonica et Metallogenia 35(1), 32-46 (in Chinese with English abstract).

Zhang, Y.Z., Wang, Y.J., Fan, W.M., Zhang, A.M., Zhang, F.F., 2012c. Geochronological and geochemical constraints on the metasomatised source for the Neoproterozoic (~825 Ma) high-mg volcanic rocks from the Cangshuipu area (Hunan Province) along the Jiangnan Domain and their tectonic implications. Precambrian Research, 220– 221, 139– 157. _in press.

Zhang, Z.L., Yuan, H.H., Nan, Y., 1998. Whole grain zircon evaporation for age of Luoyu formation, Yunkai, Group. Mineralogy Petrology 18, 85-90 (in Chinese with English abstract).

Zhao, G.C., Cawood, P.A., 1999. Tectonothermal evolution of the Mayuan assemblage in the Cathaysia Block: new evidence for Neoproterozoic collision-related assembly of the South China craton. American Journal of Sciences 299, 309-339.

Zhao, G., Cawood, P.A., 2012. Precambrian geology of China: Precambrian Research 222–223, 13-54.

Zhao, G.C., Guo, J.H., 2012. Precambrian Geology of China: Preface. Precambrian Research 222-223, 1-12.

Zhao, J.H., Zhou, M.F., Yan, D.P., Zheng, J.P., Li, J.W., 2011. Reappraisal of the ages of Neoproterozoic strata in South China: no connection with the Grenvillian orogeny. Geology 39, 299-302.

Zhejiang, BGMR (Bureau of Geology and Mineral Resources of Zhejiang Province), 1989. Regional Geology of the Zhejiang Province. Geological Publishing House, Beijing 1-688 (in Chinese with English abstract).

Zheng, Y.F., Wu, R.X., Wu, Y.B., Zhang, S.B., Yuan, H.L., Wu, F.Y., 2008. Rift melting of

Accepted Manuscript

ACCEPTED MANUSCRIPT

juvenile arc-derived crust: geochemical evidence from Neoproterozoic volcanic and granitic rocks in the Jiangnan Orogen, South China. Precambrian Research 163, 351-383.

Zheng, Y.F., Zhang, S.B., Zhao, Z.F., Wu, Y.B., Li, X.H., Li, Z.X., Wu, F.Y., 2007. Contrasting zircon Hf and O isotopes in the two episodes of Neoproterozoic granitoids in South China: implications for growth and reworking of continental crust. Lithos 96, 127–150.

Zhong, Y.F., Ma, C.Q., She, Z.B., Lin, G.C., Xu, H.J., Wang, R.J., Yang, K.G., Liu, Q., 2005. SHRIMP U-Pb zircon geochronology of the Jiuling granitic complex batholith in Jiangxi Province. Earth Science 30(6), 685-691 (in Chinese with English abstract).

Zhou, H.W., You, Z.D., Zhong, Z.Q., 1994. New findings of low pressure granulite facies metamorphic age in Yunkai uplift. Geological Science and Technology Information 13(3), 23-26 (in Chinese).

Zhou, J.C., Wang, X.L., Qiu, J.S., 2009. Geochronology of Neoproterozoic mafic rocks and sandstones from northeastern Guizhou, South China: coeval arc magmatism and sedimentation. Precambrian Research 170, 27–42.

Zhou, J.C., Wang, X.L., Qiu, J.S., Gao, J.F., 2004. Geochemistry of Meso- and Neoproterozoic mafic-ultramafic rocks from northern Guangxi, China: arc or plume magmatism? Geochemical Journal 38, 139–152.

Accepted Manuscript

ACCEPTED MANUSCRIPT

Figures Caption

Fig. 1 The main faults and tectonic subdivisions of the eastern South China Block. Inset shows the Yangtze and Cathaysia blocks along with previously defined Sibao Orogen (modified after Zhang et al., 2012c),

Fig. 2 (a) and (b) Simplified geological maps of the Wuyi and Yunkai domains showing sampling locations including Zhuyuan-Shanlintou (Songyang), Chatian (Longquan), Huangtian and Zhuhuang (Qinyuan) and Shitun (Zhenghe) in the Wuyi and Shiwo (Beiliu), Liuwan (Rongxian), Jintong and Zhaimen (Xinyi) in Yunkai domains, respectively (revised after Wang et al., 2011b). See inset in Fig. 1 for the locations in the eastern South China Block.

Fig. 3. Microscope photographs for representative rocks along the Wuyi-Yunkai domains: (a) amphibolite 09WG-66a, (b) plagioclase amphibolite 09WG-74c, (c) amphibolite 09YK-3e, (d) metagabbro WG-59B1, (e) metadiabase 09WG-53a, and (f) serpentine 09WG-51c. Amp: Amphibole, Pl: Plagioclase, Hb: Hornblende, Cpx, Clinopyroxene, Atg, Antigorite, Chl, Chlorite, Q: Quartz.

Fig. 4 Zircon CL images with U–Pb ages for (a) amphibolite (09WG-66A), (b) metadiabase (09WG-53A), (c) plagioclase amphibolite (09YK-3e), (d) plagioclase amphibolite (09WG-58D) and (e) plagioclase amphibolite (09WG-74C) along the Wuyi-Yunkai domain, respectively.

Fig. 5 Concordia diagrams of (a) SHRIMP zircon U-Pb data for 09WG-66A amphibolite from Chatian (Longquan in SW Zhejiang; N27°56.920’, E119°01.506’), (b) LA-ICP zircon U-Pb data for 09WG-66A amphibolite, (c) SIMS zircon U-Pb result for 09WG-53A metadiabase from Shitun (Zhenghe in Fujian, N27°20.895’, E118°47.712’) in the Wuyi domain; (d) LA-ICP zircon U-Pb data for 09WG-53A metadiabase; (e) LA-ICP zircon U-Pb data for 09YK-3e plagioclase amphibolite; (f) LA-ICP zircon

Accepted Manuscript

ACCEPTED MANUSCRIPT

U-Pb dating result for 09WG-58D plagioclase amphibolite from Huangtian (Qinyuan in Zhejiang; N27°50.029’, E118°52.538’) in the Wuyi domain; (g) LA-ICP zircon U-Pb result for 09WG-74C garnet-bearing plagioclase amphibolite from Shanlintou village (Songyang, Zhejiang; N28°19.552’, E119°10.469’) in Wuyi domain. The corresponding locations of the samples are shown in Figures 2a-b. (h) $\varepsilon_{Nd}(t)$ values for the Neoproterozoic inherited zircons in the Kwangsian (~400-460 Ma) granitoid gneiss in the Cathaysia Block (Wang et al., 2011b).

Fig. 6 Chondrite-normalized REE patterns for zircon grains from (a) amphibolite (09WG-66A), (b) metadiabase (09WG-53A), (c) plagioclase amphibolite (09YK-3e) and (d) plagioclase amphibolite (09WG-74C) along the Wuyi-Yunkai domain. Red dashed ad green solid lines in (a-c) denote the crystallized and xenocrystic grains with U-Pb ages of ~980 Ma and older than ~1000 Ma, respectively. Blue solid lines in (d) denote the metamorphic grains with U-Pb metamorphic ages of ~244 Ma.

Fig. 7 (a) Zr/TiO_2 vs SiO_2, (b) Zr/TiO_2 vs Nb/Y, (c) MgO vs Nb/La, and (d) Nb vs Nb/U for the metabasic rocks from the Wuyi and Yunkai domains in the Cathaysia Block. The fields of the island arc basalts and Nb-enrich basalts are from Kepezhinskas et al. (1996).

Fig. 8 Plots of SiO_2 vs. (a) FeOt, (b) TiO_2, (c) Al_2O_3, (d) MgO, (e) CaO and (f) P_2O_5 and of MgO vs (g) Cr and (h) Ni for the metabasic rocks along the Wuyi and Yunkai domains in the Cathaysia Block.

Fig. 9 Chondrite normalized rare-earth element patterns for Group 1 (a), Group 2 (b), Group 3 (c) and Group 4 (d) for the metabasic rocks along the Wuyi and Yunkai domains in the Cathaysia Block, respectively. Data for the Okinawa Trough BABB, Lesser Caucasus back-arc basalt, New Caledonia fore-arc basin basalt and Saunders island-arc basalt and are from Shinjo et al. (1999), Pearce et al. (1995), Rolland et al.

ACCEPTED MANUSCRIPT

(2009) and Hässig et al. (2012). N-MORB and E-MORB are after Sun and McDonough (1989). The Pickle Nb-enriched basalts are from Hollings and Kerrich (2004).

Fig. 10 Primitive mantle-normalized multi-element spidergram for Group 1 (a), Group 2 (b), Group 3 (c) and Group 4 (d) for the metabasic rocks along the Wuyi and Yunkai domains in the Cathaysia Block. Data for the Okinawa Trough back-arc basin basalts, Saunders island-arc basalt and New Caledonia fore-arc basin basalt are from Shinjo et al. (1999), Pearce et al. (1995), Fan et al. (2010) and Hässig et al. (2012). N-MORB and E-MORB are after Sun and McDonough (1989). The Pickle Nb-enriched basalts and ~1.0 Ga Nb-enriched basalts in the Yunkai domain are from Hollings and Kerrich (2004) and Zhang et al. (2012a), respectively.

Fig.11 (a) $^{187}Re/^{188}Os$ ratio versus Os concentrations for the Groups 2 and 3 samples, Arc lavas, MORB and OIB are from Alves et al. (2002). The plots of (b) $^{187}Re/^{188}Os$ vs $^{187}Os/^{188}Os$, and (c) Os (ppt) vs γOs for the Shitun serpentines. The fields of the residual peridotite, lava, OIB (plume mantle) and lithospheric mantle are from Shirey and Walker (1998), Widom and Shirey (1996), Widom et al. (1999), Xu et al., (2007) and Shi et al.(2006).

Fig. 12 MgO vs εNd (t) (a), MgO vs Nb/La (b), La/Sm vs Nb/La (c) La/Sm vs εNd(t) for the metabsic rocks along the Wuyi and Yunkai domains in the Cathaysia Block, respectively.

Fig. 13 Plots of (a) Y/15-La/10-Nb/8, (b) Hf/3-Th-Nb/16, (c) FeO/MgO vs TiO_2 and (d) TiO_2 vs V for the metabasic rocks along the Wuyi and Yunkai domains in the Cathaysia Block. CFB: continental flood basalt; IAB: island-arc basalt; CAMB: active continental margin basalt; CWPAB: continental within-plate alkali and transitional basalts; OIB: ocean-island basalt; BABB: back-arc basin basalt; IAT: island-arc tholeiite; IAB: island-arc calc-alkaline basalt. MORB: mid-ocean ridge basalt.

Accepted Manuscript

ACCEPTED MANUSCRIPT

N-MORB: normal mid-ocean ridge basalt, and E-MORB: enriched mid-ocean ridge basalt.

Fig. 14 La/Nb vs Nb/Th (a), Ta/Yb -Th/Yb (b), Tb/Ta-Th/Ta (c), and Zr vs Ti/Zr (e) for the metabasic rocks along the Wuyi and Yunkai domains in the Cathaysia Block (e.g., Woodhead et al., 1993; Pearce and Peate, 1995; Condie, 1997). Symbols are same as those in Fig. 8a.

Fig. 15 Plots of (a) Nb/Y vs ε_{Nd} (t), (b) Nd/Pb vs ε_{Nd} (t), (c) Th/Zr and Nb/Zr, and (d) Cr and Ni for the metabasic rocks along the Wuyi and Yunkai domains in the Cathaysia Block. The compositions of the end-members are from Elliott et al. (1997), Class et al. (2002), Petrone and Ferrari (2008), Castillo et al. (2002, 2007) and Wang et al., (2013). The expected range of the normal mantle-derived melt and Kitakami high-mg andesite in (d) are from Tsuchiya et al. (2005).

Fig. 16 The synthesis of the reported U-Pb geochronological data for the early-middle Neoproterozoic igneous rocks along the Wuyi-Yunkai, Shuangxiwu and Jiangnan domains of the eastern SCB. The data are from 1) Li, 1999; 2) Wang et al., 2006; 3) Ma et al., 2009; 4) Zhang et al., 2011a; 5) Zheng et al., 2005; 6) Wang et al., 2007a, b; 7) Li et al., 2003; 8) Wu et al., 2006; 9) Zhang et al., 2008; 11) Li et al., 1994; 12) Gao et al., 2009; 13) Li et al., 2003; 14) Ye et al., 2007; 15) Chen et al., 2009a; 17) Wang et al., 2012a; 18) Zhou et al., 2007, 2009; 19) Zhang et al., 2009; 20) Li et al., 2009; 21) Ding et al., 2008; 22) Zhang YZ et al., 2012; 23) Wang et al., 2008b; 24) Shu et al., 2006; 25) Li et al., 2010a; 26) Hu and Liu, 2002; 27) Qin et al., 2006; 28) Zhang et al., 1997; 29) Zhang et al., 2012a; 30) Shu et al., 2008; 31) Liu et al., 2001; 32) Shu et al., 2011; 33) Li et al., 2005; 34) Li et al., 2002; 35) Zhang et al., 2011b and 36) this study. Inset (a) shows the early Neoproterozoic tectonic subdivision in the eastern South China Block and associated orogenism. Inset (b) shows the age-spectra of detrital

Accepted Manuscript

ACCEPTED MANUSCRIPT

zircons for the Neoproterozoic sedimentary rocks from the Yunkai-Nanling and Jiangnan domains. Data in (b) from Wang et al. (2007b, 2008a, 2010a, b; 2012a), Zhang et al. (2012a), Yu et al. (2007, 2008, 2010), Wan et al. (2007, 2010), Li et al. (2011); Zhao et al. (2011) and Zhou et al. (2009).

Fig. 17 Neoproterozoic reconstruction of the South China Block during the assemblage of Rodinia. The South China Block situated between NW Australia and East Antarctica around the periphery of Rodinia supercontinent (modified after Torsvik et al., 2001).

Fig. 18 Schematic cartoon showing the early Neoproterozoic tectonic evolution of the eastern South China Block. (a) At ~1.0-0.90 Ga, the arc and back-arc system along the Wuyi-Yunkai and Shuangxiwu domains developed and accreted at 0.90 Ga and 0.88 Ga, respectively. (b) Development between ~860-830 Ma of the back-arc system along the Jiangnan domain and intraplate magmatism in the merged Cathaysia Block. (c) At ~830-800 Ma, the merged Cathaysia Block amalgamated with the Yangtze Block along the Jiangnan domain and finally created a united SCB.

Accepted Manuscript

Accepted Manuscript

Table 1: Major oxides, elemental and Nd isotopic analytical results for the earliest Neoproterozoic mafic rocks along the Wuyi and Yunkai domains, SCB

	Group 1													Group 2	
	Northern Yunkai domain											NE Wuyi domain		Yunkai domain	
Sample	09YK-9B	YK-9C	09YK-9C	09YK-9H	YK-09A	YK-9B	09YK-11F	1244-1[a]	1246-1[a]	3087[a]	3102[a]	LB264[b]	LB265[b]	JT-4	JT-5
	Plagioclase amphibolite				Plagioclase amphibolite		metagabbro					Plagioclase amphibolite		Plagioclase amphibolite	
	Mala village (Xinyi)				Jintong (Xinyi)		Liuwan	Shiwo (Beiliu)				Zhulu (Longquan)		Jintong (Xinyi)	
SiO_2	45.71	45.23	45.23	46.00	45.67	45.71	50.05	46.63	48.57	48.24	48.31	47.08	47.23	49.68	47.39
TiO_2	0.81	0.80	0.80	0.84	0.91	0.81	1.51	1.40	1.10	1.62	0.80	1.50	1.43	0.91	1.01
Al_2O_3	14.65	14.02	14.02	14.69	13.95	14.65	13.59	14.25	14.89	13.85	15.63	15.84	16.08	14.94	14.80
FeOt	9.54	9.24	9.24	9.25	9.05	9.54	12.23	12.59	10.98	13.23	10.05	13.20	13.73	9.61	10.39
MgO	11.52	11.70	11.70	10.91	10.48	11.52	7.18	7.09	7.83	6.92	8.67	6.02	5.93	7.73	8.41
CaO	8.88	9.36	9.36	9.06	9.69	8.88	10.27	11.59	11.86	11.55	10.11	9.96	9.58	9.41	10.79
K_2O	4.22	4.65	4.65	4.39	2.15	4.22	1.09	0.33	0.47	0.24	2.12	1.08	1.53	2.62	2.61
Na_2O	0.87	0.45	0.45	0.95	1.93	0.87	2.35	0.87	1.61	1.31	1.06	2.98	2.83	2.81	2.07
P_2O_5	0.07	0.08	0.08	0.07	0.09	0.07	0.13	0.14	0.09	0.15	0.05	0.13	0.13	0.06	0.07
MnO	0.15	0.16	0.16	0.15	0.29	0.15	0.22	0.21	0.19	0.21	0.17	0.22	0.23	0.18	0.17
LOI	3.38	4.47	4.47	3.79	2.83	3.38	1.36	0.50	0.75	0.45	1.15			1.68	1.85
Total	99.80	100.14	100.14	100.10	100.04	99.80	99.98	95.60	98.34	97.77	98.12	98.01	98.70	99.64	99.55
mg-number	71	72	72	70	69	64	54	53	59	51	63	48	46	62	62
Sc	39	40	39	42	33	35	49	48	46	52	42	29	50	31	35
V	179	191	174	184	198	175	96	351	298	342	236	233	259	193	214
Cr	806	866	805	784	250	621	107	173	269	203	204	546	539	242	280
Co	54	54	52	54	38	57	48	60	66	58	56	70	62	44	47
Ni	326	376	365	321	121	326	61	66	96	61	112	231	236	113	125
Ga	19.2	17.9	17.3	19.3	18.7	18.8	16.4					18.1	19.4	15.6	16.8
Rb	432	456	441	443	299	452	39.1	10.3	23.2	2.3	94.4	46.6	82.7	222	224
Sr	74.7	73.1	71.3	79.1	188	82.5	134	160	234	232	103	235	265	121	263
Y	24.07	22.96	22.69	24.84	33.70	24.30	34.06	33.20	25.70	37.50	25.40	29.90	32.40	32.80	31.90
Zr	66.5	65.8	63.7	67.6	66.5	65.8	111.3	96.9	57.9	115.0	39.5	90.5	90.1	69.3	72.6
Nb	1.89	2.14	2.22	2.82	2.57	3.04	2.45	5.33	1.39	4.01	1.24	3.76	3.63	3.13	4.97

Accepted Manuscript

Cs	26.47	27.19	27.07	26.17	50.20	25.60	2.65	0.55	4.35	0.11	6.62	1.78	2.87	8.40	8.16
Ba	459	484	479	444	370	447	74	18	139	25	137	87	144	572	633
La	2.59	3.05	3.16	2.93	3.13	2.55	4.55	4.25	2.61	6.25	2.23	4.20	4.74	5.59	4.87
Ce	7.86	8.51	8.81	8.77	9.50	7.64	13.24	11.90	7.43	16.70	6.55	12.20	13.30	12.61	12.8
Pr	1.38	1.44	1.48	1.50	1.52	1.23	2.29	1.92	1.23	2.59	1.05	1.95	2.22	1.92	1.86
Nd	6.94	7.12	7.37	7.56	7.73	5.74	11.76	9.74	6.68	12.70	5.61	9.93	11.00	8.57	9.02
Sm	2.29	2.22	2.19	2.30	2.64	2.10	3.81	3.29	2.39	4.12	2.21	3.41	3.62	3.03	2.97
Eu	1.01	1.09	1.07	1.05	0.92	0.92	1.30	1.24	0.99	1.43	0.88	1.35	1.54	0.90	1.00
Gd	3.02	2.79	2.90	3.04	4.09	3.46	4.83	4.83	3.62	6.17	3.41	4.85	4.95	4.12	4.21
Tb	0.60	0.55	0.55	0.60	0.76	0.56	0.91	0.83	0.68	1.01	0.62	0.82	0.90	0.67	0.70
Dy	3.94	3.78	3.71	4.01	5.01	3.73	5.63	5.92	4.57	6.98	4.55	5.43	5.25	4.43	4.52
Ho	0.88	0.85	0.81	0.92	1.12	0.85	1.20	1.25	1.01	1.56	0.98	1.17	1.23	1.00	1.00
Er	2.60	2.52	2.50	2.74	3.42	2.57	3.32	3.80	3.05	4.50	2.95	3.31	3.47	2.92	2.97
Tm	0.42	0.42	0.39	0.44	0.53	0.40	0.49	0.54	0.43	0.64	0.43	0.49	0.51	0.41	0.43
Yb	2.91	2.93	2.83	3.05	3.70	2.72	3.24	3.51	2.84	4.09	2.87	3.12	3.29	2.58	2.81
Lu	0.45	0.47	0.45	0.49	0.62	0.42	0.49	0.50	0.40	0.60	0.39	0.47	0.50	0.38	0.43
Hf	1.89	1.71	1.64	1.81	2.10	1.72	3.03	2.61	1.82	3.24	1.26	2.15	2.37	2.29	2.25
Ta	0.13	0.15	0.15	0.16	0.22	0.23	0.17	0.24	0.10	0.21	0.10	0.21	0.21	0.24	0.25
Pb	9.26	10.97	10.70	11.42	9.22	10.60	9.72	9.68	22.80	11.50	13.50	8.85	7.39	12.70	10.50
Th	0.23	0.25	0.24	0.24	0.66	0.20	0.83	0.42	0.30	0.68	0.39	0.29	0.39	0.48	0.51
U	0.29	0.32	0.33	0.32	0.91	0.33	0.84	0.08	0.07	0.15	0.27	0.20	0.08	0.29	0.18
$^{147}Sm/^{144}Nd$	0.200				0.207		0.180					0.208	0.199		0.199
$^{143}Nd/^{144}Nd$	0.512900				0.512954		0.512856					0.512929	0.512919		0.512812
2 σ	2				6		5					9	5		7
εNd (t)	4.8				4.9		4.4					4.3	5.2		3.1

ACCEPTED MANUSCRIPT

to be continued

	Group 2										Group 3				
	Northern Yunkai domain					NE Wuyi domain					NE Wuyi domain				
sample	JT-6	JT-7	1243-1[a]	1257-1[a]	1260-1[a]	WG-59B1	WG-59B2	WG-59B4	09WG-59A	09WG-59B	LB258[b]	LB259[b]	LB262[b]	LB263[b]	09WG-75A
	Plagioclase amphibolite					Metagabbro					amphibolite				Plagioclase amphibolite
	Zhaimen (Xinyi)		Guiyi (Cenxi)			Huangtian (Qinyuan)					Zhulu (Longquan)				Zhuyuan
SiO_2	49.81	47.24	49.07	48.16	49.64	48.48	48.51	48.25	48.52	48.71	46.18	50.21	47.74	48.46	46.62
TiO_2	0.95	0.95	1.52	1.61	1.56	1.58	1.50	1.44	1.51	1.43	2.42	1.76	2.20	2.13	1.89
Al_2O_3	14.76	14.72	14.71	13.67	14.21	14.10	13.82	14.49	14.10	13.88	13.64	15.92	15.92	15.19	15.31
FeOt	10.23	10.81	11.75	13.50	12.68	12.48	12.69	12.09	12.85	13.03	14.93	12.18	13.88	15.67	14.75
MgO	7.88	7.83	7.30	6.44	6.87	6.74	6.72	5.63	6.67	6.61	8.08	5.22	5.28	3.87	7.09
CaO	9.30	10.61	10.90	10.33	8.48	11.46	11.28	12.70	11.11	10.90	8.96	10.01	9.59	8.86	8.96
K_2O	2.00	1.62	0.30	0.41	0.26	0.99	1.10	0.85	0.96	1.06	0.92	0.78	1.04	1.27	1.79
Na_2O	3.30	2.69	1.74	2.78	3.63	2.32	2.30	2.47	2.38	2.47	2.67	2.97	3.01	3.40	1.62
P_2O_5	0.07	0.07	0.14	0.15	0.15	0.13	0.12	0.15	0.14	0.14	0.24	0.21	0.22	0.17	0.21
MnO	0.19	0.18	0.20	0.22	0.20	0.20	0.21	0.20	0.18	0.19	0.26	0.22	0.20	0.18	0.18
LOI	1.16	2.85	0.65	0.35	0.55	1.00	1.21	1.33	1.08	1.09					1.04
Total	99.65	99.59	98.28	97.62	98.23	99.48	99.46	99.60	99.51	99.52	98.30	99.48	99.08	99.20	99.46
mg-number	61	59	55	49	52	52	51	48	51	50	52	46	43	33	49
Sc	32	33	39			39	39	34	41	42	47	37	36	48	45
V	193	200	305			274	275	257	267	300	309	236	295	357	341
Cr	246	267	195			83	84	75	75	81	379	543	362	165	243
Co	44	46	61			51	50	44	46	49	62	61	79	47	56
Ni	116	127	76			67	66	62	53	60	195	224	168	62	64
Ga	17.8	18.1				16.4	16.5	19.8	16.3	16.8	20.9	20.9	18.7	21.4	23.7
Rb	152	109	8.1			39.1	51.6	40.4	32.6	43.1	42.9	20.4	43.0	59.0	87.1
Sr	107	163	297			226	239	231	192	244	221	257	282	244	275
Y	29.20	25.10	32.10			23.30	22.80	18.50	21.74	21.45	45.60	33.30	38.70	46.70	27.94
Zr	69.2	69.9	102			87.6	86.3	98.2	88.2	78.8	158	131	140	147	113
Nb	4.90	4.38	6.48			5.07	4.89	5.00	5.32	5.22	7.93	9.72	8.30	7.67	12.78
Cs	6.49	9.28	0.71			2.69	3.18	1.82	3.14	3.56	1.50	1.27	2.50	2.25	4.80

Accepted Manuscript

Ba	424	348	100	105	117	84	99	108	91	100	110	90	300
La	7.35	4.80	5.86	6.21	6.26	5.70	5.91	6.10	8.96	11.50	9.94	8.20	11.95
Ce	15.00	11.90	16.40	14.50	13.90	11.80	15.30	15.73	22.80	26.90	22.40	20.80	28.25
Pr	2.05	1.75	2.36	2.13	2.20	1.72	2.44	2.35	3.70	3.49	3.35	3.14	3.92
Nd	9.67	8.55	11.40	9.79	10.50	8.06	11.97	11.42	18.90	15.20	16.40	15.10	17.22
Sm	3.21	2.87	3.56	3.05	3.01	2.40	3.34	3.17	5.48	4.34	4.90	4.96	4.44
Eu	0.93	0.88	1.36	1.18	1.14	0.89	1.31	1.28	1.81	1.59	1.67	1.83	1.59
Gd	4.15	3.51	5.01	3.68	3.48	2.78	3.84	3.73	6.52	5.43	6.31	6.43	4.76
Tb	0.68	0.60	0.84	0.65	0.64	0.50	0.68	0.68	1.20	0.92	1.09	1.26	0.86
Dy	4.38	3.90	6.03	3.88	3.83	2.94	4.21	4.13	7.40	5.79	6.74	7.41	5.33
Ho	0.95	0.85	1.23	0.81	0.79	0.61	0.89	0.86	1.61	1.23	1.46	1.77	1.12
Er	2.78	2.53	3.61	2.28	2.22	1.73	2.36	2.29	4.44	3.47	3.97	4.98	2.93
Tm	0.40	0.38	0.53	0.32	0.32	0.24	0.34	0.33	0.68	0.49	0.60	0.75	0.43
Yb	2.54	2.53	3.47	2.02	2.00	1.57	2.14	2.08	4.23	3.22	3.65	4.67	2.71
Lu	0.38	0.38	0.45	0.29	0.29	0.24	0.33	0.33	0.62	0.48	0.53	0.72	0.42
Hf	2.21	2.49	2.91	2.27	2.37	2.13	2.39	2.07	3.86	3.06	3.38	3.81	2.82
Ta	0.25	0.24	0.38	0.33	0.35	0.28	0.35	0.33	0.50	0.61	0.47	0.44	0.81
Pb	11.30	7.68	19.80	13.10	11.40	18.10	11.28	10.37	4.79	9.27	5.77	6.93	16.39
Th	0.60	0.50	0.52	0.47	0.42	0.45	0.51	0.47	1.16	1.36	0.63	0.78	2.37
U	0.39	0.21	0.14	0.19	0.44	0.66	0.13	0.36	0.99	0.34	0.30	0.25	0.96
$^{147}Sm/^{144}Nd$	0.200	0.203				0.180			0.175		0.181	0.199	0.156
$^{143}Nd/^{144}Nd$	0.512880	0.512835				0.512747			0.512860		0.512761	0.512950	0.512524
2 σ	8	10				9			14		9	15	8
εNd (t)	4.2	3.1				4.2			7.0		4.4	5.9	2.9

ACCEPTED MANUSCRIPT

to be continued

	Group 3													
	NE Wuyi domain													
Sample	09WG-74A	09WG-74B	09WG-74C	09WG-74D	09WG-74F	09WG-74G	09WG-74H	09WG-74I	09WG-74K	09WG-74L	09WG-74M	09WG-74N	09WG-74O	09WG-58B
	Plagioclase amphibolite													amphibolite
	Yuyan-Shanlintuo (Songyang)													Zhuhuang
SiO_2	50.06	49.70	48.27	48.73	48.55	49.38	47.82	48.60	49.59	49.38	48.76	48.78	47.88	48.71
TiO_2	1.43	1.66	3.41	1.47	2.74	1.45	1.57	1.54	1.47	1.42	1.94	1.45	2.06	2.06
Al_2O_3	12.21	11.65	12.52	12.03	13.31	13.17	13.06	13.21	12.94	12.90	13.30	12.92	13.26	12.90
FeOt	13.21	13.56	17.64	15.77	17.19	14.88	15.55	15.25	14.33	13.81	14.70	14.94	14.63	15.38
MgO	5.39	5.08	5.75	6.27	6.56	6.42	7.21	7.06	6.64	6.59	7.08	6.81	4.90	6.13
CaO	11.79	12.53	7.59	10.12	7.53	9.04	9.60	9.00	9.57	10.21	8.43	9.82	11.52	9.31
K_2O	1.33	0.94	1.11	1.32	0.74	0.53	0.34	0.50	0.48	1.06	1.45	0.41	1.30	1.24
Na_2O	2.79	3.03	1.36	2.56	1.31	3.44	3.12	3.16	3.45	2.93	2.48	3.13	2.27	2.31
P_2O_5	0.17	0.19	0.38	0.16	0.29	0.16	0.15	0.18	0.16	0.14	0.18	0.16	0.24	0.21
MnO	0.22	0.24	0.26	0.23	0.25	0.20	0.22	0.19	0.19	0.20	0.20	0.22	0.24	0.21
LOI	0.96	0.99	1.24	0.95	1.03	1.01	1.01	0.97	0.84	0.96	1.03	1.02	1.23	1.10
Total	99.55	99.57	99.52	99.61	99.50	99.68	99.66	99.66	99.66	99.60	99.57	99.65	99.52	99.57
mg-number	45	43	39	44	43	46	48	48	48	49	49	48	40	44
Sc	41	40	45	47	39	44	46	48	47	43	44	46	39	47
V	299	317	490	350	374	316	331	352	330	305	362	306	366	400
Cr	119	100	114	98	74	134	143	150	149	128	108	79	83	79
Co	46	47	48	46	45	50	49	53	48	46	50	46	43	50
Ni	57	53	62	66	45	59	61	64	61	60	72	58	43	49
Ga	14.1	12.5	19.4	13.5	18.0	16.0	15.3	15.6	15.4	15.2	20.6	15.1	20.6	20.1
Rb	69.7	48.3	41.4	59.7	35.1	20.3	9.8	20.0	18.6	48.7	60.9	17.1	61.4	47.2
Sr	452	347	99.0	306	68.9	79.8	73.7	132	168	301	315	108	197	254
Y	25.03	25.92	52.90	27.00	41.88	26.35	29.21	25.95	25.96	24.38	29.25	25.85	35.97	42.58
Zr	90.2	105	256	96.9	203	91.2	95.3	95.1	98.1	90.4	136	92.8	162	124
Nb	10.92	12.16	23.91	10.36	20.56	10.51	12.01	10.38	10.43	9.94	13.59	9.57	17.67	9.70
Cs	1.99	0.89	0.81	1.27	2.69	0.58	0.31	0.60	0.44	1.26	1.64	0.43	1.55	1.24
Ba	125	89	200	258	98	35	19	38	27	125	313	294	294	219

Accepted Manuscript

ACCEPTED MANUSCRIPT

La	11.94	13.83	24.07	10.24	15.75	8.60	8.56	8.72	9.08	8.78	11.57	9.03	19.81	12.81
Ce	28.31	30.19	56.81	23.62	39.48	20.85	21.03	20.97	21.90	20.41	30.06	21.48	47.83	32.58
Pr	3.91	4.06	7.77	3.40	5.81	2.93	2.99	3.10	3.18	2.91	4.50	3.16	6.58	4.80
Nd	16.97	17.88	35.40	15.48	26.48	13.40	13.66	14.30	14.18	13.48	21.00	14.04	28.71	22.97
Sm	4.09	4.34	8.90	4.08	6.65	3.52	3.80	3.70	3.61	3.55	5.37	3.67	6.72	6.18
Eu	1.49	1.37	2.30	1.42	2.22	1.22	1.25	1.34	1.31	1.37	1.62	1.26	2.09	2.09
Gd	4.29	4.72	9.43	4.50	7.21	3.98	4.52	4.16	4.16	4.11	5.68	4.16	6.64	7.14
Tb	0.75	0.82	1.63	0.81	1.30	0.72	0.87	0.77	0.75	0.74	0.96	0.79	1.15	1.24
Dy	4.64	5.07	9.82	4.95	7.99	4.64	5.40	4.95	4.78	4.63	5.75	4.92	7.08	7.71
Ho	0.97	1.04	2.06	1.05	1.66	0.99	1.12	1.06	1.01	0.98	1.16	1.04	1.50	1.58
Er	2.67	2.87	5.58	2.92	4.52	2.79	3.16	2.98	2.78	2.73	3.09	2.94	4.01	4.33
Tm	0.40	0.42	0.81	0.43	0.66	0.40	0.46	0.44	0.41	0.40	0.43	0.41	0.61	0.62
Yb	2.54	2.67	5.01	2.83	4.16	2.59	3.09	2.75	2.66	2.56	2.78	2.80	3.85	3.92
Lu	0.39	0.41	0.79	0.45	0.64	0.41	0.49	0.44	0.41	0.41	0.42	0.42	0.60	0.60
Hf	2.42	2.59	6.10	2.03	4.76	2.30	2.47	2.44	2.46	2.33	3.54	2.01	4.19	3.15
Ta	0.70	0.74	1.44	0.62	1.22	0.61	0.73	0.64	0.61	0.60	0.90	0.59	1.17	0.50
Pb	20.92	12.93	3.27	7.54	5.94	6.47	4.70	4.30	7.96	11.39	10.54	4.06	10.94	6.20
Th	2.85	2.01	3.44	1.09	3.29	0.96	1.97	0.96	0.92	1.01	2.04	1.36	3.81	0.74
U	2.22	1.67	0.94	0.32	1.02	0.39	0.85	0.32	0.32	0.31	1.28	0.29	1.47	0.69
$^{147}Sm/^{144}Nd$	0.146							0.157	0.154				0.142	0.163
$^{143}Nd/^{144}Nd$	0.512507							0.512557	0.512526				0.512428	0.512540
2 σ	6							9	6				7	8
εNd (t)	3.8							3.5	3.2				2.8	2.4

ACCEPTED MANUSCRIPT

to be continued

	Group 3													
	NE Wuyi domain													
Sample	09WG-58C	09WG-58D	09WG-58E	WG-58B1	WG-58B2	WG-58D1	WG-58D2	WG-59B3	09WG-59B3	09WG-59B6	09WG-66A	09WG-66A7	09WG-66A9	XT3086-1[d]
	Plagioclase amphibolite							metagabbro			amphibolite			metamafic
	Zhuhuang (Qinyuan)							Huangtian (Qinyuan)			Chatian (Longquan)			
SiO_2	49.24	48.05	47.62	48.62	48.62	47.90	47.89	44.46	44.66	49.33	42.31	43.30	43.46	48.54
TiO_2	1.78	2.14	2.53	2.18	2.18	2.25	2.26	1.60	1.54	1.01	1.77	2.04	1.79	1.65
Al_2O_3	13.49	13.01	12.69	12.86	12.83	12.94	12.93	13.16	13.30	14.29	13.39	11.63	11.36	14.30
FeOt	13.90	15.47	16.15	14.89	14.91	14.99	14.98	15.03	15.50	12.04	13.89	14.58	13.48	12.56
MgO	5.95	6.20	5.67	6.15	6.18	6.26	6.26	9.40	9.26	7.42	9.18	10.13	9.28	7.15
CaO	9.56	9.69	9.90	9.60	9.60	10.02	9.98	9.89	9.59	9.75	12.60	11.88	13.97	11.82
K_2O	1.78	1.35	1.35	1.28	1.29	1.38	1.42	0.97	0.94	1.30	1.39	1.30	0.81	0.30
Na_2O	2.32	2.21	2.04	2.29	2.30	2.15	2.18	1.93	1.96	2.77	0.56	0.63	0.53	1.27
P_2O_5	0.19	0.22	0.26	0.19	0.19	0.20	0.20	0.21	0.22	0.23	0.21	0.07	0.11	0.15
MnO	0.18	0.22	0.20	0.23	0.23	0.25	0.24	0.25	0.24	0.18	0.81	0.78	0.92	0.22
LOI	1.11	0.99	1.14	1.06	1.02	1.00	1.00	2.42	2.40	1.22	3.30	3.12	3.72	
Total	99.52	99.55	99.54	99.34	99.34	99.33	99.33	99.30	99.59	99.55	99.40	99.45	99.43	97.96
mg-number	46	44	41	45	45	46	46	56	54	55	57	58	58	53
Sc	42	44	47	43	44	42	40	46	51	37	36	42	39	47
V	330	354	550	381	387	397	392	320	347	239	277	300	279	322
Cr	59	70	80	81	87	82	79	65	55	117	15	18	26	187
Co	45	44	48	49	49	48	48	60	60	42	65	67	68	44
Ni	40	38	42	52	55	49	48	78	74	61	42	45	47	54
Ga	18.5	18.9	20.3	19.9	20.3	19.9	19.1	15.3	15.9	17.4	21.0	17.1	19.5	21.6
Rb	70.4	50.4	48.3	57.4	58.0	62.0	62.1	28.6	23.8	39.8	41.9	30.3	19.2	9.0
Sr	245	200	234	246	251	246	247	161	139	289	421	219	396	182
Y	34.42	34.41	45.46	45.60	44.80	37.00	37.60	36.10	33.46	26.86	44.74	47.78	60.85	37.15
Zr	125	125	142	123	123	126	124	82.4	84.2	77.0	112	132	122	121
Nb	7.97	7.18	11.55	8.50	8.51	7.90	7.97	16.00	18.05	18.10	14.99	20.32	29.87	10.59
Cs	2.34	1.20	1.24	1.15	1.12	1.08	1.11	1.01	1.13	3.40	3.18	2.15	1.48	0.61
Ba	248	197	321	208	212	221	219	241	271	200	588	532	142	70

Accepted Manuscript

ACCEPTED MANUSCRIPT

Accepted Manuscript

La	13.22	11.47	15.00	13.30	13.50	11.40	11.80	14.90	14.88	8.23	11.39	12.01	9.80	7.87
Ce	31.06	28.41	37.67	24.50	25.00	21.90	22.10	23.70	33.59	19.12	27.76	30.31	25.46	17.43
Pr	4.23	4.08	5.48	4.67	4.59	3.87	3.87	4.03	4.39	2.58	4.31	4.43	3.75	3.08
Nd	19.12	19.74	26.01	21.40	21.40	18.30	17.40	16.00	19.05	11.32	21.00	21.80	18.81	14.27
Sm	4.94	5.18	7.02	6.08	6.06	5.00	4.91	4.32	4.72	3.06	5.79	6.16	5.58	4.54
Eu	1.76	1.91	2.36	1.97	2.03	1.79	1.77	1.49	1.61	1.02	2.01	2.27	2.12	1.66
Gd	5.65	5.90	8.11	7.71	7.76	6.49	5.65	4.93	5.30	3.65	6.40	7.52	7.16	6.29
Tb	1.00	1.05	1.45	1.23	1.26	1.05	1.03	0.94	0.98	0.72	1.16	1.33	1.47	1.07
Dy	6.07	6.62	8.76	7.36	7.51	6.25	6.15	5.76	6.37	4.69	7.52	8.68	10.55	7.11
Ho	1.25	1.37	1.86	1.53	1.55	1.29	1.28	1.23	1.34	0.99	1.64	1.84	2.34	1.48
Er	3.41	3.84	4.92	4.36	4.39	3.69	3.62	3.60	3.87	2.72	4.61	4.95	6.48	4.33
Tm	0.49	0.54	0.71	0.62	0.62	0.53	0.52	0.54	0.59	0.40	0.67	0.71	0.94	0.68
Yb	3.19	3.52	4.42	3.84	3.91	3.39	3.27	3.48	3.83	2.56	4.41	4.36	5.76	4.29
Lu	0.48	0.53	0.70	0.58	0.58	0.51	0.49	0.53	0.60	0.39	0.69	0.64	0.82	0.65
Hf	2.74	3.15	3.51	3.18	3.28	3.07	3.07	2.50	2.59	2.32	3.07	3.52	3.29	2.50
Ta	0.44	0.53	0.67	0.56	0.48	0.50	0.58	0.99	0.99	1.10	0.99	1.07	1.25	1.07
Pb	7.56	6.22	8.26	7.73	6.93	8.36	7.80	8.29	7.53	14.63	12.70	10.55	11.34	22.40
Th	0.17	0.38	0.21	0.78	0.68	0.37	0.38	0.97	0.92	1.28	0.80	0.86	0.93	0.95
U	0.33	0.44	0.34	0.73	0.70	0.45	0.50	1.64	1.85	2.91	1.20	1.01	1.55	0.83
$^{147}Sm/^{144}Nd$			0.163						0.150		0.167		0.179	
$^{143}Nd/^{144}Nd$			0.512619						0.512533		0.512653		0.512740	
2 σ			6						8		6		6	
εNd (t)			3.8						3.8		4.1		4.2	

ACCEPTED MANUSCRIPT

to be continued

Sample	Group 3										Shitun ultramafic rocks coeval with Group 4			
	Northern Yunkai domain													
Sample	XT3088-1[c]	XT3090-2[c]	XT3101-1[c]	XT3090-3[c]	09YK-1d [d]	09YK-1e [d]	09YK-1f [d]	09YK-3e [d]	09YK-3f [d]	JXW-1[d]	09WG-51C	09WG-51D	09WG-51E	09WG-51M
	Plagioclase amphibolite				Plagioclase amphibolite						serpentinite			
	Shiwo-Qingshuikou (Eastern Guangxi)				Fenjie-Guizi (north Guangdong)						Shitun (Zhenghe)			
SiO_2	47.58	47.16	47.32	48.11	51.70	50.58	51.51	49.30	50.89	50.32	37.25	39.18	38.77	38.08
TiO_2	1.69	1.14	1.28	1.57	2.21	2.25	2.20	1.80	1.88	1.76				
Al_2O_3	15.07	15.77	15.04	15.21	13.92	14.09	14.08	15.02	14.72	14.84	0.57	0.55	1.14	0.70
FeOt	12.83	11.29	10.99	11.58	5.43	5.74	5.55	6.34	6.07	6.26	7.79	6.44	7.55	5.83
MgO	7.69	8.30	8.47	7.63	13.23	13.65	13.33	13.35	13.19	13.54	39.18	39.39	39.12	39.93
CaO	11.17	10.75	10.79	11.22	8.93	8.84	8.70	8.92	8.76	9.44	0.12	0.23	0.08	0.29
K_2O	0.32	0.83	1.45	0.56	0.31	0.64	0.43	2.00	1.51	0.48				
Na_2O	1.03	2.43	1.41	1.81	3.05	3.00	3.08	1.67	1.55	3.09	0.14	0.12	0.13	0.13
P_2O_5	0.15	0.09	0.13	0.13	0.27	0.27	0.27	0.11	0.22	0.20				
MnO	0.21	0.22	0.22	0.21	0.10	0.10	0.10	0.21	0.21	0.18	0.10	0.08	0.07	0.07
LOI					0.80	0.79	0.74	1.25	0.96		14.90	13.87	12.65	15.13
Total	97.74	97.98	97.10	98.03	99.95	99.96	99.98	99.98	99.96		100.08	99.89	99.56	100.18
mg-number	55	60	61	57	49	50	49	53	52	66				
Sc	49	44	44	46	44	42	42	56	49	36				
V	345	257	270	302	366	335	343	367	342	268				
Cr	129	206	182	279	36	32	36	35	38	37				
Co	47	43	42	42	91	81	81	120	116	185				
Ni	60	80	68	63	36	35	36	43	47	62				
Ga	14.5	20.3	16.7	16.5	19.70	21.37	20.82	25.29	24.77	18.47				
Rb	11.0	20.0	55.0	23.0	7.56	21.05	12.58	87.37	71.60	26.37				
Sr	118	108	109	237	339	340	341	152	144	218				
Y	37.55	26.20	33.59	32.80	39.51	40.05	40.50	33.41	35.04	28.63				
Zr	120	76.0	90.3	113	172.1	168.4	169.5	83.5	137.3	114.6				
Nb	14.42	16.94	16.79	13.45	12.70	12.44	12.37	11.09	10.87	8.55				
Cs	0.67	1.22	1.21	0.87	0.47	1.06	0.62	2.60	1.83					

Accepted Manuscript

ACCEPTED MANUSCRIPT

Ba	51	135	150	92	23.9	77.8	40.7	502.3	319.4	130.4
La	7.60	5.31	7.50	8.41	18.11	21.82	19.07	12.93	12.61	11.61
Ce	21.67	13.85	13.89	15.44	41.20	47.58	43.21	27.46	29.34	26.34
Pr	3.13	2.14	2.45	3.06	5.59	6.23	5.71	3.71	4.22	3.64
Nd	14.62	10.13	13.71	15.03	23.84	26.72	24.48	15.04	18.77	16.01
Sm	4.57	3.18	3.95	4.16	6.03	6.20	6.07	3.56	4.73	4.08
Eu	1.75	1.24	1.48	1.62	2.05	2.12	2.16	1.15	1.35	1.38
Gd	6.40	4.25	5.36	5.52	6.62	6.74	6.78	4.05	5.29	5.15
Tb	1.12	0.76	0.96	1.00	1.13	1.14	1.16	0.76	0.95	0.86
Dy	7.32	5.14	6.59	6.60	6.68	6.88	6.95	5.09	5.87	5.16
Ho	1.54	1.05	1.36	1.37	1.38	1.40	1.42	1.16	1.25	1.10
Er	4.41	3.04	3.84	3.78	3.77	3.82	3.83	3.52	3.63	2.91
Tm	0.72	0.50	0.62	0.60	0.54	0.55	0.56	0.57	0.55	0.43
Yb	4.41	3.03	3.94	3.80	3.44	3.51	3.62	3.74	3.69	2.86
Lu	0.68	0.46	0.59	0.58	0.51	0.52	0.54	0.56	0.54	0.45
Hf	2.39	1.57	1.71	2.20	4.23	4.22	4.34	2.36	3.64	2.02
Ta	1.29	1.35	1.55	1.05	0.89	0.90	0.88	0.89	0.84	0.69
Pb	13.50	6.80	8.80	14.10	4.19	4.13	7.10	7.27	6.60	
Th	0.99	0.50	0.98	0.72	2.20	2.23	2.13	3.67	1.49	1.95
U	1.03	0.49	0.73	0.53	0.63	0.56	0.60	0.79	0.54	0.45
$^{147}Sm/^{144}Nd$						0.1457			0.1524	0.1599
$^{143}Nd/^{144}Nd$						0.512476			0.512593	0.512617
2 σ						8			7	
εNd (t)						3.93			4.69	4.22

Accepted Manuscript

ACCEPTED MANUSCRIPT

1369 to be continued

Sample	Group 4					
	Diabase coeval with ultramafic rocks from Wuyi		Northern Yunkai domain			
	09WG-53A	09WG-53E	1252-1 [a]	09YK-11A	09YK-12B	09YK-12E
	Shitun (Zhenghe)		Dajin	Liuwan (Rongxian)		
	metadiabase			Plagioclase amphibolite		
SiO_2	43.30	43.53	49.04	47.73	51.64	51.29
TiO_2	1.07	1.28	0.47	1.50	1.19	1.20
Al_2O_3	17.99	17.11	16.04	14.91	14.50	14.62
FeOt	11.30	13.46	8.61	12.98	11.63	11.62
MgO	10.43	12.09	9.62	7.16	6.83	7.01
CaO	6.14	5.06	9.83	11.35	9.77	9.52
K_2O	6.00	4.66	0.77	1.12	0.91	0.98
Na_2O	0.07	0.14	1.27	2.24	2.26	2.12
P_2O_5	0.16	0.24	0.06	0.11	0.10	0.10
MnO	0.34	0.22	0.15	0.20	0.17	0.17
LOI	3.14	2.21	2.30	0.68	0.96	1.34
Total	99.94	100.01	98.16	99.98	99.96	99.98
mg-number	65	64	69	52	54	55
Sc	25	33	33	49	43	43
V	284	316	162	332	272	269
Cr	137	113	314	201	137	168
Co	60	23	67	45	47	45
Ni	98	45	124	71	67	73
Ga	16.3	13.1		19.4	17.8	18.1
Rb	323.5	191.3	52.0	19.6	16.0	21.9
Sr	416	137	262	138	90.9	76.7
Y	14.64	10.73	9.47	51.83	41.92	42.97
Zr	52.8	51.0	36.9	110	108	107
Nb	3.56	3.52	2.38	2.66	2.46	2.50
Cs	15.40	18.15	5.24	0.60	0.43	0.73

ACCEPTED MANUSCRIPT

Ba	1306	839	104	67	82	75
La	8.27	8.23	7.21	10.05	15.36	15.70
Ce	18.17	18.99	15.70	25.01	34.31	37.09
Pr	2.51	2.67	1.94	3.62	4.61	4.98
Nd	11.26	11.20	7.76	16.71	19.29	21.15
Sm	2.68	2.56	1.73	5.34	5.16	5.73
Eu	1.05	0.62	0.58	1.57	1.47	1.56
Gd	2.82	2.39	1.87	7.11	6.20	6.67
Tb	0.41	0.38	0.29	1.42	1.13	1.20
Dy	2.31	2.18	1.84	8.94	6.82	7.31
Ho	0.45	0.43	0.39	1.82	1.43	1.49
Er	1.19	1.16	1.17	4.89	3.93	4.11
Tm	0.16	0.17	0.16	0.72	0.58	0.60
Yb	1.01	1.06	1.13	4.43	3.77	3.98
Lu	0.15	0.16	0.13	0.65	0.57	0.60
Hf	1.46	1.56	1.23	2.91	2.93	3.06
Ta	0.24	0.26	0.17	0.19	0.22	0.24
Pb	3.88	3.79	8.59	7.71	8.34	6.19
Th	0.70	0.95	2.22	0.55	2.04	2.10
U	0.21	0.25	0.46	0.16	0.50	0.98
$^{147}Sm/^{144}Nd$	0.144			0.193	0.162	
$^{143}Nd/^{144}Nd$	0.512586			0.512732	0.512554	
2 σ	10			2	3	
εNd (t)	5.6			2.3	2.7	

The samples with “a”, “b”, “c” and “d” are from Qin et al. (2007), Li XH et al. (1999a, b), Qin et al. (2005) and Zhang et al. (2012), respectively. εNd (t) values are calculated assuming t = 980 Ma

Accepted Manuscript

ACCEPTED MANUSCRIPT

Table 2: Re-Os isotopic analytical results for the earliest Neoproterozoic amphibolites and Shitun serpentinite along the Wuyi domain, SCB

sample			Re (ppt)	±	Os (ppt)	±	$^{187}Re/^{188}Os$	±	$^{187}Os/^{188}Os$	±	$^{187}Os/^{188}Os_{(t\ Ma)}$	±	$\gamma Os_{(t\ Ma)}$ ±
Group 2	metagabbro	WG-59B1	8.9	1.2	4.6	0.1	11.58	1.55	1.85676	0.0110	1.6662	0.12040	1284± 12
	metagabbro	WG-59B4	9.4	1.2	52.9	0.1	0.87	0.11	0.2596	0.0010	0.2453	0.00079	104± 0.7
Group 3	plagioclase amphibolite	09WG-59B3	13.2	1.1	11.1	0.1	6.51	0.54	1.1568	0.0110	1.0492	0.00225	772±1.9
		09WG-59B6	13.2	1.1	12.2	0.2	5.87	0.49	1.0756	0.0202	0.9791	0.01209	713± 10
	amphibolite	09WG-66A2	54.0	0.0	46.2	0.2	6.04	0.02	0.6997	0.0028	0.6002	0.00239	399±2.0
		09WG-66A7	74.5	1.2	42.8	0.1	8.76	0.15	0.4795	0.0018	0.3351	0.00060	178±0.5
		09WG-66A9	74.5	1.2	42.8	0.1	8.77	0.15	0.4825	0.0012	0.3382	0.00121	181±1.0
Group 4	serpentinite	09WG-51C	33.9	2.8	2613	62.1	0.06	0.01	0.1147	0.0002	0.1136	0.00014	-5.6±0.1
	serpentinite	09WG-51D	19.0	2.4	3275.1	74.0	0.03	0.00	0.1143	0.0003	0.1138	0.00022	-5.5±0.2
	serpentinite	09WG-51E	21.4	1.4	51.2	0.1	2.02	0.13	0.1442	0.0006	0.1110	0.00153	-7.8±1.3
	serpentinite	09WG-51M	38.1	3.8	2961.1	33.9	0.06	0.01	0.1216	0.0003	0.1205	0.00020	0.1 ±0.2

$\gamma Os_{(t\ Ma)}$ values are calculated assuming t = 980 Ma

Accepted Manuscript

ACCEPTED MANUSCRIPT

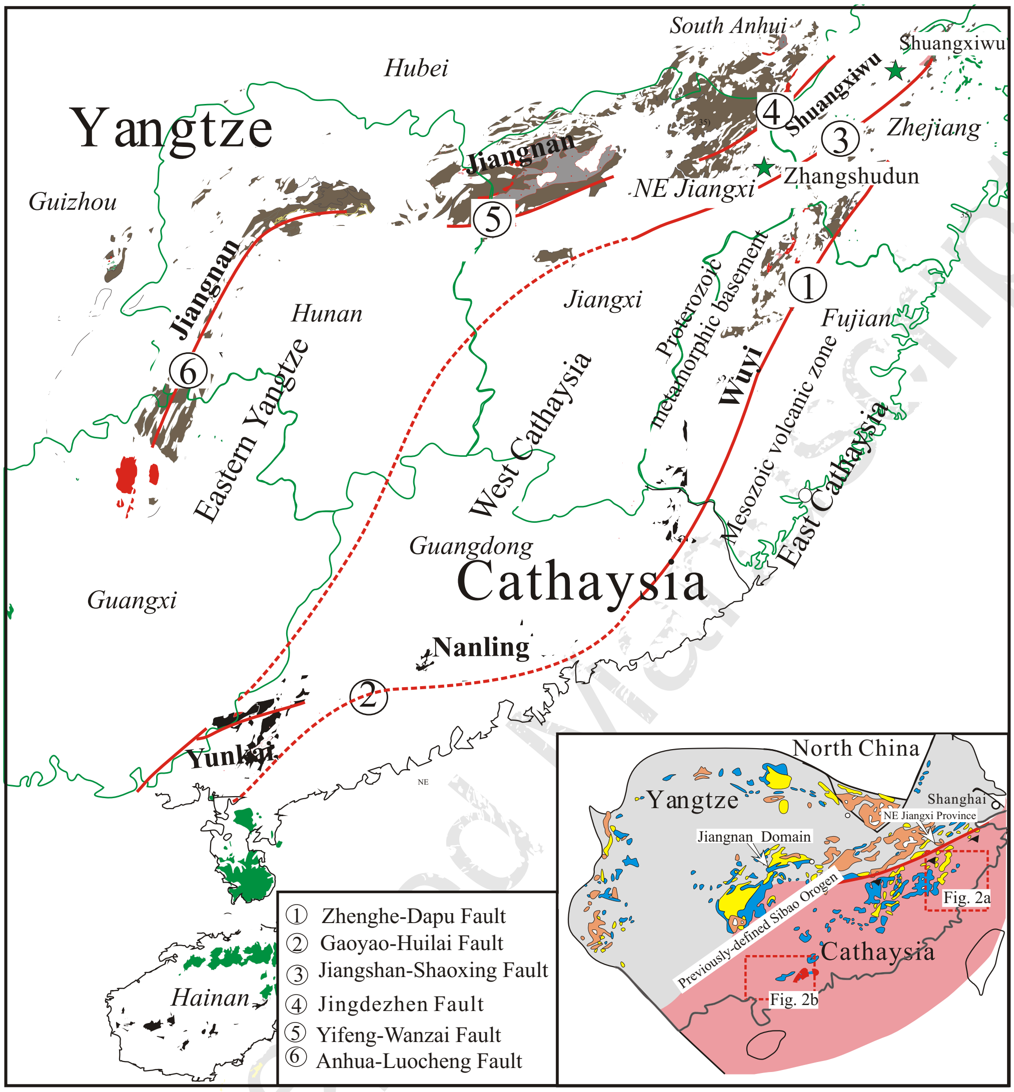

Fig. 1 Y-J Wang & coauthors

ACCEPTED MANUSCRIPT

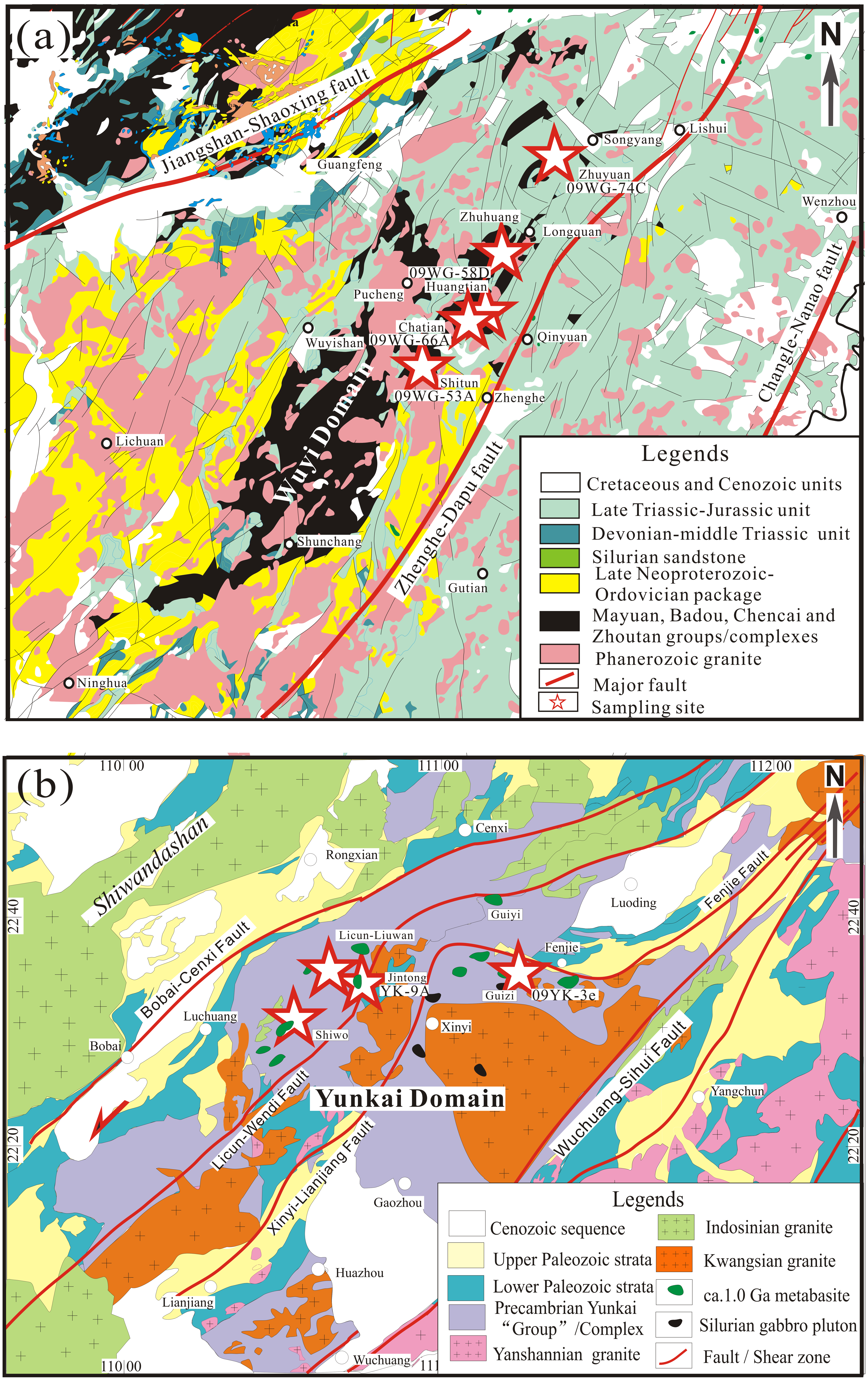

Fig. 2 Y-J Wang & coauthors

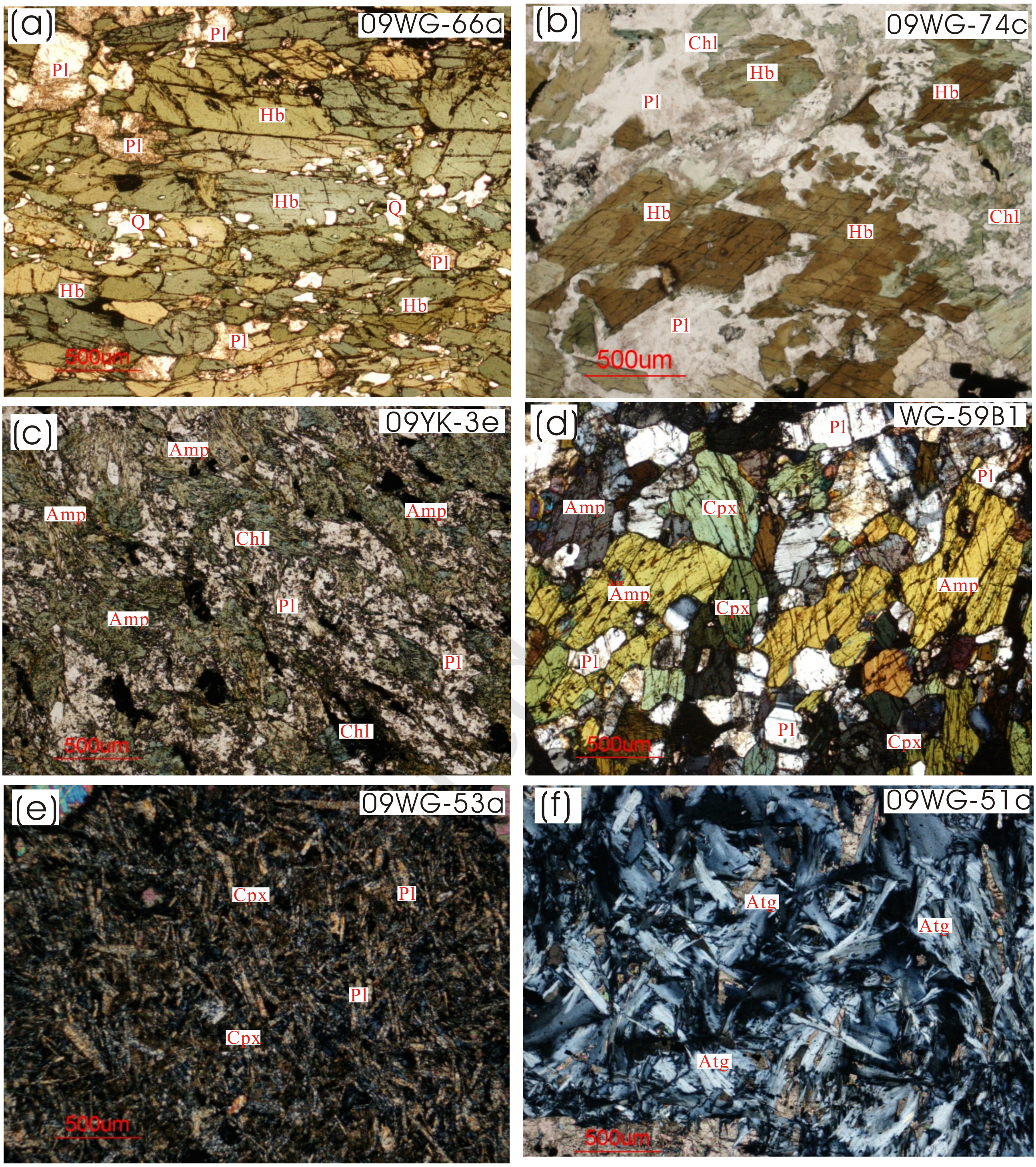

Fig. 3 Y-J Wang & coauthors

ACCEPTED MANUSCRIPT

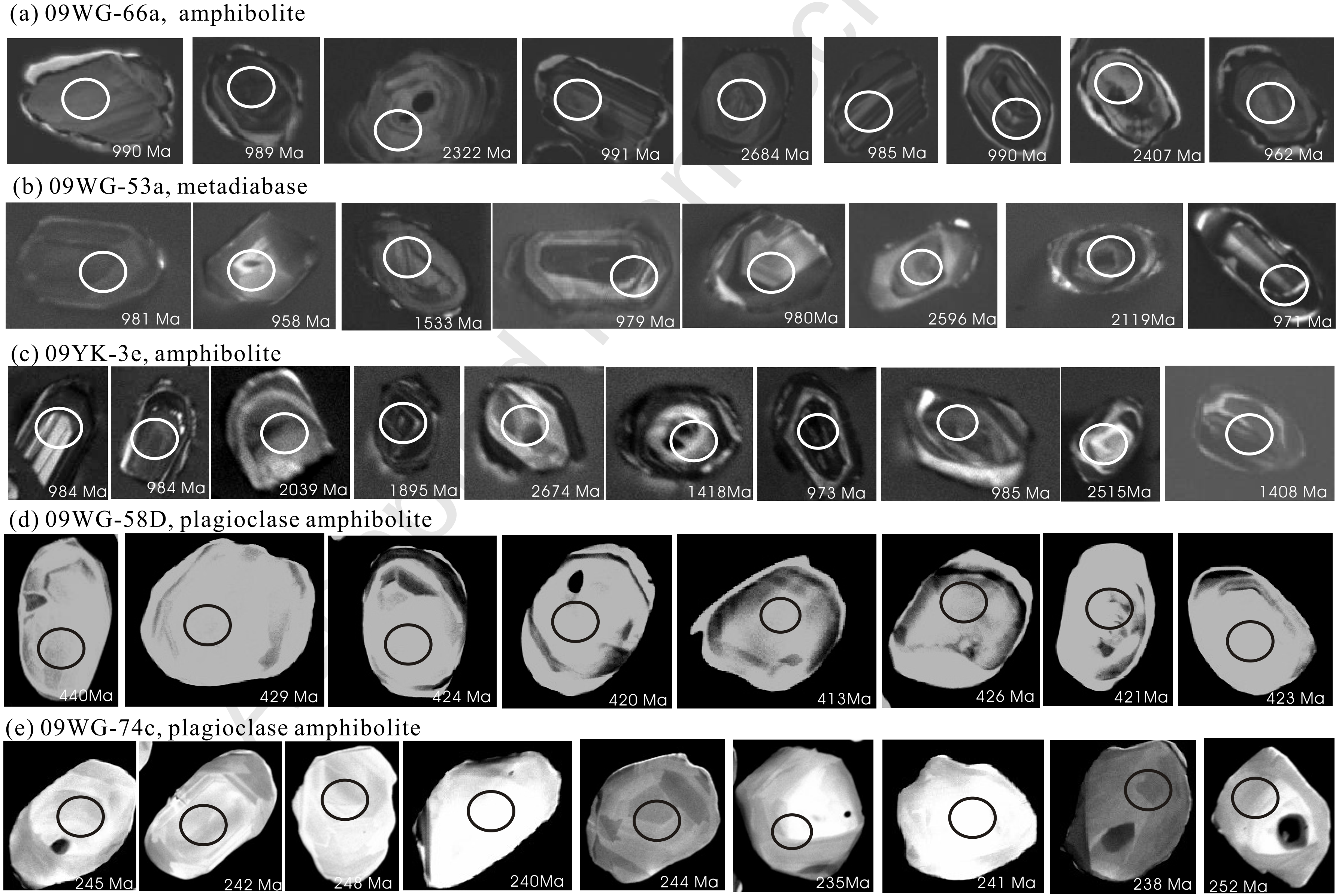

Fig. 4 Y-J Wang & coauthors

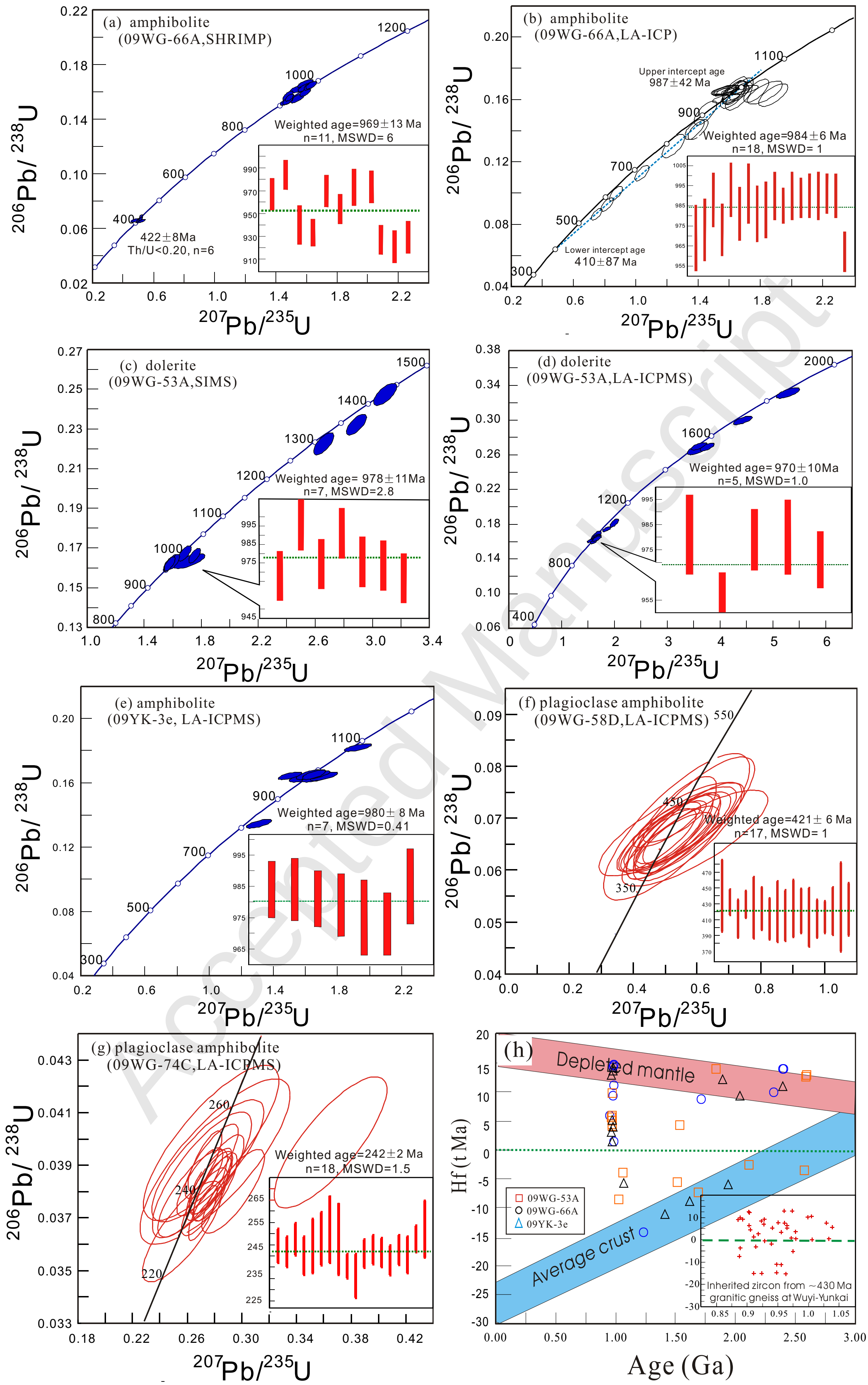

Fig. 5Y-J Wang & coauthors

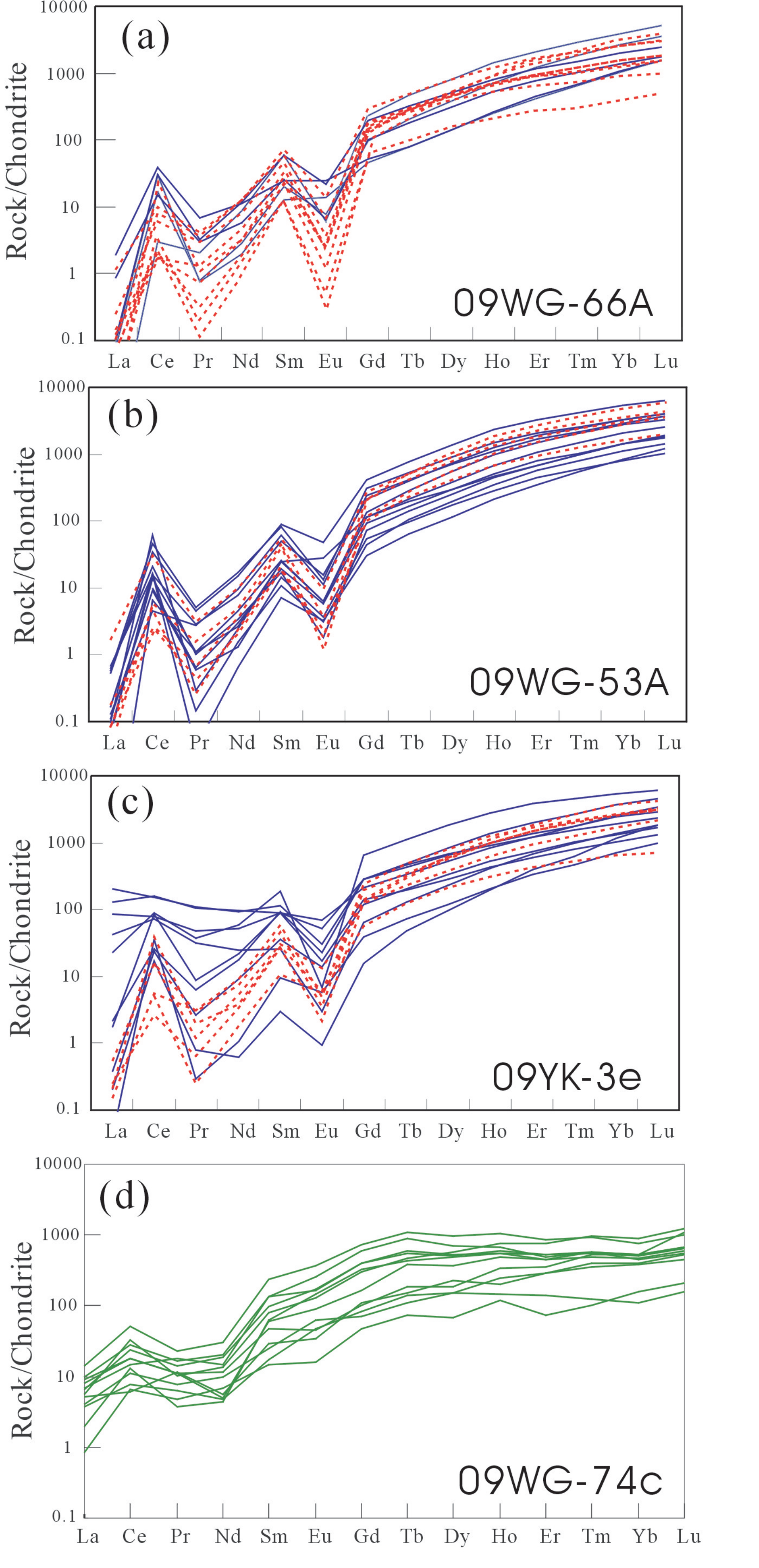

Fig. 6 Y-J Wang & coauthors

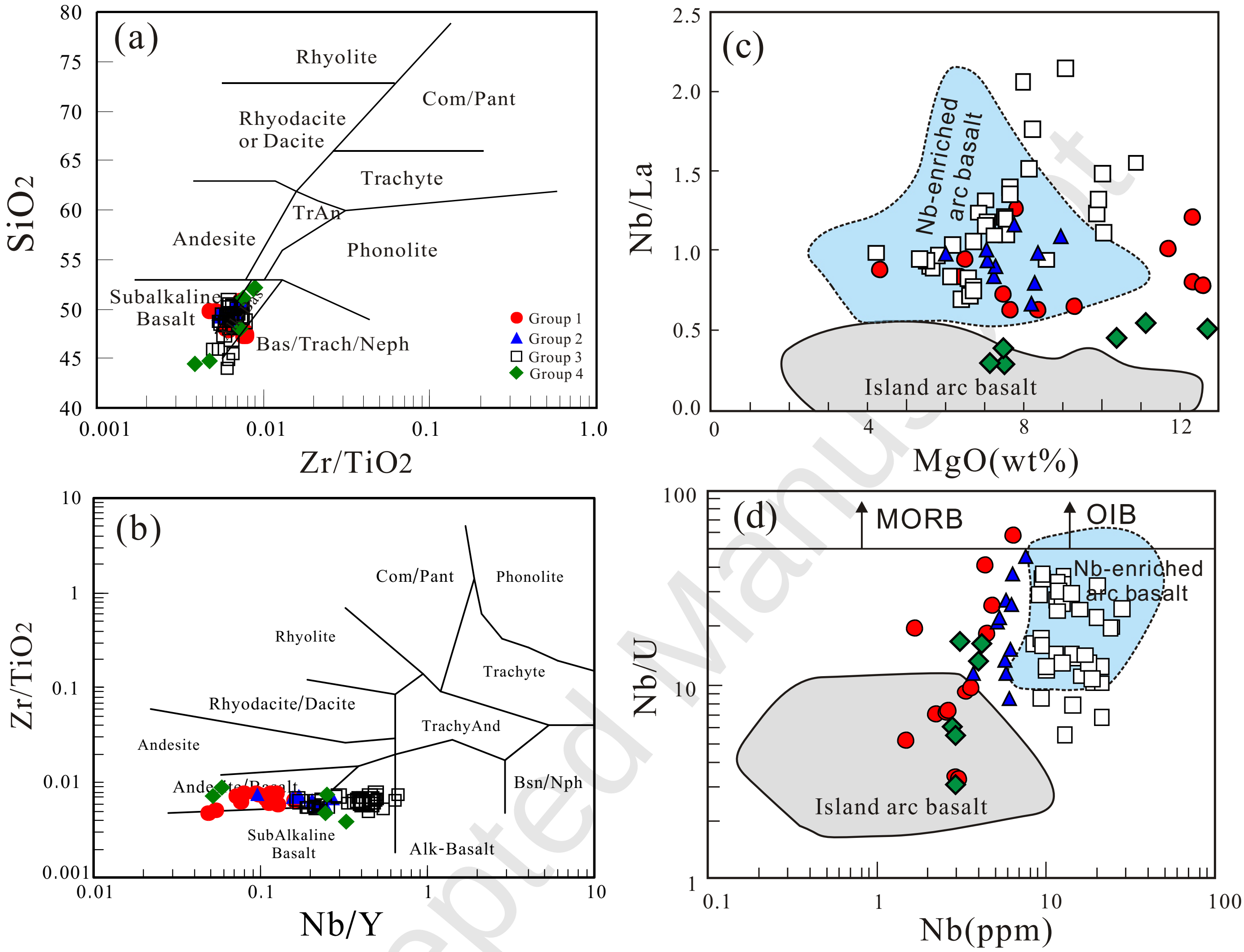

Fig. 7 Y-J Wang and coauthors

Accepted Manuscript

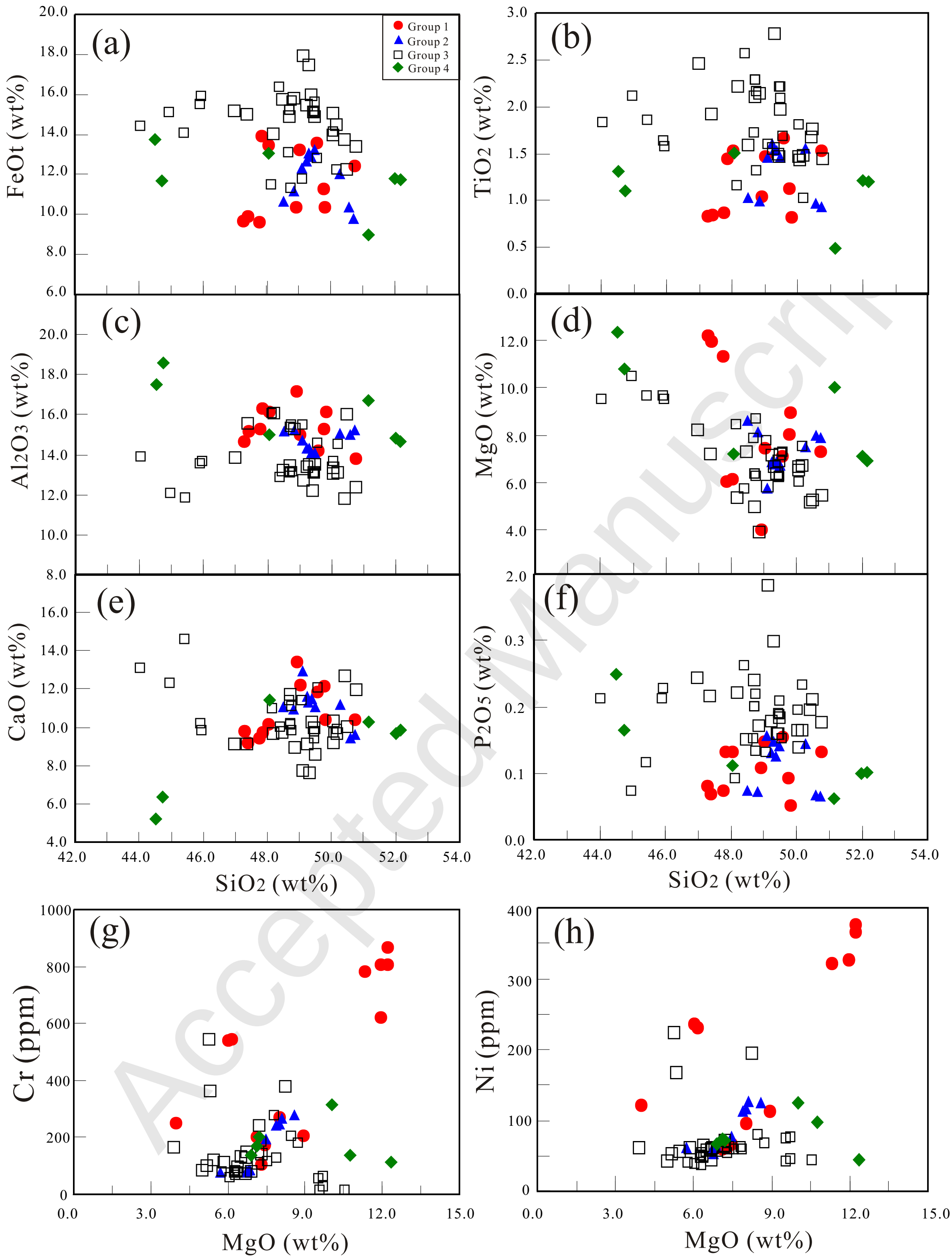

Fig. 8 Y-J Wang & coauthors

ACCEPTED MANUSCRIPT

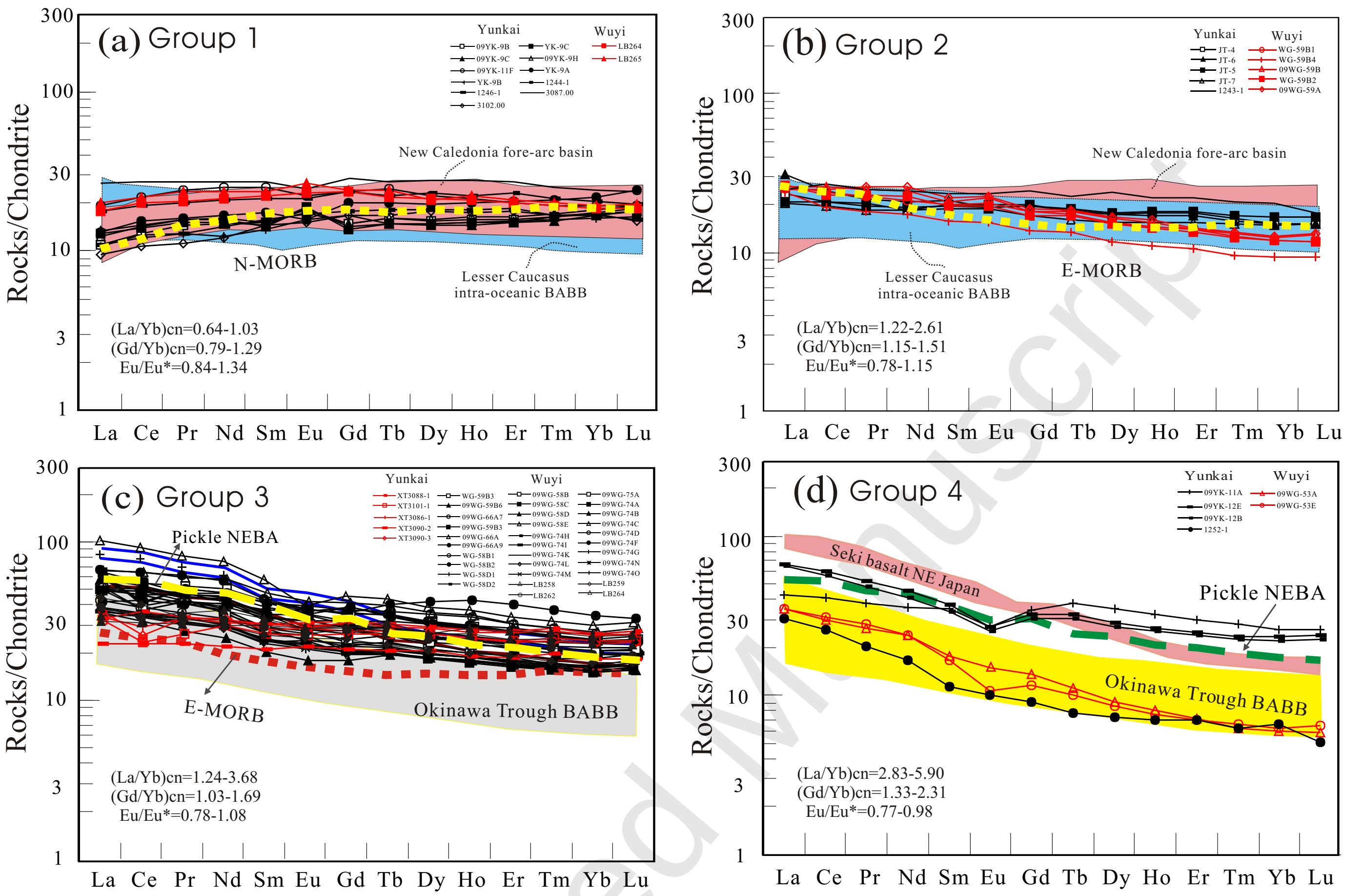

Fig. 9 Y-J Wang and coauthors

ACCEPTED MANUSCRIPT

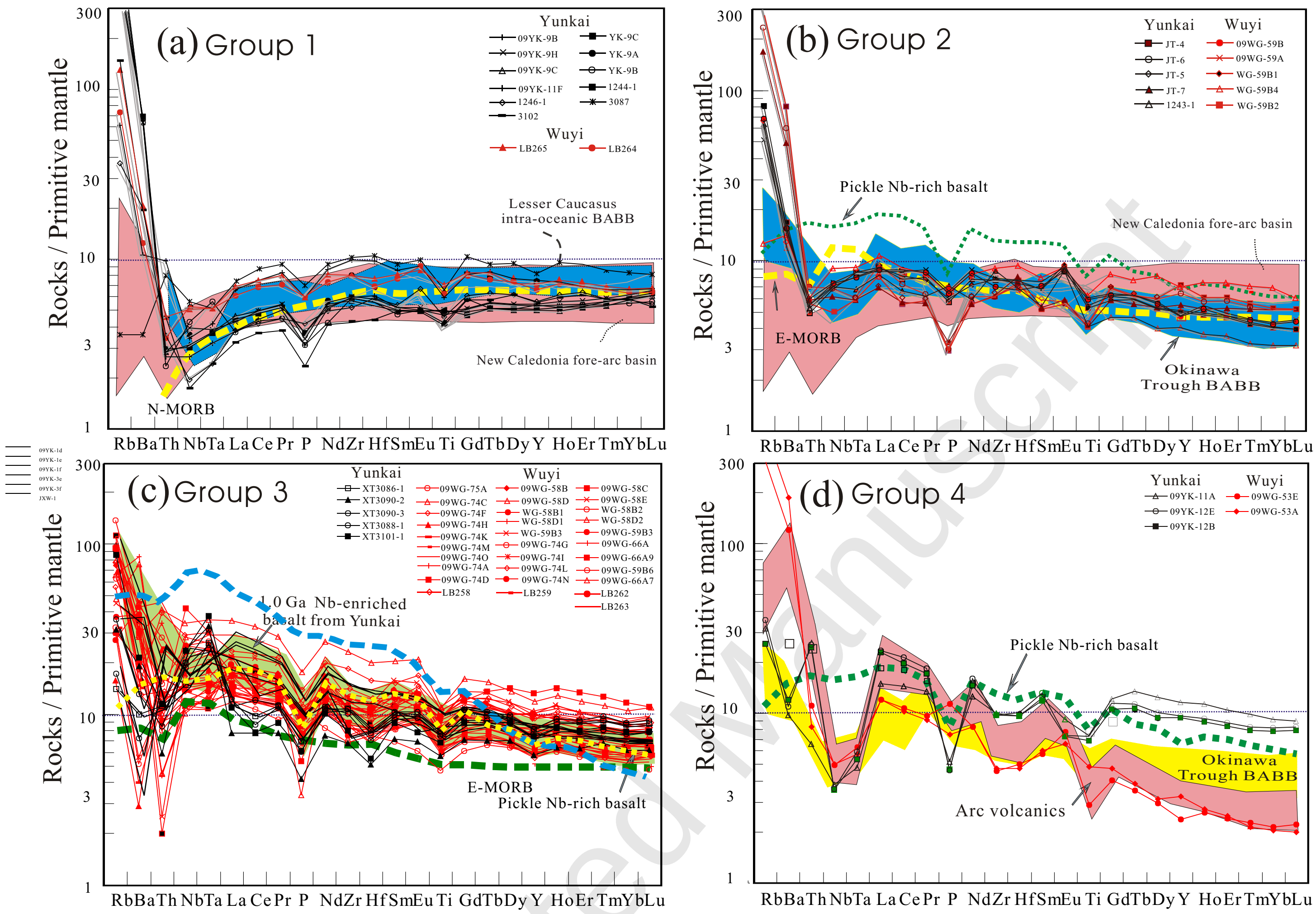

Fig. 10 Y-J Wang and coauthors

Accepted Manuscript

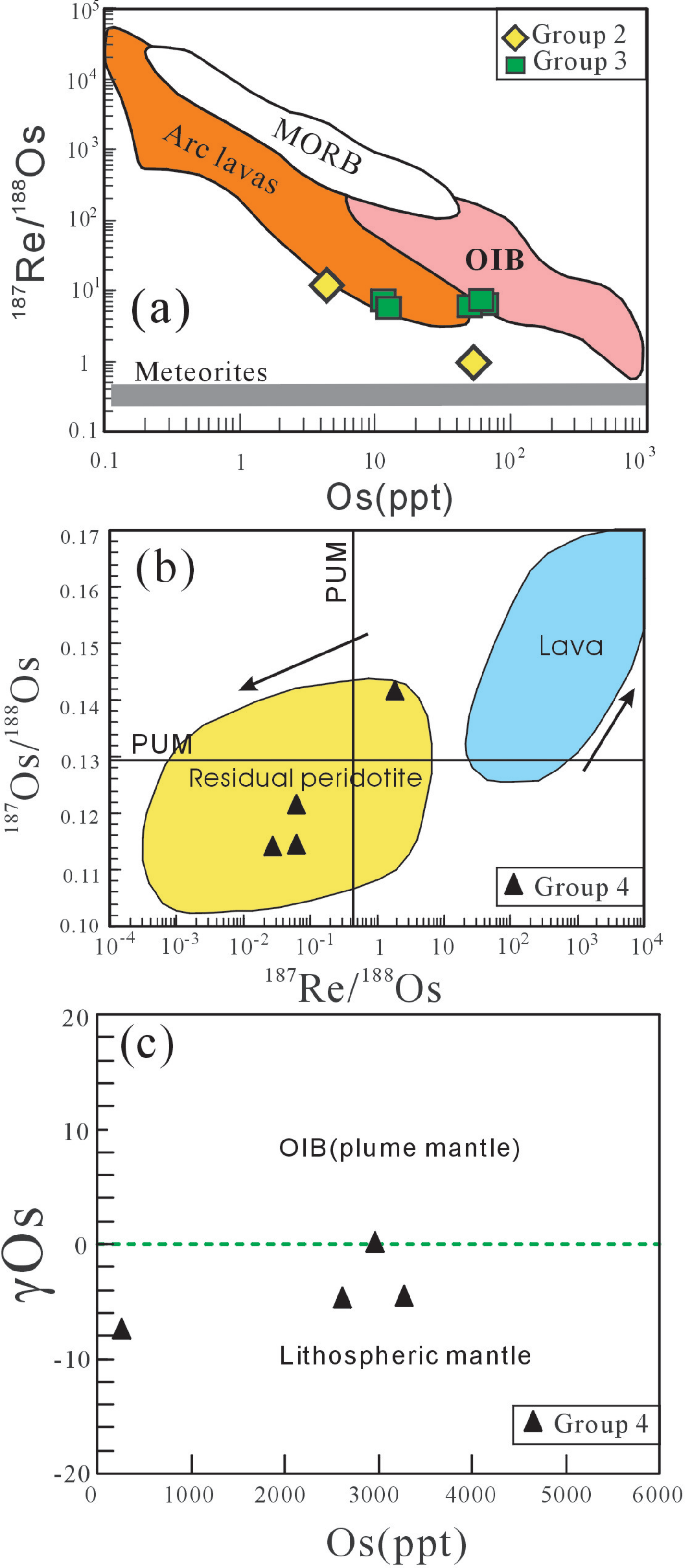

Fig. 11 Y-J Wang & coauthors

ACCEPTED MANUSCRIPT

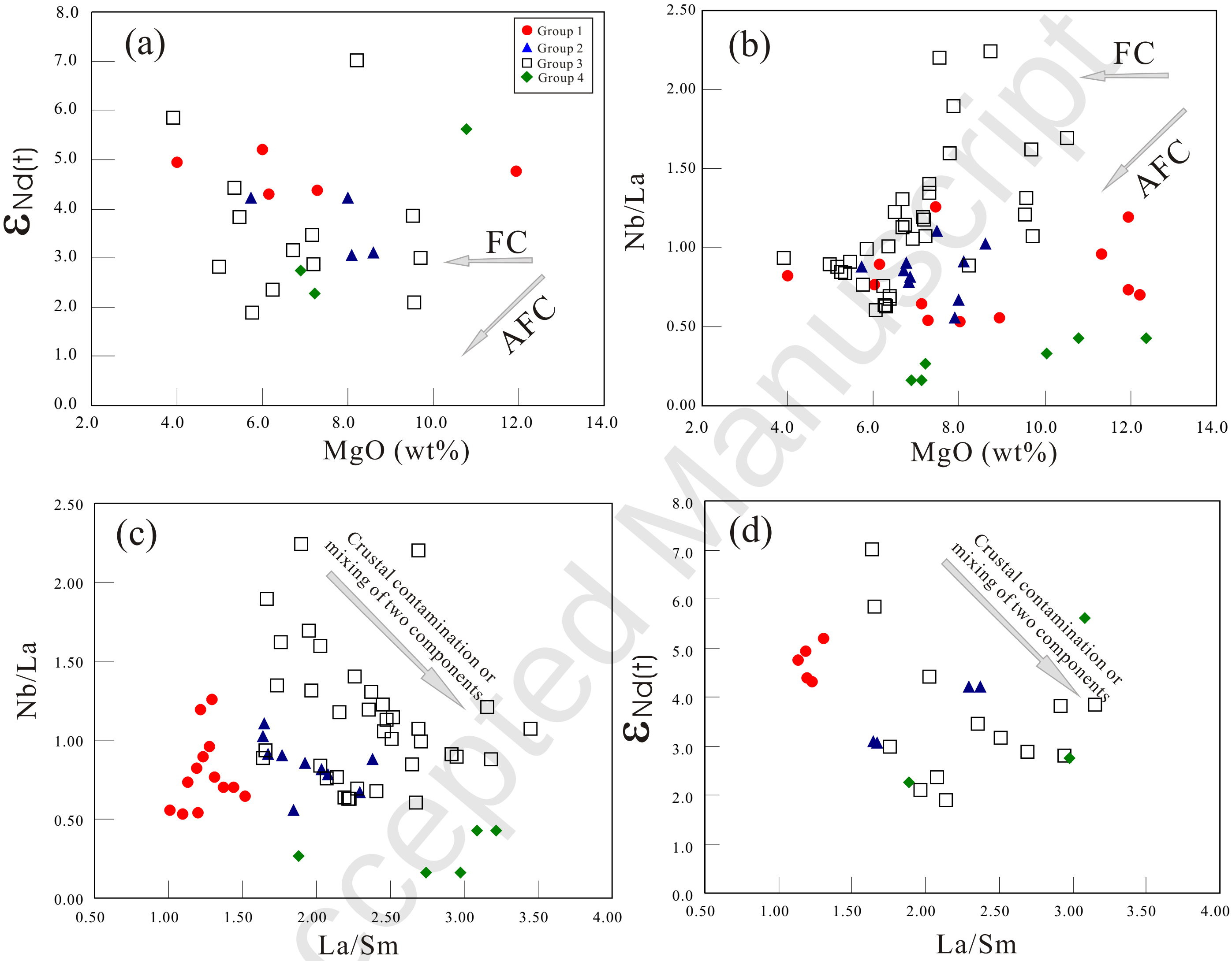

Fig. 12 Y-J Wang & coauthors

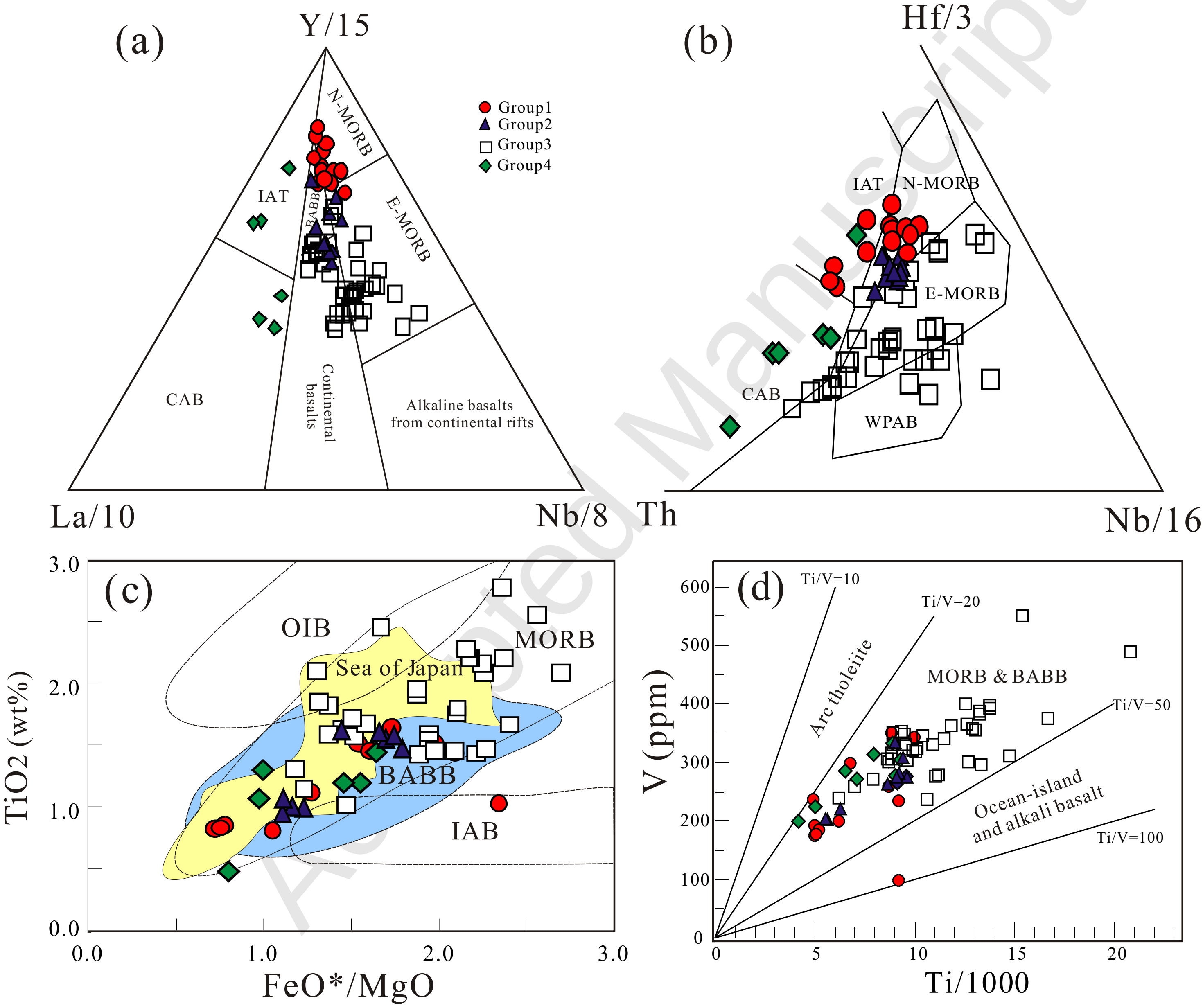

Fig. 13 Y-J Wang & coauthors

Accepted Manuscript

ACCEPTED MANUSCRIPT

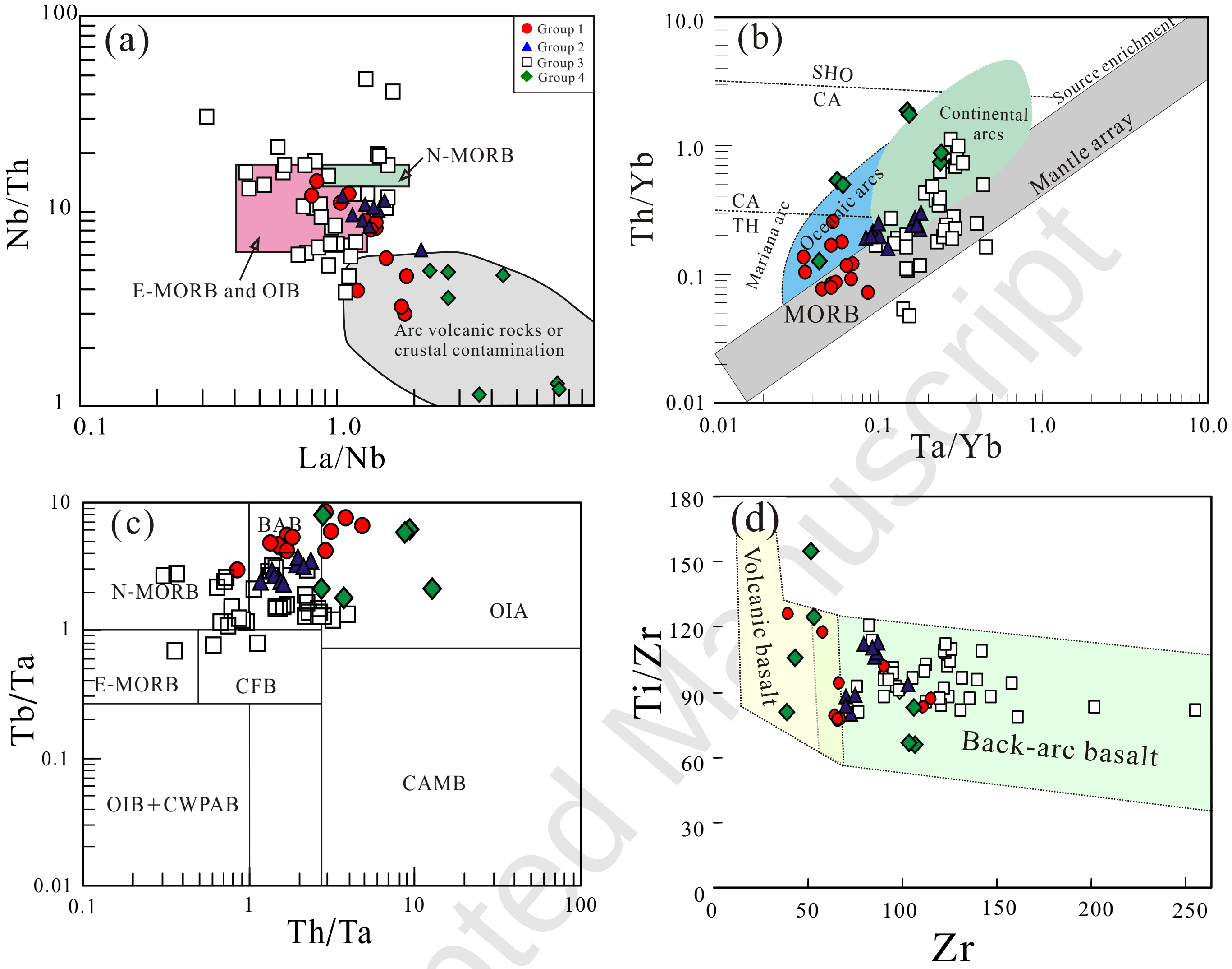

Fig. 14 Y-J Wang & coauthors

Accepted Manuscript

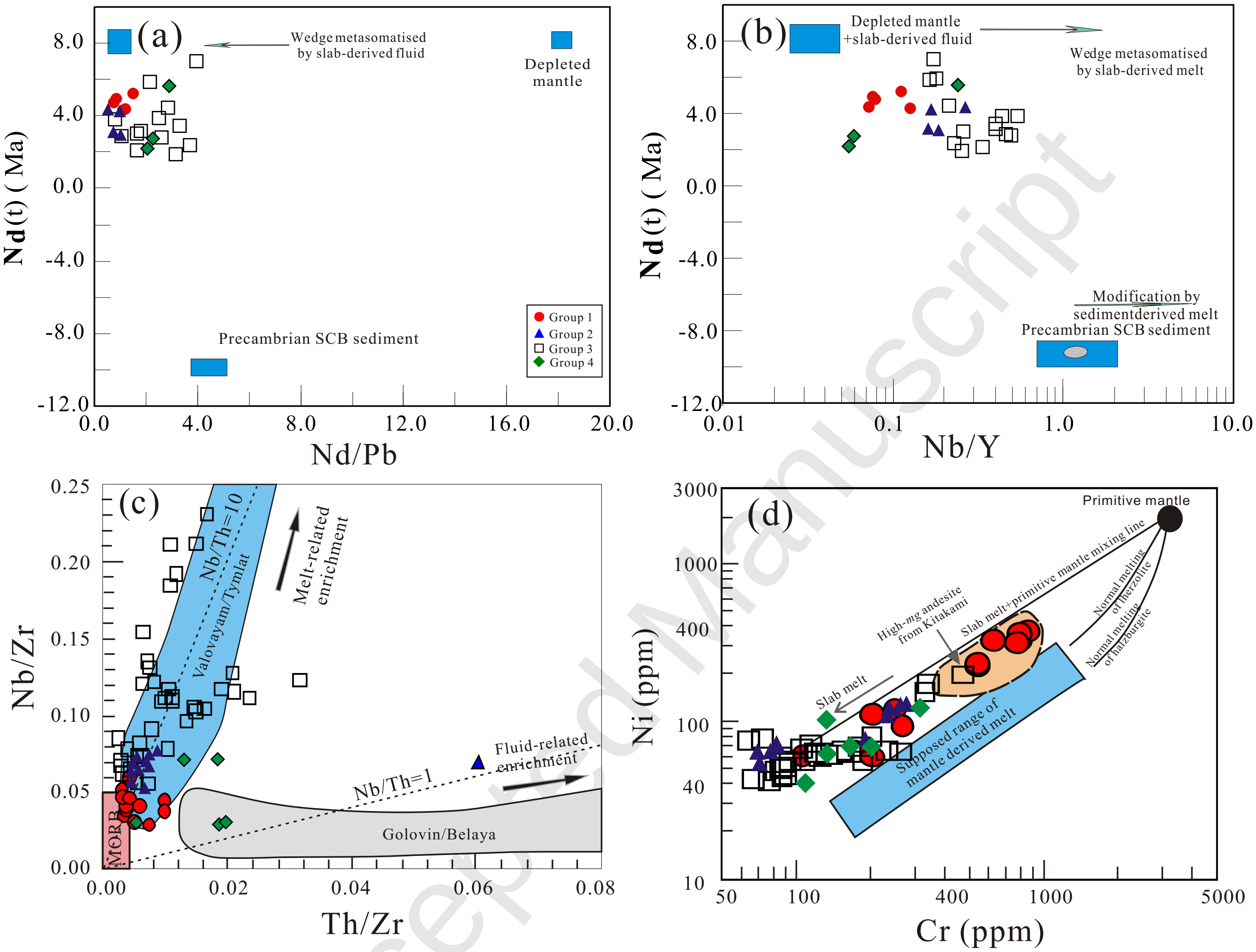

Fig. 15 Y-J Wang & coauthors

Accepted Manuscript

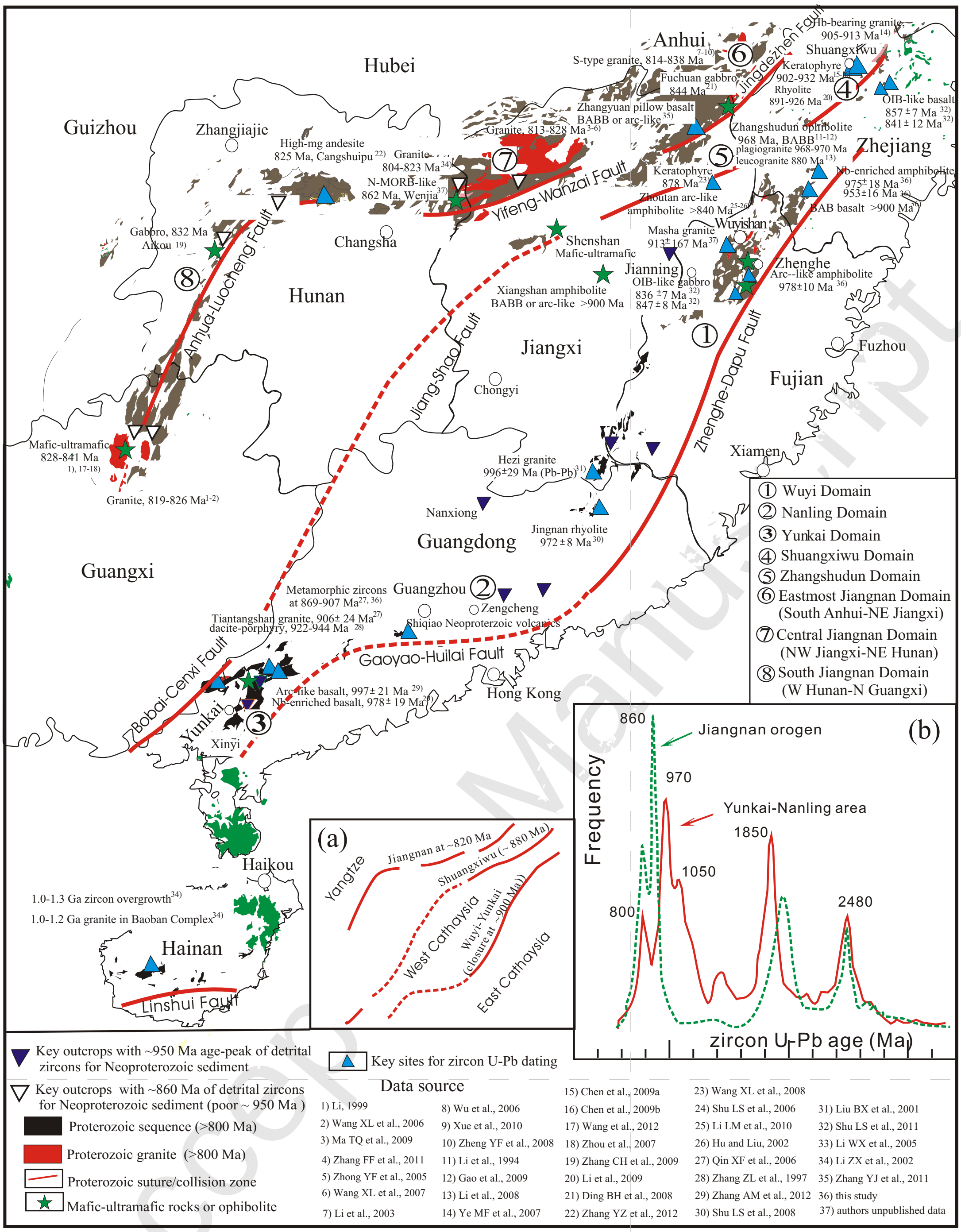

Fig. 16 Y-J Wang & coauthors

Accepted Manuscript

ACCEPTED MANUSCRIPT

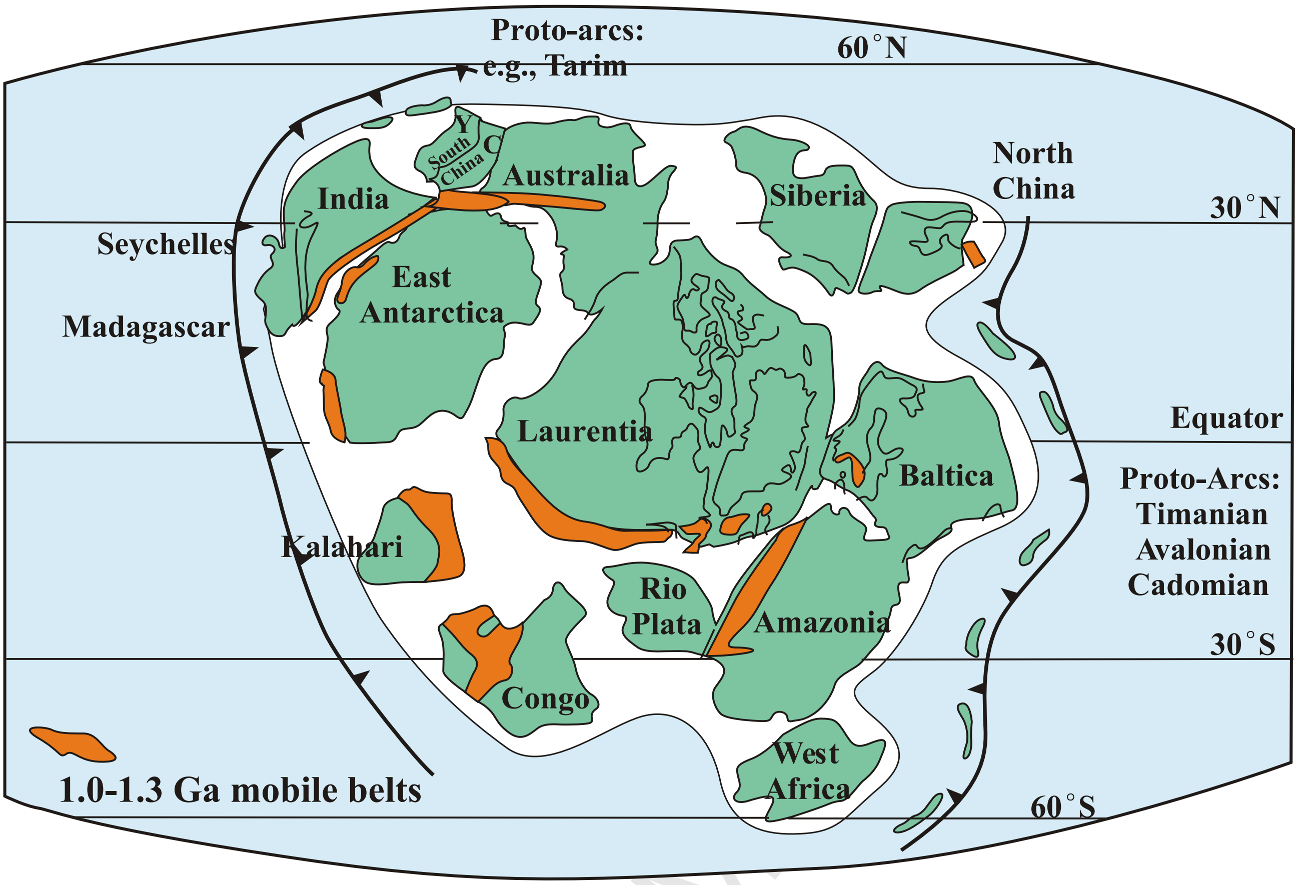

Fig. 17 Y-J Wang & coauthors

Accepted Manuscript

ACCEPTED MANUSCRIPT

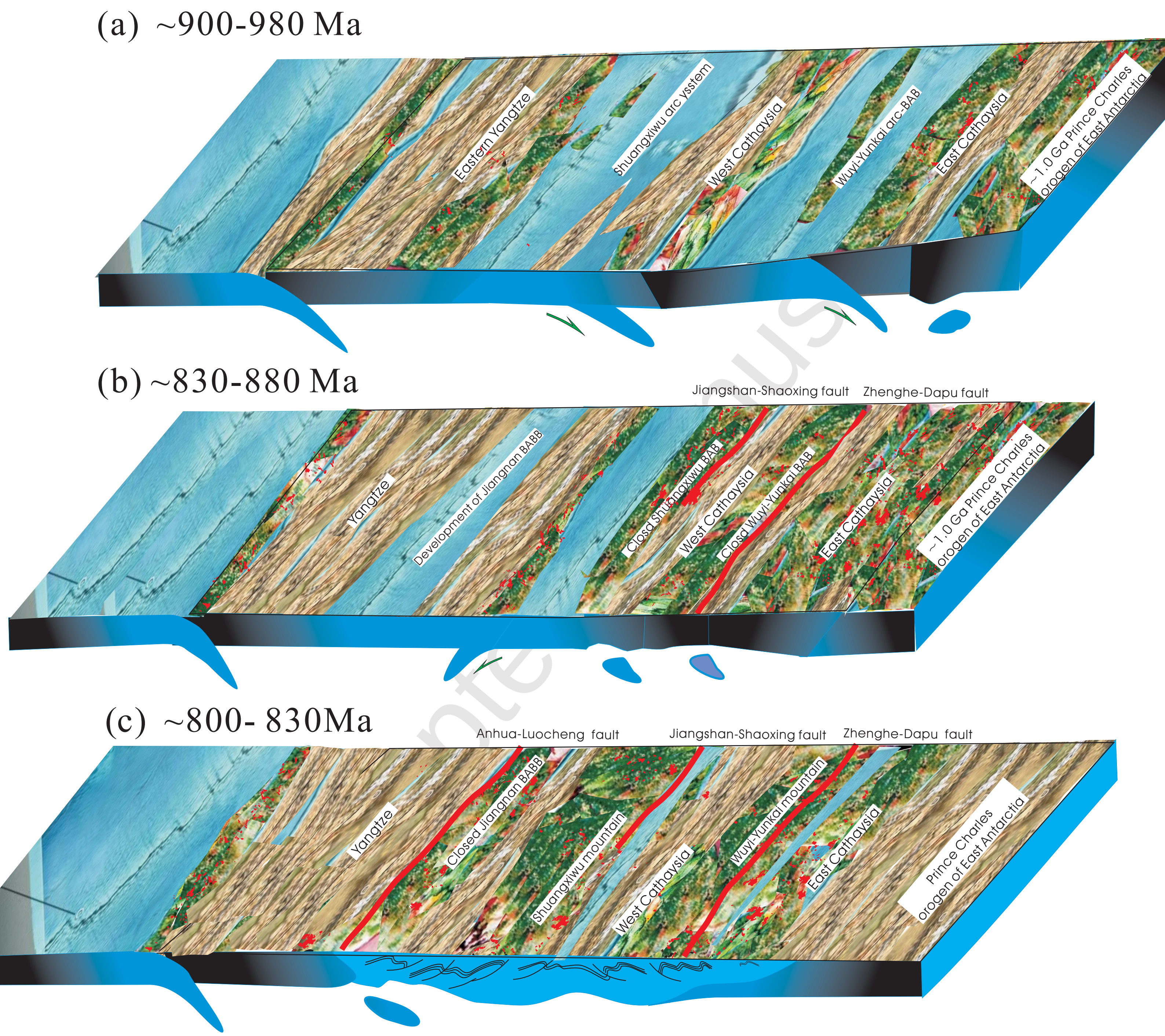

Figure 18 Y-J Wang & coauthors